

**UPGRADE OF NOS LAKE SUPERIOR OPERATIONAL  
FORECAST SYSTEM TO FVCOM: MODEL DEVELOPMENT  
AND HINDCAST SKILL ASSESSMENT**

Silver Spring, Maryland

May 2022



**noaa** National Oceanic and Atmospheric Administration

---

U.S. DEPARTMENT OF COMMERCE  
National Ocean Service  
Coast Survey Development Laboratory

**Office of Coast Survey  
National Ocean Service  
National Oceanic and Atmospheric Administration  
U.S. Department of Commerce**

**The Office of Coast Survey (OCS) is the Nation's only official chart maker. As the oldest United States scientific organization, dating from 1807, this office has a long history. Today it promotes safe navigation by managing the National Oceanic and Atmospheric Administration's (NOAA) nautical chart and oceanographic data collection and information programs.**

**There are four components of OCS:**

**The Coast Survey Development Laboratory develops new and efficient techniques to accomplish Coast Survey missions and to produce new and improved products and services for the maritime community and other coastal users.**

**The Marine Chart Division acquires marine navigational data to construct and maintain nautical charts, Coast Pilots, and related marine products for the United States.**

**The Hydrographic Surveys Division directs programs for ship and shore-based hydrographic survey units and conducts general hydrographic survey operations.**

**The Navigational Services Division is the focal point for Coast Survey customer service activities, concentrating predominately on charting issues, fast-response hydrographic surveys, and Coast Pilot updates.**

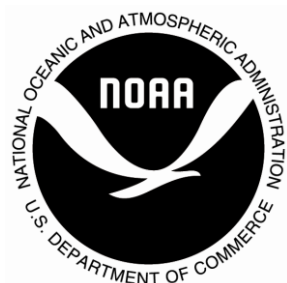
**UPGRADE OF NOS LAKE SUPERIOR OPERATIONAL FORECAST SYSTEM TO FVCOM: MODEL DEVELOPMENT AND HINDCAST SKILL ASSESSMENT**

**John G. W. Kelley and Yi Chen**  
National Ocean Service  
Office of Coast Survey, Coast Survey Development Laboratory  
Silver Spring, Maryland

**Eric J. Anderson and Gregory A. Lang**  
Office of Oceanic and Atmospheric Research  
Great Lakes Environmental Research Laboratory  
Ann Arbor, Michigan

**Machuan Peng**  
National Ocean Service  
Center for Operational Oceanographic Products and Services  
Silver Spring, Maryland

**May 2022**



**noaa** National Oceanic and Atmospheric Administration

---

**U. S. DEPARTMENT  
OF COMMERCE**  
Gina Raimondo,  
Secretary

**National Oceanic and  
Atmospheric Administration**  
Richard Spinrad,  
Under Secretary

**National Ocean Service**  
Nicole LeBoeuf,  
Assistant Administrator

**Office of Coast Survey**  
RDML Admiral Benjamin Evans  
Director

**Coast Survey Development Laboratory**  
Shachak Pe'eri  
Division Chief

## NOTICE

**Mention of a commercial company or product does not constitute an endorsement by NOAA. Use of information from this publication concerning proprietary products or the tests of such products for publicity or advertising purposes is not authorized.**

## TABLE OF CONTENTS

TABLE OF CONTENTS .....	ii
LIST OF FIGURES .....	iv
LIST OF TABLES .....	vii
LIST OF ACRONYMS .....	ix
EXECUTIVE SUMMARY .....	xi
1. INTRODUCTION .....	1
2. LAKE SUPERIOR .....	3
3. MODEL SYSTEM AND SETUP FOR HINDCASTS .....	5
3.1. Description of Model .....	5
3.2. Grid Configuration .....	6
3.3. Lateral Boundary Conditions .....	8
3.4. Surface Boundary Forcing .....	11
3.5. Initial Conditions .....	12
4. DESCRIPTION OF HINDCAST PERIODS .....	13
5. METHOD OF EVALUATION .....	15
5.1. Evaluation of Water Level Hindcasts .....	17
5.2. Evaluation of Surface Water Temperature Hindcasts .....	21
5.3. Evaluation of Sub-Surface Water Temperature Hindcasts .....	24
5.4. Evaluation of Water Currents Hindcasts .....	25
6. HINDCAST SKILL ASSESSMENT RESULTS .....	27
6.1. Assessment of Water Level Hindcasts .....	27
6.1.1. Hourly Water Levels .....	27
6.1.2. Extreme High-Water Level Events .....	35
6.1.3. Extreme Low Water Level Events .....	43
6.2. Assessment of Surface Water Temperature Hindcasts .....	50
6.2.1. Open Lake .....	50

6.2.2. Nearshore Buoys .....	54
6.3. Assessment of Sub-Surface Water Temperature Hindcasts .....	58
6.4. Assessment of Surface Water Currents Hindcasts .....	63
7. SUMMARY AND DISCUSSION .....	67
ACKNOWLEDGEMENTS .....	69
REFERENCES .....	71
APPENDIX .....	75

## LIST OF FIGURES

Figure 1. Map of the Lake Superior bathymetry (m) used by LSOFS, referenced to Low Water Datum (LWD) of 183.2 m (601.1 ft). The average depth is 147 m (482 ft) and the maximum depth is 389 m (1276 ft).....	7
Figure 2. Map depicting the FVCOM grid domain for LSOFS. The horizontal resolution ranges from around 200 m (0.12 mi) near the shore to approximately 2.5 km (1.6 mi) offshore with 21 vertical sigma levels. ....	8
Figure 3. LSOFS lateral boundary conditions.....	10
Figure 4. Locations where surface water temperatures are specified on the lateral boundaries of LSOFS. ....	11
Figure 5. 6-minute water level observations from the NOS/CO-OPS gage at Marquette Coast Guard Station, MI for Oct. 22-25, 2017. ....	13
Figure 6. 6-minute water level observations from the NOS/CO-OPS gage at Duluth, MN during April 13-15, 2018.....	14
Figure 7. Locations of NOS and CHS water-level gages used to evaluate LSOFS water level hindcasts. ....	18
Figure 8. Time series plots of hourly LSOFS-FVCOM hindcasts (red) and operational LSOFS-POMGL nowcasts (blue) of water level vs. original observations (black) at 1) COOPS-NWLON gauge Duluth, MN (9099064) and 2) CHS gauge Rosspport, ON (10220) during 2017. MAE and RMSE (m) at each station are shown individually on each panel.....	20
Figure 9. Time series plots of hourly LSOFS-FVCOM hindcasts (red) and LSOFS-POMGL nowcasts (blue) of water level vs. bias-removed observations (black) at 1) COOPS-NWLON gauge Duluth, MN (9099064) and 2) CHS gauge Rosspport, ON (10220) during 2017. MAE and RMSE (m) at each station are shown individually on each panel. ....	21
Figure 10. Locations of buoys used to evaluate LSOFS surface water temperature hindcasts....	22
Figure 11. Locations of buoys used to evaluate LSOFS sub-surface water temperature hindcasts. The water depths at the buoys are also depicted.....	24
Figure 12. Location of the buoy used to evaluate LSOFS hindcasts of water currents. The numbers of depths at which data are available for 2017 and 2018 are also given.....	25
Figure 13. Time series plots of hourly LSOFS-POMGL nowcasts (blue) and LSOFS-FVCOM hindcast of water level (red) vs. bias-corrected observations (black) at NOS/CO-OPS NWLON gauges (1. Duluth, MN, 2. Grand Marais, MN, 3. Ontonagon, MI, 4. Marquette C.G. Station, MI, and 5. Point Iroquois, MI), Lake Superior during 2017. MAE and RMSE (m) at each station are shown individually on each panel. ....	28
Figure 14. Time series plots of hourly LSOFS-FVCOM hindcasts of water level (red) vs. bias-corrected observations (black) at NOS/CO-OPS NWLON gauges (1. Duluth, MN, 2. Grand Marais, MN, 3. Ontonagon, MI, 4. Marquette C.G. Station, MI, and 5. Point Iroquois, MI),	

Lake Superior during 2018. MAE and RMSE (m) at each station are shown individually on each panel. ....30

Figure 15. Time series plots of hourly LSOFS-POMGL nowcasts (blue) and LSOFS-FVCOM hindcasts of water level (red) vs. bias-corrected observations (black) at CHS Water Level gauges (1. Thunder Bay, ONT, 2. Rosspport, ONT, and 3. Michipicoten, ONT), Lake Superior during 2017. MAE and RMSE (m) at each station are shown individually on each panel.....32

Figure 16. Time series plots of hourly LSOFS-FVCOM hindcasts of water level (red) vs. bias-corrected observations (black) at CHS Water Level gauges (1. Thunder Bay, ONT, 2. Rosspport, ONT, and 3. Michipicoten, ONT), Lake Superior during 2018. MAE and RMSE (m) at each station are shown individually on each panel. ....34

Figure 17. Time series plots of hourly LSOFS-POMGL nowcasts (blue) and LSOFS-FVCOM hindcast of water level (red) vs. bias-corrected observations (black) at NOS/CO-OPS NWLON gauge at Duluth, MN Oct. 24 (297) to Oct. 29, 2017 (302) including the high water level event of Oct. 27 (300), 2017. ....36

Figure 18. Time series plots of hourly LSOFS-FVCOM hindcast of water level (red) vs. bias-corrected observations (black) at NOS/CO-OPS NWLON gauge at Duluth, MN for the period from April 12 (103) to April 17 (107) 2018 including the high-water level event of April 12 (103) to April 17 (107) 2018 including the high-water level event of April 13-15, 2018. ....37

Figure 19. Time series plots of hourly LSOFS-FVCOM hindcast of water level (red) vs. bias-corrected observations (black) at NOS/CO-OPS NWLON gauge at Duluth, MN Oct. from Oct. 9 (282) to Oct. 12 (285), 2018 including the high-water level event of Oct. 10 – 11, 2018. ....38

Figure 20. Time series plots of hourly LSOFS-POMGL nowcasts (blue) and LSOFS-FVCOM hindcast of water level (red) vs. bias-corrected observations (black) at NOS/CO-OPS NWLON gauge at Duluth, MN from January 10 to 14, 2017 including low water level events of January 11 and 13, 2017.....44

Figure 21. Time series plots of hourly LSOFS-FVCOM hindcast of water level (red) vs. bias-corrected observations (black) at NOS/CO-OPS NWLON gauge at Duluth, MN for the period from Oct. 3 (276) to Oct. 7 (280) 2018 including the low water level event of Oct. 4 (277), 2018.....45

Figure 22. Time series plots of hourly LSOFS-POMGL nowcasts (blue) and LSOFS-FVCOM hindcasts of surface water temperature (red) vs. observations (black) at NDBC and buoys (1. 45001, Mid. Superior, MI, 2. 45006, W. Superior, MI, and 3. 45136, and Slate Island, ON during 2017. MAE and RMSE (°C) at each station are shown individually on each panel. .51

Figure 23. Time series plots of hourly LSOFS-FVCOM hindcasts of surface water temperature (red) vs. observations (black) at NDBC and ECCC buoy (1. 45001, Mid. Superior, MI, 2. 45004, E. Superior, MI, 3. 45006, W. Superior, MI, and 4. 45136, Slate Island, ON, during 2018. MAE and RMSE (°C) at each station are shown individually on each panel.....53

Figure 24. Time series plots of hourly LSOFS-FVCOM hindcasts of surface water temperature (red) vs. observations (black) at GLOS nearshore buoys (1. 45023, North Entry Buoy, MI, 2. 45025 South Entry Buoy, MI, 3. 45027, McQuade Harbor Nearshore, MN, 4. 45028, Western Lake Superior, MN, 5. 45171, Granite Island Buoy, MI, and 6. 45173, Munising Buoy, MI) during 2017. MAE and RMSE (°C) at each station are shown individually on each panel. .... 55

Figure 25. Time series plots of hourly LSOFS-FVCOM hindcasts of surface water temperature (red) vs. observations (black) at GLOS nearshore buoys (1. 45023, North Entry Buoy, MI, 2. 45027, McQuade Harbor Nearshore, MN, 3. 45028, Western Lake Superior, MN, and 4. 45173, Munising Buoy, MI) during 2018. MAE and RMSE (°C) at each station are shown individually on each panel. .... 57

Figure 26. Time series plots of 2017 hourly LSOFS-FVCOM hindcasts of sub-surface water temperature (red) at nine depths vs. observations (black) at the GLOS buoy 45025, South Entry Buoy. .... 60

Figure 27. Time series plots of 2017 hourly LSOFS-FVCOM hindcasts of sub-surface water temperature (red) at eight depths vs. observations (black) at GLOS buoy 45028, Western Lake Superior. .... 62

Figure 28. Time series plots of 2018 hourly LSOFS-FVCOM hindcasts of sub-surface water temperature (red) at eight depths vs. observations (black) at GLOS buoy 45028, Western Lake Superior. .... 63

Figure 29. Time series plots of 2017 (left) and 2018 (right) hourly LSOFS-FVCOM hindcasts of water currents at top obs-layer (-2.0 m in 2017, and -3.0 m in 2018) (red) vs. observations (black) at the GLOS North Entry Buoy 45023. The upper plots are current directions in degrees and the lower plots are current speeds in m/s. The MAE and RMSE values on the plots are for those hindcasts where both the hindcasts and observations had speeds greater than 0.26 m/s. .... 64

Figure 30. Time series plots of 2017 (left) and 2018 (right) hourly LSOFS-FVCOM hindcasts of water currents at -4.0 m (red) vs. observations (black) at the GLOS North Entry Buoy 45023. The upper plots are current directions in degrees and the lower plots are current speeds in m/s. The MAE and RMSE values on the plots are for those hindcasts where both the hindcasts and observations had speeds greater than 0.26 m/s. .... 65

## LIST OF TABLES

Table 1. Description of NOS skill assessment statistics (Modified from Hess et al., 2003) along with NOS Acceptance Criterion (targets) used to evaluate LSOFS hindcasts. ....	16
Table 2. Information on NOAA/NOS/CO-OPS NWLON and CHS stations whose water level observations were used to evaluate the LSOFS hindcasts. N/A indicates that an official NWS station ID has not been assigned to the station yet or not available since it is a Canadian station.....	18
Table 3. Information about NWS/NDBC and ECCC open lake fixed buoys whose surface water temperature observations were used to evaluate the LSOFS hindcasts at open lake locations. ....	23
Table 4. Information on GLOS buoys whose surface water temperature observations were used to evaluate the LSOFS surface water temperature hindcasts along the shore. ....	23
Table 5. Information about buoys whose subsurface water temperature observations were used to evaluate the LSOFS water temperature hindcasts. ....	24
Table 6. Information about GLOS buoy whose water currents observations were used to evaluate the LSOFS water currents hindcasts. ....	26
Table 7. Summary of skill assessment statistics evaluating the ability of the LSOFS-FVCOM hindcasts and LSOFS-POMGL nowcasts to predict hourly water levels at NOS NWLON gauges in Lake Superior during 2017. Gray shading, if present, indicates that it did not meet the NOS acceptance criteria.....	29
Table 8. Summary of skill assessment statistics evaluating the ability of the LSOFS-FVCOM hindcasts to predict hourly water levels at NOS NWLON gauges in Lake Superior during 2018. Gray shading, if present, indicates that it did not meet the NOS acceptance criteria..	31
Table 9. Summary of skill assessment statistics of LSOFS-FVCOM hindcasts and LSOFS-POMGL nowcasts of hourly water levels at CHS gauges in Lake Superior during 2017. Gray shading, if present, indicates that it did not meet the NOS acceptance criteria.....	33
Table 10. Summary of skill assessment statistics of LSOFS-FVCOM hindcasts of hourly water levels at CHS gauges in Lake Superior during 2018. Gray shading, if present, indicates that it did not meet the NOS acceptance criteria. ....	35
Table 11. Summary of skill assessment statistics evaluating the ability of the LSOFS-FVCOM hindcasts and LSOFS-POMGL nowcasts to predict extreme high water level events at NOS NWLON gauges during 2017. Gray shading, if present, indicates that it did not meet the NOS acceptance criteria. ....	40
Table 12. Summary of skill assessment statistics evaluating the ability of the LSOFS-FVCOM hindcasts to predict extreme high water level events at NOS NWLON stations in Lake Superior during 2018. Gray shading, if present, indicates that it did not meet the NOS acceptance criteria. ....	41

Table 13. Summary of skill assessment statistics evaluating the ability of LSOFS-FVCOM hindcasts to predict extreme high water level events at CHS gauges in Lake Superior during 2017. Gray shading, if present, indicates that it did not meet the NOS acceptance criteria..42

Table 14. Summary of skill assessment statistics evaluating the ability of LSOFS-FVCOM hindcasts to predict extreme high water level events at CHS stations in Lake Superior during 2018. Gray shading, if present, indicates that it did not meet the NOS acceptance criteria..43

Table 15. Summary of skill assessment statistics evaluating the ability of the LSOFS-FVCOM hindcasts and LSOFS-POMGL nowcasts to predict extreme low water level events at NOS NWLON gauges in Lake Superior during 2017. Gray shading, if present, indicates that it did not meet the NOS acceptance criteria.....46

Table 16. Summary of skill assessment statistics evaluating the ability of the LSOFS-FVCOM hindcasts to predict extreme low water level events at NOS NWLON stations in Lake Superior during 2018. Gray shading, if present, indicates that it did not meet the NOS acceptance criteria. ....47

Table 17. Summary of skill assessment statistics evaluating the ability of LSOFS-FVCOM hindcasts and LSOFS-POMGL nowcasts to predict extreme low water level events at CHS gauges in Lake Superior during 2017. Gray shading, if present, indicates that it did not meet the NOS acceptance criteria.....49

Table 18. Summary of skill assessment statistics evaluating the ability of LSOFS-FVCOM hindcasts to predict extreme low water level events at CHS gauges in Lake Superior during 2018. Gray shading, if present, indicates that it did not meet the NOS acceptance criteria..50

Table 19. Summary of skill assessment statistics of the hourly LSOFS-FVCOM hindcasts and LSOFS-POMGL nowcasts of surface water temperature at NDBC and ECCC fixed buoys in Lake Superior during 2017. Gray shading, if present, indicates that it did not meet the NOS acceptance criteria. ....52

Table 20. Summary of skill assessment statistics of the hourly LSOFS-FVCOM hindcasts of surface water temperatures at open lake NDBC and ECCC fixed buoys in Lake Superior during 2018. Gray shading, if present, indicates that it did not meet the NOS acceptance criteria. ....54

Table 21. Summary of skill assessment statistics of the hourly LSOFS-FVCOM hindcasts of surface water temperatures at GLOS stations and the fixed buoys in Lake Superior during 2017. Gray shading, if present, indicates that it did not meet the NOS acceptance criteria..56

Table 22. Summary of skill assessment statistics of the hourly LSOFS-FVCOM hindcasts of surface water temperatures at GLOFS stations and the fixed buoys in Lake Superior during 2018. Gray shading, if present, indicates that it did not meet the NOS acceptance criteria..58

Table 23. Summary of skill assessment statistics of the hourly LSOFS-FVCOM hindcasts of sub-surface water temperatures at GLOS buoys 45025 for 2017 and 45028 for 2017 and 2018. ....61

## LIST OF ACRONYMS

AGL	Above Ground Level
ASOS	Automated Surface Observing System
AWOS	Automated Weather Observing System
CHS	Canadian Hydrographic Service
CMMB	Coastal Marine Modeling Branch
C-MAN	Coastal-Marine Automated Network
COARE	The Center for Oceanic Awareness, Research, and Education
CO-OPS	Center for Operational Oceanographic Products and Services
CSDL	Coast Survey Development Laboratory
ECCC	Environment and Climate Change Canada
FVCOM	Finite Volume Community Ocean Model
GLCFS	Great Lakes Coastal Forecast System
GLERL	Great Lakes Environmental Research Laboratory
GLOFS	Great Lakes Operational Forecast System
GLOS	Great Lakes Observing System
GLSEA	Great Lakes Surface Environmental Analysis
GRIB2	GRIdded Binary (Version 2)
HRRR	High Resolution Rapid Refresh numerical weather prediction system
HPSS	High Performance Storage System
LBC	Lateral boundary conditions
LEOFS	Lake Erie Operational Forecast System
LHOFS	Lake Huron Operational Forecast System
LMOFS	Lake Michigan Operational Forecast System
LMHOFS	Lake Michigan-Huron Operational Forecast System
NAM	North America Mesoscale Model
NCEP	National Centers for Environmental Prediction
NCO	NCEP Central Operations
NDBC	National Data Buoy Center
NDFD	National Digital Forecast Database
NGDC	National Geophysical Data Center
NOAA	National Oceanic and Atmospheric Administration
NOS	National Ocean Service
NWLON	National Water Level Observation Network
NWS	National Weather Service
OBC	Open boundary conditions
OCS	Office of Coast Survey
OSU	The Ohio State University
POMGL	Princeton Ocean Model – Great Lakes version
UMASS	University of Massachusetts
USGS	United States Geological Survey

WCOSS  
WFO  
WPC

Weather and Climate Operational Supercomputer System  
Weather Forecast Office  
Weather Prediction Center

## EXECUTIVE SUMMARY

NOS Lake Superior Operational Forecast System (LSOFS) is a 3-D lake numerical forecast modeling system which uses near real-time atmospheric analyses, river observations and numerical weather prediction model forecast guidance to generate hourly nowcasts and short-range forecast guidance of 3-D water temperatures and currents and two-dimensional water levels for Lake Superior out to 60 hours. The present operational LSOFS, uses the Great Lakes version of the Princeton Ocean Model (POMGL) as its core numerical oceanographic forecast model with a horizontal resolution of 10 km (6.2 mi) and 21 vertical sigma levels.

A new version of LSOFS has been developed using the Finite Volume Community Ocean Model (FVCOM) with a horizontal resolution ranging from approximately 200 m (0.12 mi) near the shore to about 2.5 km (1.6 mi) offshore and with 21 vertical sigma levels. The upgrade of LSOFS is a collaborative project among NOAA's Great Lakes Environmental Research Laboratory (GLERL), the National Ocean Service's (NOS) Coast Survey Development Laboratory (CSDL), the Center for Operational Oceanographic Products and Services (CO-OPS), and the FVCOM Development Team at the University of Massachusetts-Dartmouth. The forecast systems for Lakes Erie, Huron, and Michigan have already been upgraded to FVCOM.

The accuracy of predictions of the upgraded LSOFS are evaluated by comparisons to observations for two NOS skill assessment scenarios: 1) hindcasts and 2) the semi-operational nowcast and forecast guidance. This report describes the results of the hindcast skill assessment. A similar skill report of the semi-operational nowcasts and forecast guidance is being prepared by NOS/CO-OPS.

The hindcast simulations were conducted by GLERL for year 2017 and year 2018. FVCOM Version 4.3.1 and the COARE Version 2.6 bulk flux algorithm were used for the LSOFS hindcast runs. CICE was turned on and five categories of ice thickness were defined: 5, 25, 65, 125, and 205 cm along with a sea-ice floe diameter of 300 m. The lateral boundary conditions for the hindcasts, especially the water level lateral boundary conditions (LBCs) were significantly more complicated than the present POMGL-based LSOFS. The over-lake precipitation, over-lake evaporation and inflow from tributaries, and inflow and outflow of connecting channels are all taken into account in order to simulate lake levels. First, the inflows and outflows were estimated through near-real-time discharge observations from four USGS river gauges and four ECCC river gauges in Ontonagon River, Bad River, St. Louis River, St. Mary's River, Kaministiquia River, Black Sturgeon River, Nipigon River, and Pic & Black Rivers and specified in the FVCOM river discharge file as river forcing. Second, the observed water level change over the previous five days at three NOS CO-OPS gauges and three Canadian Hydrographic Service (CHS) gauges were averaged and used to calculate the unaccounted inflow/outflow due to a combination of inflow from additional tributaries, runoff, and over-lake precipitation and evaporation. This term is then added to the model using FVCOM's formulation for mass addition/subtraction via the precipitation/evaporation forcing file.

The temperature of waters flowing into Lake Superior were specified at seven locations (Fig. 4). The temperatures of water flowing into the northern Lake Superior from the Kaministiquia River, Black Sturgeon River, Nipigon River, and Pic & Black Rivers were specified with hourly water temperature observations from the ECCC gauges located in Ontario in the Kaministiquia River, Black Sturgeon River, Nipigon River, and Pic River, respectively. The temperature of water entering the St. Louis

River, Bad River, and Ontonagon River were specified with hourly water temperatures from USGS gauges on these three rivers.

Surface meteorological forcing for the LSOFS hindcasts were provided by 2-hr (HRRR V2) or 1-hr (HRRR V3) forecast guidance from the hourly forecast cycles of NOAA's High-Resolution Rapid Refresh (HRRR) analysis and forecast modeling system. Output from HRRR Version 2 was used for forcing the hindcasts from Jan. 1, 2017 to July 11, 2018 and HRRR Version 3 was used for July 12, 2018 to Dec. 31, 2018. The specific HRRR meteorological variables used to force LSOFS-FVCOM (COARE) were the following: surface air temperature (2 m Above Ground Level (AGL)), surface relative humidity (2 m AGL), surface wind velocity (10 m AGL), mean sea level pressure, downward short-wave radiation, and downward long-wave radiation. HRRR has a horizontal resolution of 3 km (1.86 miles).

The 2017 and 2018 hindcasts of water levels, surface and subsurface water temperatures, and currents were evaluated by comparisons to observations from NWS, NOS, ECCC, and GLOS platforms (The hindcasts of ice concentration and thickness were not evaluated but will be done in a separate report). The hindcasts demonstrated good skill for simulating hourly water levels during both years. The RMSE ranged from approximately 3 cm to 6 cm at locations at U.S. gauges and 2.7 cm to 4 cm at the Canadian gauges. The NOS acceptance criteria was met at all U.S. and Canadian gauges. In comparison to nowcasts at U.S. gauges from the present POMGL-based LSOFS during 2017, the average RMSE for hindcasts was 4.2 cm while the average for the nowcasts was 5.6 cm. At Canadian gauges, the average RMSE for hindcasts was 3.3 cm and 5.0 cm for nowcasts. Thus overall, the hindcasts did better at predicting water levels than the nowcasts. However, it is not known if this is due to FVCOM, or the meteorological forcing (i.e. interpolation of in-situ surface weather observations for nowcasts vs. HRRR predictions for hindcasts). The hindcasts did well at predicting the amplitudes of extreme high and low water level events with the acceptance criteria being met at the majority of gauges. However, the CF criteria for timing was not met at several of the U.S. and Canadian gauges.

The hindcasts did not do as well for simulating hourly surface water temperatures during these two years, especially at open lake buoys. The average RMSE for U.S. and Canadian open lake buoys for 2017 was 3.8 °C and 3.6 °C for 2018. The average for nearshore buoys was 2.6 °C for 2017 and 2.4 °C for 2018. The hindcasts did not meet all acceptance criteria at the three to four open lake buoys. The hindcasts also did not meet all the acceptance criteria at two of the nearshore buoys but came close to meeting the criteria. In addition, the hindcasts for the open lake buoys overestimated the rate and amplitude of the spring warmup more than the nearshore locations. The nowcasts exhibited the same issue. The spring warmup issue has been an issue since LSOFS first became operational at NOS.

Observations from two nearshore thermistor chains in western part of Lake Superior were available in 2017 and from one in 2018 to evaluate the water temperature hindcasts at depths ranging from 3 m to 32 m. Thus, a thorough lake-wide comparison could not be made. The average RMSE for hindcasts across all depths at the two sites was 2.6 °C.

Hindcasts at two depths (2 m and 4 m – where the currents are the strongest) were compared to observations at the North Entry Buoy near Keweenaw Waterway. The MAEs for speed ranged from -1.6 cm/s to -6.3 cm/s and RMSEs ranged from 7.3 cm/s to 10.7 cm/s.

The new version of LSOFS is expected to be implemented operational in late FY22 to generate forecast guidance including ice concentration and thickness out to 120 hours.

## 1. INTRODUCTION

NOS' Great Lakes Operational Forecast System (GLOFS) provides hourly nowcasts and short-range forecast guidance of two-dimensional water levels and three-dimensional currents and water temperatures. GLOFS has been operational at NOS for Lakes Erie and Michigan since September 30, 2005 and for Lakes Ontario, Huron, and Superior since March 30, 2006. GLOFS predictions are used by commercial and recreational mariners, NWS weather and marine weather forecasters, and by U.S Coast Guard Search and Rescue Operations.

The original GLOFS used the Great Lakes version of the Princeton Ocean Model (POMGL) (Blumberg and Mellor, 1987) with separate computational (Rectangular) grids for each lake. The horizontal grid resolution used for Erie, Michigan, Ontario, and Huron was 5 km (3.1 mi) and was 10 km (6.2 mi) for Lake Superior. The number of vertical sigma levels was 21 for each of the four lakes. GLOFS had four daily nowcast and forecast cycles, which generate forecasts out to 60 hours. The nowcast cycles were forced by surface meteorological analyses of near-real-time meteorological observations from overwater and adjusted overland observing platforms, which are used to provide heat and radiation fluxes and wind stress to POMGL. The forecast cycles were forced by gridded surface wind and air temperature forecasts (2.5 km resolution) from the NWS National Digital Forecast Database. There are no heat or radiation fluxes input during the forecast cycle, only wind forcing. The only significant changes to GLOFS since 2005/2006 were the following: 1) switched from NAM to NDFD surface wind forecasts to force the forecast cycles, 2) forecast horizon increased from 48 to 60 hours, 3) reduced the frequency of nowcast cycles from hourly to every six hours, and 4) refactored code to minimize GLOFS nowcast cycle failures due to missing surface weather observations and/or missing GLSEA lake-wide average water temperatures.

Starting in 2013, NOS and NOAA's Great Lakes Environmental Research Laboratory (GLERL) began a collaborative project to develop a new version of GLOFS to provide improved lake predictions and to extend the forecast horizon out to 120 hours. The Finite Volume Community Ocean Model (FVCOM) was selected as the core numerical ocean circulation or hydrodynamic forecast model for the new version due to its unstructured grid design that would allow for higher horizontal resolution along the shore and incorporation of predicted heat and radiation fluxes during the forecast cycles. The Lake Erie Operational Forecast System (LEOFS) was migrated to FVCOM and became operational in May 2016 on NOAA Weather and Climate Operational Supercomputer System (WCOSS) with the resolution varies from approximately 100 m (0.1 mi) near the shore to about 2.5 km (1.6 mi) offshore. The separate Lake Huron Operational Forecast System (LHOFS) and the Lake Michigan Operational Forecast System were replaced by the FVCOM-based Lake Michigan and Huron Operational Forecast System (LMHOFS) with 200 m (0.2 mi) near the shore to about 2.5 km (1.6 mi) offshore and with 21 vertical levels. LMHOFS became operational on WCOSS in July 2019. The remaining GLOFS lake domains to be migrated to FVCOM are the Lake Superior Operational Forecast System (LSOFS) and Lake Ontario Operational Forecast System (LOOFS).

This report documents the development and testing of the upgraded forecast modeling system for Lake Superior (LSOFS) using FVCOM as well as the results of a skill assessment of hindcasts for water level, water currents, and surface and subsurface water temperature during 2017 and 2018. The skill assessment of the semi-operational nowcasts and forecast guidance running on

WCOSS will be conducted by CO-OPS and its results will be published in a separate technical report. A brief overview of the physical limnology of Lake Superior is given first.

## 2. LAKE SUPERIOR

Lake Superior is the coldest of the Great Lakes of North America and contains 10 percent of the world's surface freshwater. The lake's name comes from the French word *lac supérieur*, which means "upper lake". Lake Superior is about 563 km (350 mi) in length and 257 km (160 mi) in width, with a surface area of 82,170 sq. km (31,700 sq mi), and a shoreline including islands of 4,387 km (2,726 mi). The average elevation of Lake Superior is about 183 m (602 ft) above sea level. The deepest point is 400 m (1,300 ft) about 64 km (40 mi) north of Munising, Michigan. Over 300 streams and rivers empty into the lake. The largest tributaries include the Nipigon River in Ontario, Canada and the St. Louis River in Minnesota. Lake Superior drains into Lake Huron via the St. Mary's River.

Lake Superior can be considered a mini-freshwater ocean, but with non-dominant tides. However, the lake does experience seiches, and periodically the water levels rise and fall. Small seiches occur frequently, but occasionally stronger ones occur that can cause problems in harbors and shore areas. Seiches in Lake Superior take approximately eight hours to cross the lake and come back, sometimes changing nearshore water levels by more than 91 cm (3 ft) (Mortimer et al., 1976).

In addition, Lake Superior, like the other Great Lakes, experiences meteotsunamis, meteorologically generated water waves that have temporal and spatial characteristics similar to seismic tsunamis. According to Bechle et al. (2016), meteotsunami waves, which typically have periods from two minutes to two hours, are caused mainly by atmospheric pressure and wind perturbations associated with frontal passages, cyclones, atmospheric gravity waves, and mesoscale convective systems. In 2014, Lake Superior meteotsunami overtopped the Soo Locks, interrupted shipping operations, and prompted homes to be evacuated in Sault Ste. Marie, ON, Canada (Bechle et al., 2016).

Each year, Lake Superior undergoes twice-per-year formation and destruction of thermal stratification (Boyce et al., 1989). Positive stratification occurs in the summer when a warm layer of water develops over colder water. During the fall, the buoyant surface waters cool and the difference in density between layers becomes increasingly small. When the density is very similar, strong winds can mix the entire lake with the sinking of heavy water and mixing by wind results in the exchange of surface and bottom waters. This is referred to as fall turnover. During the icy winter, negative stratification occurs with very cold water (0 – 3.93 °C) on top of cold water. The winter stratification breaks down during June when the surface water temperature warms to 3.94 °C (39.1 °F), the temperature at which freshwater reaches its maximum density (<http://www.waterencyclopedia.com/Hy-La/Lakes-Physical-Processes.html>). Spring turnover occurs with the water again being able to freely circulate through the water column. The average annual water temperature of Lake Superior is 4 °C (40 °F).

During most winters, the lake is 40 to 95% covered with ice. Occasionally the lake freezes over completely but only for several hours. The last complete freezing of Lake Superior occurred in 1979. The lake almost frozen over in 2014 with a 91% ice cover. During the 2019-2020, ice coverage only reached about 13.9% in mid-February (USGS, 2020). Freezing of the lakes can affect hydropower generation, commercial shipping, and fishing. Lake water temperatures and

ice coverage affect the timing, intensity, and locations of lake-effect snowfalls. The area prone to lake-effect snowfalls in the vicinity of Lake Superior extends from Marathon, ON southeast to Sault Ste. Marie and then along the south coast of the lake from Sault Ste. Marie to the Wisconsin-Michigan border.

Lake Superior formed about 10,000 years ago, which dates back to the last glacial retreat. The basin continues to spring back following the retreat of the glaciers. This phenomenon, known as Post-Glacial Rebound (PGR), is the reason why the Great Lakes vertical control datum requires updating approximately every 30 – 35 years (Gill et al. 2014). This topic will be further discussed in Section 6.1.1 in reference to evaluating water level hindcasts.

### 3. MODEL SYSTEM AND SETUP FOR HINDCASTS

This section provides descriptions of the three-dimensional hydrodynamic (ocean circulation) numerical forecast model FVCOM, the grid configuration, and how the lateral boundary, surface boundary, and initial conditions were specified for the LSOFS hindcast runs. The configurations for LSOFS, when it is run operationally on WCOSS, will be different in terms of surface meteorological forcing and lateral boundary conditions for water temperatures and water levels due to operational decisions by NOS/CO-OPS personnel.

#### 3.1. Description of Model

FVCOM is a prognostic, unstructured-grid, finite-volume, free-surface, three-dimensional primitive equation coastal ocean circulation prediction model developed by the researchers at the UMASS-Dartmouth and Woods Hole Oceanographic Institution (Chen and Beardsley, 2003; Chen et al., 2013). The model consists of momentum, continuity, water temperature, salinity, and density equations and is closed physically and mathematically using turbulence closure sub-models. The horizontal grid is comprised of unstructured triangular cells with a generalized terrain-following vertical coordinate system. Several different turbulent closure schemes (TCS) are available in FVCOM. For LSOFS, the Mellor Yamada 2.5 TCS was used for the vertical and the Smagorinsky TCS was utilized for the horizontal. FVCOM is solved numerically by a second-order-accurate discrete flux calculation in the integral form of the governing equations over an unstructured triangular grid. The three-dimensional model solution is determined using a mode-splitting technique by which a two-dimensional external mode is updated at frequent intervals while the more slowly evolving internal mode is obtained less frequently. Thus, the free surface, defined as the external mode, is integrated by solving vertically averaged equations with a smaller time step and the 3-D momentum and tracer equations, defined as the internal mode, are integrated with a larger time step. Following every internal time step, an adjustment is made to maintain numerical consistency between the modes (Chen et al., 2013).

An unstructured grid version of the Los Alamos Sea Ice model (UG-CICE; Hunke et al., 2010; Fujisaki-Manone, 2020) has been included and coupled within FVCOM (Anderson et al., 2018). The CICE model includes components for ice thermodynamics and ice dynamics, using elastic-viscous-plastic rheology (deformation and flow matter) for internal stress, and produces two-dimensional fields of ice concentration, thickness, and velocity. A multi-category ice thickness distribution (ITD) model is employed in CICE to resolve mechanical deformation as well as growth and decay. The CICE allows the specification of several categories of ice thickness. The ice surface albedo depends on surface temperature and thickness of ice, as well as the visible and infrared spectral bands of the incoming solar radiation. At ice-covered cells, the net momentum transfer is calculated as a weighted average of the air-water and ice-water stresses by areal fraction of ice. The air-ice drag coefficient  $CD_{ai}$  is a function of wind speed  $U$ , given as  $CD_{ai} = (1.43 + 0.052U) \times 10^{-3}$  and the ice-water drag coefficient is  $5.5 \times 10^{-3}$  (Anderson et al., 2018). Similarly, the net heat transfer is calculated as a weighted average of the air-water and ice-water heat fluxes (Anderson et al., 2018). The ice-water heat fluxes are calculated based on the bulk

transfer formula (BTF). BTF are linear equations relating surface latent and sensible heat fluxes to corresponding humidity or temperature gradients multiplied by empirical wind speed. An average sea-ice floe, a cohesive sheet of ice floating in water, size diameter can be set depending on water body.

The FVCOM-CICE has two options for heat flux calculations. The first option is the SOLAR flux algorithm. The SOLAR algorithm was developed at the NOAA Great Lakes Environmental Research Laboratory (GLERL) for application to the Great Lakes with a few modifications by researchers at The Ohio State University. SOLAR solves standard bulk flux expressions for latent and sensible heat based on Monin-Obukhov Similarity Theory (Foken, 2006; Kantha and Clayson, 2004). SOLAR served as the flux algorithm for the POMGL-based implementation of GLOFS. The second option is the Coupled Ocean Atmosphere Response Experiment (COARE) Bulk Air Sea Flux algorithm (Fairall et al., 2003, BTFs are linear equations relating surface latent and sensible heat fluxes to corresponding humidity and temperature gradient multiplied by empirical wind speed dependent transfer coefficients). A freshwater parameterization of COARE is included within FVCOM starting with Version 4.0. It uses Monin-Obukhov Similarity Theory with minor differences in stability functions relative to SOLAR (Gronewold et al., 2019). The FVCOM-based LEOFS uses SOLAR while the FVCOM-based LMHOFS uses the COARE algorithm.

FVCOM has been successfully applied in several coastal ocean regions to simulate oceanographic conditions. FVCOM is used by NOS' Northern Gulf of Mexico Operational Forecast System (Wei et al., 2014; Wei et al., 2015), LEOFS (Kelley et al, 2018), LMHOFS (Kelley et al, 2020, Peng et al., 2019), and the San Francisco Operational Forecast System (Schmalz, 2014).

For LSOFS, FVCOM Version 4.3.1 and the COARE Version 2.6 bulk flux algorithm were used for the LSOFS hindcast runs due to investigation of GLERL personnel (Eric Anderson's personal reference). CICE was turned on and five categories of ice thickness were defined: 5, 25, 65, 125, and 205 cm along with a sea-ice floe (sheet of floating ice) diameter of 300 m.

### **3.2. Grid Configuration**

An unstructured model grid was generated for LSOFS by GLERL using the Surface-Water-Modeling System (SMS) software. The grid size distribution is configured as dependent on the GLERL bathymetry (NOAA/NCEI, 3 arc-second). The model bathymetry was obtained by interpolating the GLERL digital bathymetry onto each unstructured FVCOM model grid node, referenced to the Low Water Datum (LWD) or chart datum for Lake Superior, which is 183.2 m (601.1 ft) above the International Great Lakes Datum (IGLD) of 1985. The model bathymetry is shown in Fig. 1.

High resolution NOAA coastline data were applied to delineate the land boundary. The model grid in the horizontal is composed of 174,000 triangular elements and 90,000 nodes. The resolution varies from approximately 200 m (0.12 mi) near the shore to about 2.5 km (1.6 mi) offshore. The grid is depicted in Fig. 2. The model has 21 uniform sigma levels with distribution

referenced to the Great Lakes low water datum for Lake Superior. The sigma levels are the following: 0.0, -0.05, -0.1, -0.15, -0.2, -0.25, -0.3, -0.35, -0.4, -0.45, -0.5, -0.55, -0.6, -0.65, -0.7, -0.75, -0.8, -0.85, -0.9, -0.95, and -1.0.

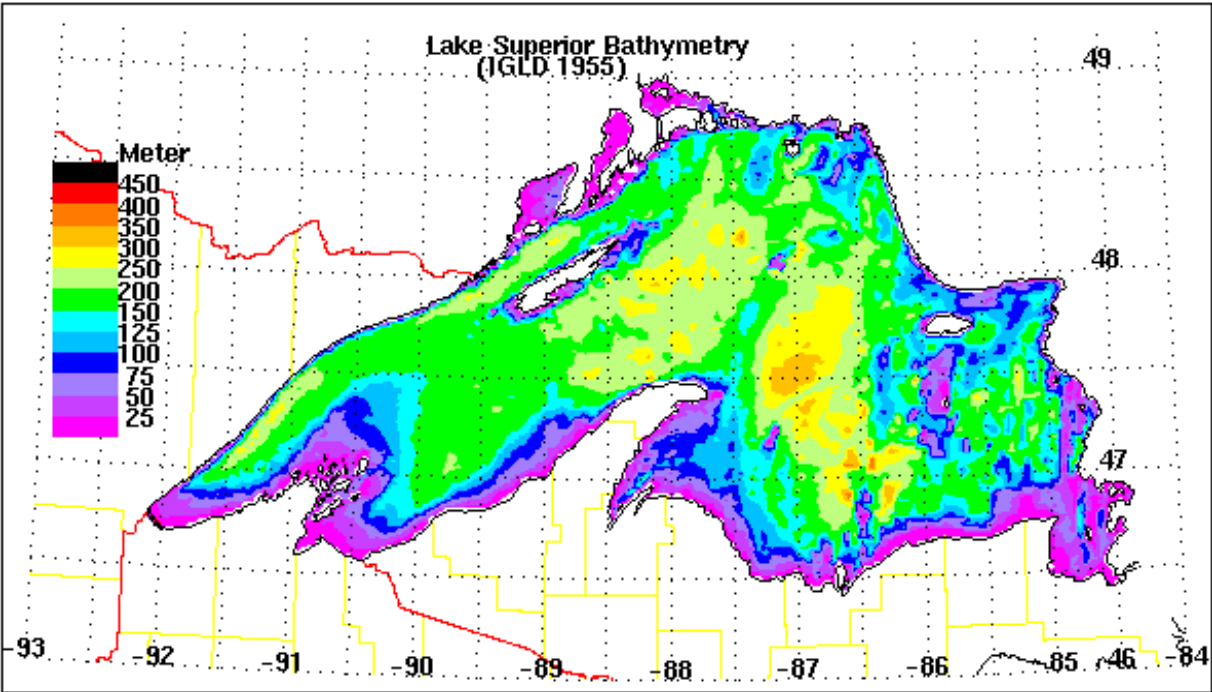


Figure 1. Map of the Lake Superior bathymetry (m) used by LSOFS, referenced to Low Water Datum (LWD) of 183.2 m (601.1 ft). The average depth is 147 m (482 ft) and the maximum depth is 389 m (1276 ft).



Figure 2. Map depicting the FVCOM grid domain for LSOFS. The horizontal resolution ranges from around 200 m (0.12 mi) near the shore to approximately 2.5 km (1.6 mi) offshore with 21 vertical sigma levels.

### 3.3. Lateral Boundary Conditions

The lateral boundary conditions (LBCs) for the hindcasts were prescribed for water temperatures and inflows/outflows. The assignment of water level LBCs was the most complicated. Since over-lake precipitation, over-lake evaporation and inflow from tributaries and inflow and outflow of connecting channels are the same order of magnitude for Lake Superior, all these components must be estimated for LSOFS to track low-frequency changes (e.g., seasonal) in lake levels.

The components were estimated in the following equation

$$dV/dt = Q_{\text{Tributaries}^*} - Q_{\text{St. Marys River}} + Q_{\text{Residual}}$$

where  $dV$  = change in lake volume, and  $Q$  = discharge.

$Q_{\text{St. Marys River}}$  outflow is estimated using near-real-time discharge observations from the USGS gauge, *St. Marys River at Sault Sainte-Marie, MI* (Station ID 04127885). The estimation of  $Q_{\text{Tributaries}^*}$ , the inflow from other tributaries, is determined from near-real-time (and long-term daily climatological when near-real-time data is not available) discharge observations from both U.S. Geological Survey (USGS) and Environment and Climate Change Canada (ECCC) gauges. The three USGS gauges are *St. Louis River at Scanlon, MN* (04024000), *Bad River near Odanah, WI* (04027000), and *Ontonagon River near Rockland, MI* (04040000). The four ECCC gauges are *Black Sturgeon River at Highway No. 17, ON* (02AC002), *Nipigon River below Alexander Generating Station, ON* (02AD012), *Kaministiquia River at Kaministiquia, ON* (02AB006), and

*Pic River near Marathon, ON (02BB003)*. These inflows and outflows were specified in the FVCOM river discharge data file, *casename\_river.nc*.

The unaccounted inflow/outflow due to a combination of inflow from additional tributaries, runoff, and over-lake precipitation and evaporation is represented in the term,  $Q_{\text{Residual}}$ . The  $Q_{\text{Residual}}$  is added to FVCOM using its formulation for mass addition/subtraction via the precipitation/evaporation forcing file, *casename\_pre\_evap.nc*.

The  $dV/dt$  is calculated by multiplying the lake surface area by the average observed water level change over the previous five days at the following six ‘Master’ Water Level Gauges (Figure 3.b): 1) NOS 9099064, 2) NOS 9099018, 3) NOS 9099004, 4) CAN 10750, 5) CAN 10220, 6) CAN 10050. GLERL tested different averaging time periods to find the optimal number of days which minimized lags in tracking lake levels while at the same time minimized high frequency variations that may not accurately represent resting lake levels. As a result of this approach, five days end up being the best balance of these two objectives.

The prescribed inflows and outflows are depicted in Figure 3.

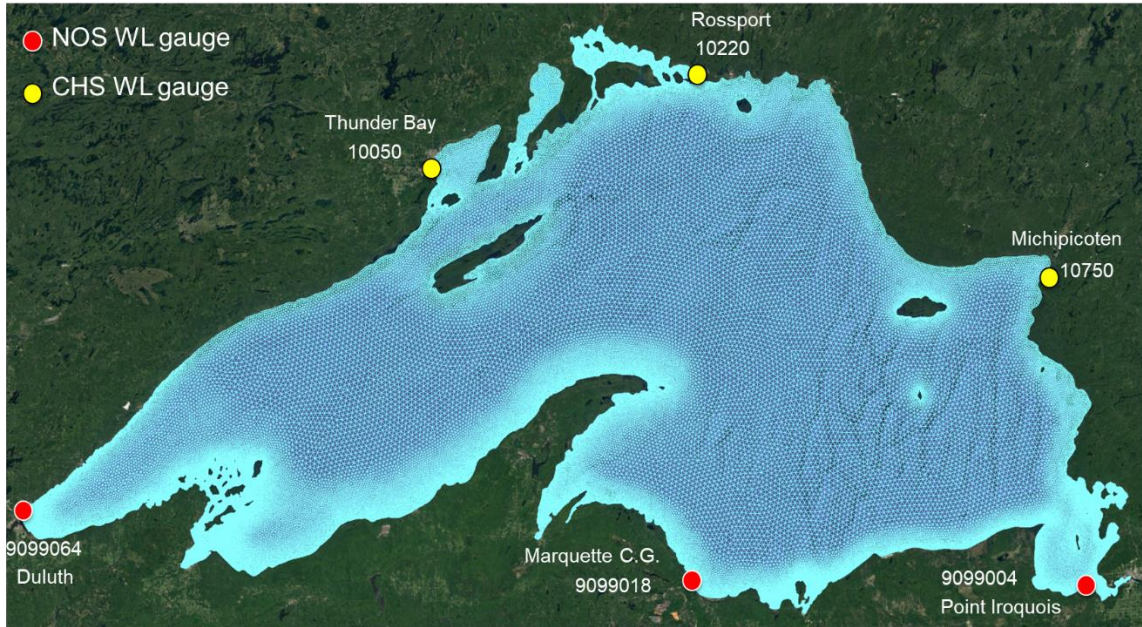
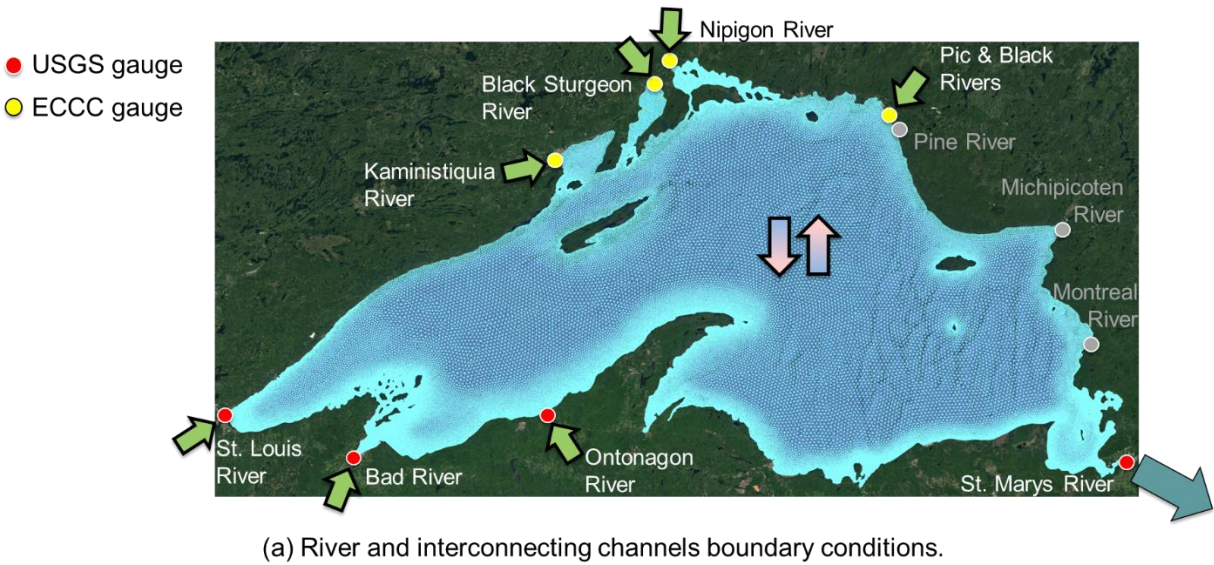


Figure 3. LSOFS lateral boundary conditions.

The temperature of waters flowing into Lake Superior were specified at seven locations (Fig. 4). The temperatures of water flowing into the northern Lake Superior from the Kamimistiquia River, Black Sturgeon River, Nipigon River, and Pic & Black Rivers were specified with hourly water temperature observations from the ECCC gauges individually at *Kaministiquia River at Kaministiquia, ON (02AB006)*, *Black Sturgeon River at Highway No. 17, ON (02AC002)*,

*Nipigon River below Alexander Generating Station, ON (02AD012), and Pic River near Marathon, ON (02BB003), respectively. The temperature of water entering the St. Louis River, Bad River, and Ontonagon River were specified with hourly water temperatures from the USGS gauges at St. Louis River at Scanlon, MN (04024000), Bad River near Odanah, WI (04027000), and Ontonagon River near Rockland, MI (04040000), respectively. The water temperatures for these locations are specified in the *casename\_river.nc* file.*

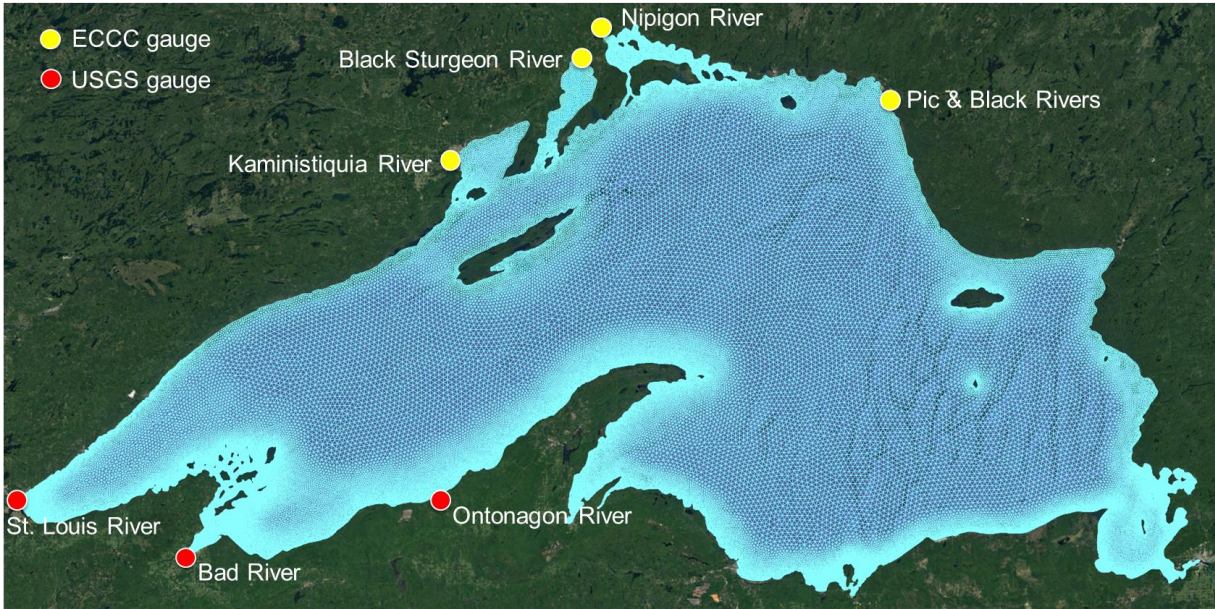


Figure 4. Locations where surface water temperatures are specified on the lateral boundaries of LSOFS.

### 3.4. Surface Boundary Forcing

The surface meteorological forcing for the hindcasts was supplied using very-short range forecast guidance from the hourly forecast cycles of the NOAA High-Resolution Rapid Refresh (HRRR) System, a 3-D numerical weather prediction analysis and forecast modeling system (Benjamin et al., 2016). HRRR provided analyses and forecast guidance out to 18 hours at a horizontal resolution of 3 km (1.86 mi). The HRRR variables used to force FVCOM (SOLAR) are: 1) surface air temperature (2m AGL), 2) surface dew point temperature (2 m AGL), 3) total cloud/sky cover, 4) u- and v-wind components [ $\sim 7.8$  m (HRRR V2) or 10 m AGL (HRRR V3)]. The HRRR variables used to force FVCOM (COARE) are the following: 1) surface air temperature (2m AGL), 2) relative humidity, 3) mean sea level pressure (2 m AGL), 4) u- and v-wind components [ $\sim 7.8$  m (HRRR V2) or 10 m AGL (HRRR V3)], 5) net downward short-wave radiation, and 6) downward long-wave radiation. All variables were obtained from the 2-hr forecast (HRRR V2) or the 1-hr forecast (HRRR V3). The HRRR analyses (0-hr) and the 1-

hr (for V2) forecasts were not used because of artificially sharp gradients, artifacts from the HRRR's assimilation system (Stan Benjamin, personal communication).

Output from HRRR Version 2 was used for forcing the hindcasts from Jan. 1, 2017 to July 11, 2018 and HRRR Version 3 was used for July 12, 2018 to Dec. 31, 2018 (Upgrade to the RAP and HRRR Analysis and Forecast System: Effective July 11, 2018, available at: [https://www.weather.gov/media/notification/pdfs/scn18-58rap\\_hrrr.pdf](https://www.weather.gov/media/notification/pdfs/scn18-58rap_hrrr.pdf)). The HRRR output was obtained from the NOAA High Performance Storage System (HPSS) runtime history archives, the required variables were extracted, and subsetted for the Great Lakes Region by CSDL personnel. The processed HRRR output was then provided to GLERL researchers. The latent and sensible heat fluxes were calculated from several of the meteorological variables using the freshwater version of the COARE Version 2.6 algorithm of FVCOM (HEATING\_CALCULATED\_GL).

### **3.5. Initial Conditions**

LSOFS required initial three-dimensional conditions including surface elevation field and three-dimensional velocity and water temperature fields at the beginning of the hindcasts. The model was initialized one year prior to the start of the hindcast period on January 1, 2017 with surface water temperatures derived from NOAA Advanced Very High-Resolution Radiometer (AVHRR) imagery obtained through the Great Lakes CoastWatch program and prescribed from the NOAA Great Lakes Surface Environmental Analysis (GLSEA). The GLSEA is valid at an approximate depth of 10  $\mu\text{m}$  or  $1 \times 10^{-6}$  m (Songzhi Liu, Personal Communication). Surface to 10m was based on GLSEA analysis. Sub-surface water temperatures below 10 m (32.8 ft) were set to a uniform water temperature of 2 °C (36 °F). The water level was set to the observed lake level on Jan. 1, 2017 and the water currents were set to 0 m/s. The model was continuously forced with observed LBCs and surface meteorological analyses of near-real-time adjusted overland and overwater weather observations. The restart file after the one-year run (spin-up) was used as the initial conditions for the start of the hindcasts. Details on the hindcast period are given in the next section.

#### 4. DESCRIPTION OF HINDCAST PERIODS

Two hindcast model simulations using LSOFS were conducted by GLERL on their Linux cluster in Ann Arbor, MI. Hindcast Period #1 covered from Jan. 1, 2017 to Dec. 31, 2017. Hindcast Period #2 was from Jan. 1, 2018 to Dec. 31, 2018. One of the most notable extra-tropical cyclones occurred in 2017 on Oct. 24<sup>th</sup> and tracked across the central Great Lakes. During the storm, wind gusts of 80 – 123 KPH (50 – 77 MPH) were reported over Lake Superior. The high winds resulted in lakeshore flooding and large waves of 7.6 m to 9.1 m (25 ft to 30 ft) along the shoreline from Big Bay down to Grand Marais (NWS, 2017). Water level observations during Oct. 22-23, 2017 at the NOS gage at Marquette are depicted in Fig. 5.

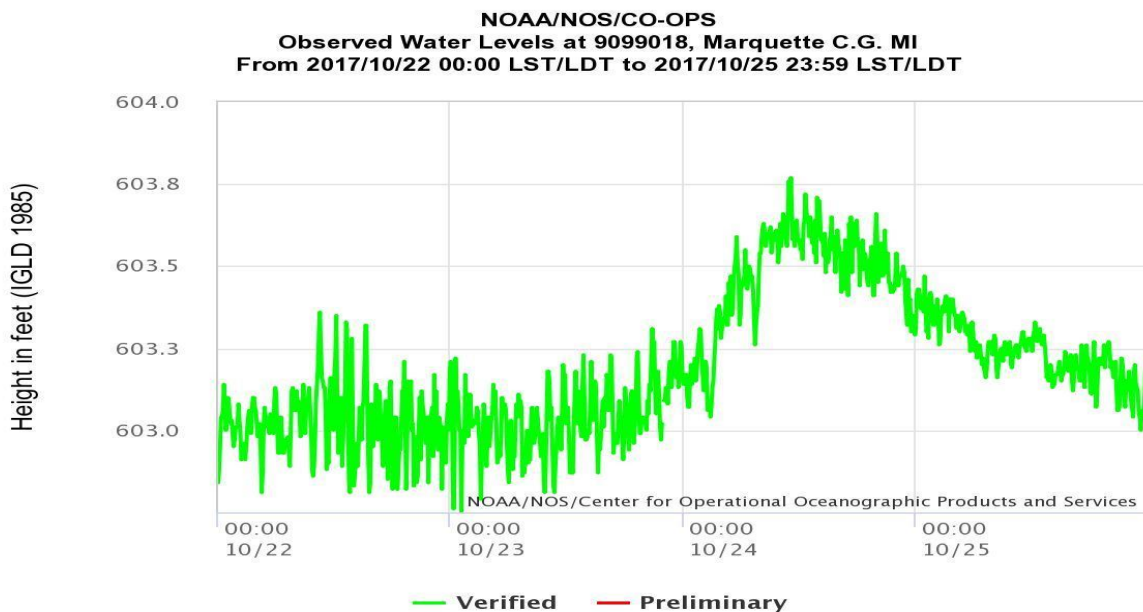


Figure 5. 6-minute water level observations from the NOS/CO-OPS gage at Marquette Coast Guard Station, MI for Oct. 22-25, 2017.

The most notable storm of 2018 was the extra-tropical cyclone of April 13-15<sup>th</sup> which resulted in wind gusts of 80 – 111 KPH (50 – 69 MPH) on Lake Superior and wave heights of at least 4.6 m (15 ft) over the lake and along the South Shore to the Duluth and Superior area (NWS, 2018). According to the NWS, the late season blizzard caused flooding near the Duluth Ship Canal and Duluth Lift Bridge. Water level observations during April 13-15, 2018 at the NOS Duluth gage is given in Fig. 6.

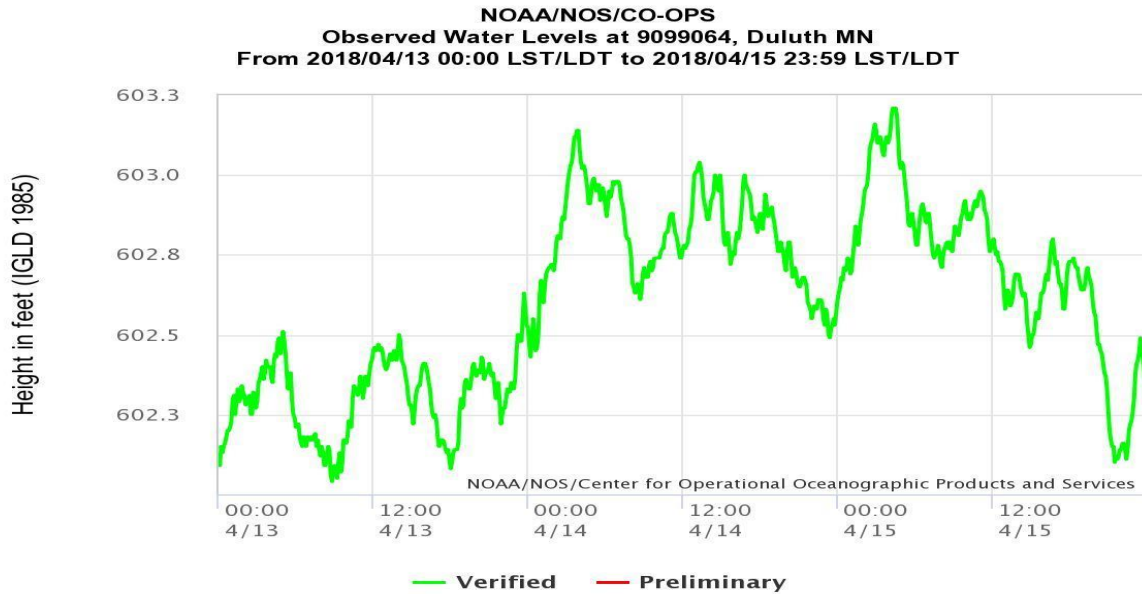


Figure 6. 6-minute water level observations from the NOS/CO-OPS gage at Duluth, MN during April 13-15, 2018.

The daily ice coverage maps for the Great Lakes for the 2016-2017 ([https://www.glerl.noaa.gov/data/pgs/glicd/glicd\\_2017.html](https://www.glerl.noaa.gov/data/pgs/glicd/glicd_2017.html)) indicate that most of the Lake Superior was ice free for most of the winter. However, during the 2017-2018 ice season, Lake Superior had an extensive ice coverage, especially from Feb 1<sup>st</sup> to until March 25<sup>th</sup> and then again from April 9 through 11<sup>th</sup>.

## 5. METHOD OF EVALUATION

Hourly hindcasts of water levels, water currents, and water temperatures for 2017 and 2018 were compared to hourly observations from observing platforms in Lakes Superior. In addition, the LSOFS water level and water temperature hindcasts for 2017 were also compared to nowcasts from the operational POMGL-based LSOFS where available.

The evaluation used the standard NOS suite of skill assessment statistics. These statistics included Mean Error, or more commonly referred to as Mean Algebraic Error (MAE), Root Mean Squared Error (RMSE), Standard Deviation (SD), Central Frequency (CF), Positive Outlier Frequency (POF), Negative Outlier Frequency (NOF), Maximum Duration of Positive Outliers (MDPO), and Maximum Duration of Negative Outliers (MDNO). These statistics are described briefly in Table 1 while more detailed descriptions can be found in Hess et al. (2003). The comparisons were done using the NOS standard skill assessment software (Zhang et al., 2010 and Zhang et al., 2013).

The calculation of the target frequency of skill statistics, CF, POF, NOF, MDPO and MDNO, required the assignment of 1) acceptable magnitude errors for water level and water temperature amplitudes, 2) acceptable timing error for water levels, and 3) maximum allowable time durations for consecutive positive and negative water level outliers. The same acceptable errors and maximum allowable time duration used to evaluate GLOFS, when it was first implemented operationally at NOS, were employed in evaluating these hindcasts (see last column in Table 1). These specific values for the water level and temperature skill assessments will be discussed in later sections.

The standard skill assessment code has a coarse quality assurance function that is applied to all downloaded observational data. It calculates a "quality control range" first; any data that is out of this range will be regarded as unrealistic and will then be deleted. The quality-control-range is calculated in the subroutine *refwl.f*. The code in the subroutine calculates average and standard deviation for the whole data set and uses average  $\pm 5$  times SD as upper and lower boundaries and writes out data that are within this range. This  $\pm 5$  SD quality assessment (QA) check erroneously removed several high amplitude water level events at NOS/CO-OPS in the Great Lakes. This QA check was commented out in order to include all high amplitude water level and water temperature events when assessing the hindcasts' performance skills. However, both the water level and water temperature observational data were plotted and obviously erroneous spikes were manually deleted from the data prior to running the skill assessment program.

Extreme high or low water events were selected from the observed data and hindcasts using the equations  $h_{upper} = \text{mean} + \text{factor} \times \text{SD}$  and  $h_{lower} = \text{mean} - \text{factor} \times \text{SD}$  where the value for factor was set to 2.0 (Zhang et al., 2013).

The resulting values for each statistic were then judged against the NOS Acceptance Criteria (Table 1) for that statistic. These criteria include target frequencies for CF, NOF, and POF and limits on the duration of errors (i.e. maximum length of time of consecutive) for MDPO and MDNO. Any new or upgraded NOS operational oceanographic modeling system is expected to meet or exceed most of the NOS Acceptance Criteria (targets) in order to be implemented operationally.

Table 1. Description of NOS skill assessment statistics (Modified from Hess et al., 2003) along with NOS Acceptance Criterion (targets) used to evaluate LSOFS hindcasts.

Statistic	Units	Description	NOS Acceptance Criterion
Mean Algebraic Error (MAE)	Meters or Hours	The error is defined as the predicted value, p, minus the reference (observed value)	None
SD	Meters or Hours	Standard Deviation	None
RMSE	Meters or Hours	Root Mean Square Error	None
SM	Meters or Hours	Series Mean. The mean value of a series y	None
CF(X)	%	Central Frequency. Fraction (percentage) of errors that lie within the limits $\pm X$ .	$\geq 90\%$
POF(X)	%	Positive Outlier Frequency. Fraction (percentage) of errors that are greater than X.	$POF(2X) \leq 1\%$
NOF(X)	%	Negative Outlier Frequency. Fraction (percentage) of errors that are less than -X.	$NOF(2X) \leq 1\%$
MDPO(X)	Hours	Maximum Duration of Positive Outliers. A positive outlier event is two or more consecutive occurrences of an error greater than X. MDPO is the length of time in hours (based on the number of consecutive occurrences) of the longest positive outlier event.	$MDPO(2X) \leq L$
MDNO(X)	Hours	Maximum Duration of Negative Outliers. A negative outlier event is two or more consecutive occurrences of an error less than -X. MDNO is the length of time in hours (based on the number of consecutive occurrences) of the negative outlier longest event.	$MDNO(2X) \leq L$
NOS Standard Criteria		<p>where X = acceptable error magnitude (cm or minutes)</p> <p>X = +- 15 cm for water level amplitude errors</p> <p>X = +- 1.5 hours (90 minutes) for water level timing errors</p> <p>X = +- 3.0 °C for water temperature amplitude errors</p>	<p>Where</p> <p>L = time limit or max. allowable duration</p> <p>L = 24 hours</p>

## 5.1. Evaluation of Water Level Hindcasts

The evaluation of hourly water levels was based on comparisons of time series from the hindcasts to observations during 2017 and 2018 and also on comparisons to nowcasts from the operational POMGL-based LSOFS during 2017. The comparison of time series from 2017 and 2018 water level hindcasts used the statistics SM, RMSE, SD, NOF, POF, MDPO, and MDNO as described in the previous section. The assessment evaluated the ability of the hindcasts to predict hourly water levels and also extreme high and low water events. The identification of extreme high and low water events during the hindcast periods in the Great Lakes was accomplished using the method described in Chu et al. (2007).

The acceptable magnitude errors for water levels were set at +/- 15 cm (0.5 ft) and the acceptable timing error was set at +/- 1.5 hours. In addition, for the calculation for the MDPO and MDNO statistics, a maximum allowable time duration of consecutive occurrences with an error greater than the acceptable amplitude or timing error was specified as 24 hours.

The water level time series from hourly hindcasts were compared to observed hourly water levels recorded at NOS/CO-OPS NWLON and Canadian Hydrographic Service (CHS) stations along the shores of Lakes Superior (Fig. 5). Information about these stations is given in Table 2. The hourly water level observations from the NOS NWLON gauges were obtained from CO-OPS online archives at <http://tidesandcurrents.noaa.gov>. The hourly water levels from the CHS gauges were obtained from Canada's Dept. of Fisheries and Oceans online archives at <http://www.meds-sdmm.dfo-mpo.gc.ca/isdm-gdsi/twl-mne/inventory-inventaire/list-liste-eng.asp?user=isdm-gdsi&region=CA&tst=1>. All observations were plotted as time series and visually inspected for erroneous data. Any erroneous data was removed prior to conducting the skill assessment.



Figure 7. Locations of NOS and CHS water-level gauges used to evaluate LSOFS water level hindcasts.

Table 2. Information on NOAA/NOS/CO-OPS NWLON and CHS stations whose water level observations were used to evaluate the LSOFS hindcasts. N/A indicates that an official NWS station ID has not been assigned to the station yet or not available since it is a Canadian station.

Station Name	State or Prov.	NOS or CHS Station ID	NWS Station ID	Coordinates	
				Lat. (deg N)	Lon. (deg W)
Point Iroquois	MI	9099004	PTIM4	46.485	84.630
Marquette C.G.	MI	9099018	MCGM4	46.545	87.378
Ontonagon	MI	9099044	OGOM4	46.875	89.323
Duluth	MN	9099064	DULM5	46.775	92.092
Grand Marais	MN	9099090	GDMM5	47.748	90.342
Thunder Bay	ON	C10050	N/A	48.409	89.217
Rosspport	ON	C10220	N/A	48.834	87.520
Michipicoten	ON	C10750	N/A	47.961	84.901

Current crustal movement in the Great Lakes basin is the result of the natural rebound of the Earth's crust following the removal of the weight of the glaciers that covered the region some 10,000 years ago. When the ice began melting, the crust started rebounding. This rebounding results in a slow rate of apparent vertical movement of the land area, and water levels are affected as lake basins tilt by a gradual rising of their northeastern rims (Neff and Nicholas, 2005). In general, the land north of the Great Lakes is rising and the land south of the Great Lakes, never covered by the glaciers, is subsiding. The crustal movement has a significant effect on the vertical datum planes used to reference water levels and also changes the hydraulic flow characteristics of the connecting channels. Due to variations in the thickness of the glaciers, the time they receded, regional geology and other differences such as changes in global sea levels, the Earth's gravity field, induced earthquakes, and changes in the rotational motion etc., the rate of vertical movement at any location varies throughout the region. This phenomenon is called glacial isostatic adjustment (GIA) and is the key reason why the Great Lakes vertical control datum requires updating approximately every thirty years (i.e. water level datum elevations relative to the land must be updated over time) (Heck and Craymer, 2021).

The International Great Lakes Datum (IGLD) is the reference system by which Great Lakes-St. Lawrence River Basin water levels are measured. It consists of benchmarks at various locations on the lakes and St. Lawrence River that roughly coincides with sea level. The new reference zero point of IGLD 1985 is located at Rimouski, Quebec. All water levels are measured in feet or meters above this point. Movements in the earth's crust (isostatic rebound) necessitate updating this datum every 25-30 years (<https://www.in.gov/dnr/water/3659.htm>). Since the latest update for the IGLD was in 1985, the present NOS and CHS Great Lakes water level observations are all referenced to this datum.

A linear drift over time was apparent in the NOS and CHS observations. The magnitude of water level drift differs for each gauge, where Canadian gauges tend to reveal a negative drift and US gauges reveal a positive drift. Overall, the maximum drift in 2019 was up to 10 cm, found at NOS gage 9099064 and CHS gage 10220. This bias needed to be removed before an evaluation could be conducted. To implement the water level de-bias, firstly the historical water level data (1980-2019) from all eight stations was collected; and the monthly lake mean water levels were calculated by averaging all available data on each month. The drifting trend of each station was then calculated by applying linear regression on the difference between its monthly water levels and the Lake-wide-mean. In another words,  $\Delta_{WL} = A \times Date + B$ . Where A and B are coefficients. Having the linear regression coefficients, the bias was able to be removed from observation values according to the linear trend:  $WL_{db} = WL - \Delta_{WL}$ .

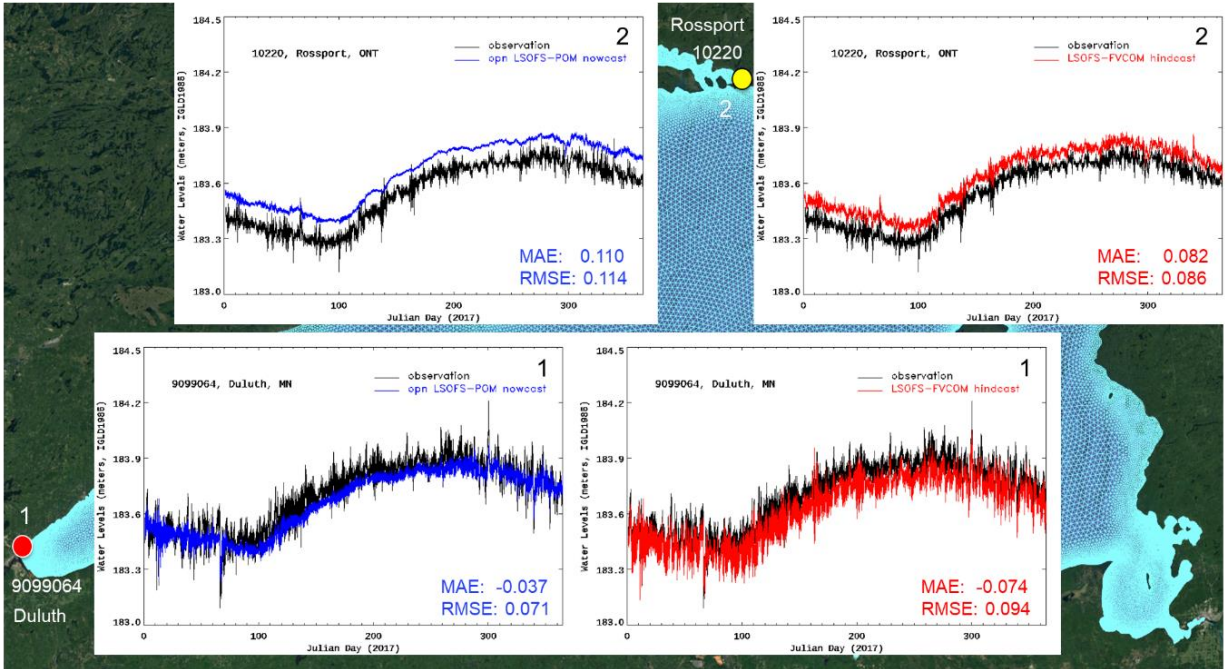


Figure 8. Time series plots of hourly LSOFS-FVCOM hindcasts (red) and operational LSOFS-POMGL nowcasts (blue) of water level vs. original observations (black) at 1) COOPS-NWLON gauge Duluth, MN (9099064) and 2) CHS gauge Rosspart, ON (10220) during 2017. MAE and RMSE (m) at each station are shown individually on each panel.

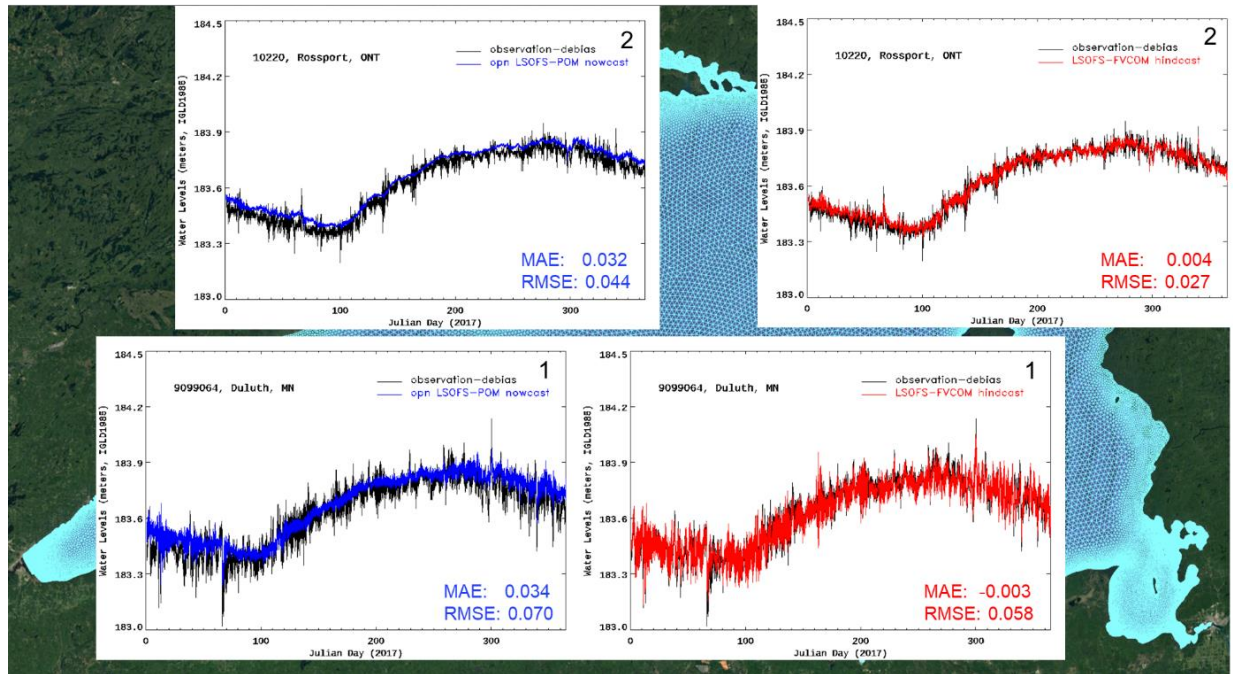


Figure 9. Time series plots of hourly LSOFS-FVCOM hindcasts (red) and LSOFS-POMGL nowcasts (blue) of water level vs. bias-removed observations (black) at 1) COOPS-NWLON gauge Duluth, MN (9099064) and 2) CHS gauge Rossport, ON (10220) during 2017. MAE and RMSE (m) at each station are shown individually on each panel.

Figures 6 and 7 showed the MAEs and RMSEs differences between before and after WL observation data de-bias as well as time series plots at two sample stations for both LSOFS-POMGL and LSOFS-FVCOM. It is apparent that predictions from both LSOFS-POMGL and LSOFS-FVCOM more closely matched the de-biased water level observations compared to the non-de-biased data. Since the de-biased observation data better represent the ‘true’ water levels for all stations, the de-biased water level observations were used in the skill assessment of the FVCOM-based LSOFS hindcasts as well as the POMGL-based nowcasts.

## 5.2. Evaluation of Surface Water Temperature Hindcasts

The evaluation of hourly hindcasts of surface water temperatures was based on comparisons of time series from the hindcasts to observations at both offshore and shore locations in Lake Superior. The hindcasts during 2017 were also compared to operational nowcasts from the LSOFS-POMGL. The comparisons were done using MAE (SM), RMSE, SD, NOF, POF, MDPO, and MDNO. In evaluating predicted water temperatures in tidal regions, NOS sets an acceptable error of 7.7 °C to meet the acceptable error of draft of 7.5 cm (3 inches). Water density is a function of water temperature and salinity, and contributes to the underwater draft.

However, since the Great Lakes are considered freshwater and non-tidal, there is no preset standard for lake temperature predictions. Based on ten years of experience in running the Great Lakes Forecasting System and input from the Great Lakes user community, Dr. David Schwab formerly of NOAA/GLERL suggested a 3 °C criteria for water temperature skill assessment in the Great Lakes region (personal communication). Thus, a 3 °C (5.4 °F) criteria for water temperature was assigned, the same criteria used in earlier evaluations of GLOFS (Chu et al., 2007; Kelley et al., 2018).

Hindcasts at nearshore and open lake locations were compared to observations at 10 fixed buoys in the lakes (Fig. 8). The buoys are operated by the NOAA/NWS/National Data Buoy Center (NDBC), ECCC or the Great Lakes Observing System (GLOS). The point evaluations were conducted by comparing surface (highest sigma layer) water temperature hindcasts at the nearest grid points to the buoys. Geographic information for the buoys is given in Tables 3 and 4.

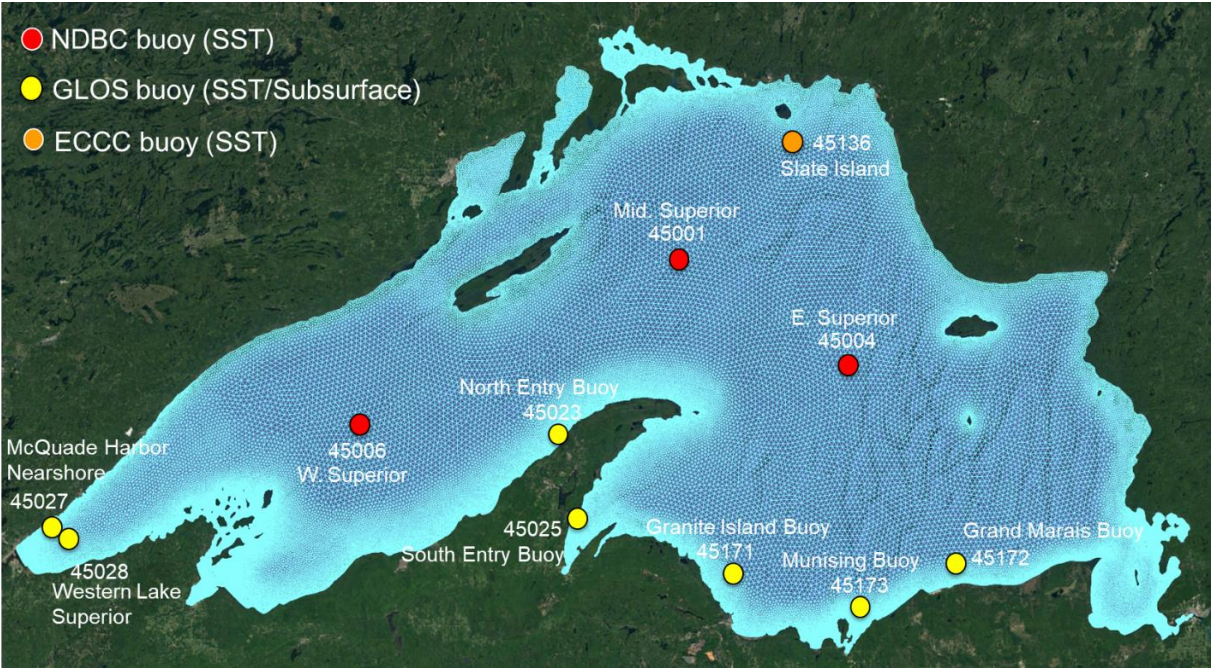


Figure 10. Locations of buoys used to evaluate LSOFS surface water temperature hindcasts.

Table 3. Information about NWS/NDBC and ECCC open lake fixed buoys whose surface water temperature observations were used to evaluate the LSOFS hindcasts at open lake locations.

Buoy Name	Agency	Prov. or State	NWS Buoy Platform ID	Water Depth (m)	Coordinates	
					Latitude (deg N)	Longitude (deg W)
Mid. Superior	NWS/NDBC	MI	45001	247	42.674	87.026
E. Superior	NWS/NDBC	MI	45004	274	44.283	82.416
W. Superior	NWS/NDBC	WI	45006	195	43.100	87.850
Slate Island	Envir. Canada	ON	45136	170	43.973	86.556

The water temperature sensors at the NWLON stations are located approximately 1.5 m below the low water datum (LWD) for the Great Lakes. According to Grodsky (personal communication), the sensors are located fairly close to the shore structure that the water level gauges are mounted to.

Table 4. Information on GLOS buoys whose surface water temperature observations were used to evaluate the LSOFS surface water temperature hindcasts along the shore.

Buoy Name	Agency	Prov. or State	NWS Buoy Platform ID	Water Depth (m)	Coordinates	
					Latitude (deg N)	Longitude (deg W)
North Entry	GLOS	MI	45023	25	44.800	87.760
South Entry	GLOS	MI	45025	28	46.969	88.398
McQuade Harbor Nearshore	GLOS	MN	45027	52	41.714	87.527
Western Lake Superior	GLOS	MN	45028	49	46.814	91.829
Granite Island	GLOS	MI	45171	27	41.783	87.573
Munising	GLOS	MI	45173	40	45.403	85.088

### 5.3. Evaluation of Sub-Surface Water Temperature Hindcasts

The evaluation of hourly hindcasts of sub-surface water temperatures was based on comparisons of time series of the hindcasts to observations at two GLOS near-shore buoys containing thermistor strings in Lake Superior (Fig. 9). The comparisons were done using SM, RMSE, SD, NOF, POF, MDPO, and MDNO. The point evaluations were conducted by comparing sub-surface water temperatures (at multiple depth) hindcasts at the nearest grid points to the two buoys and at the approximate depths. Geographic information for the two buoys is given in Table 5.

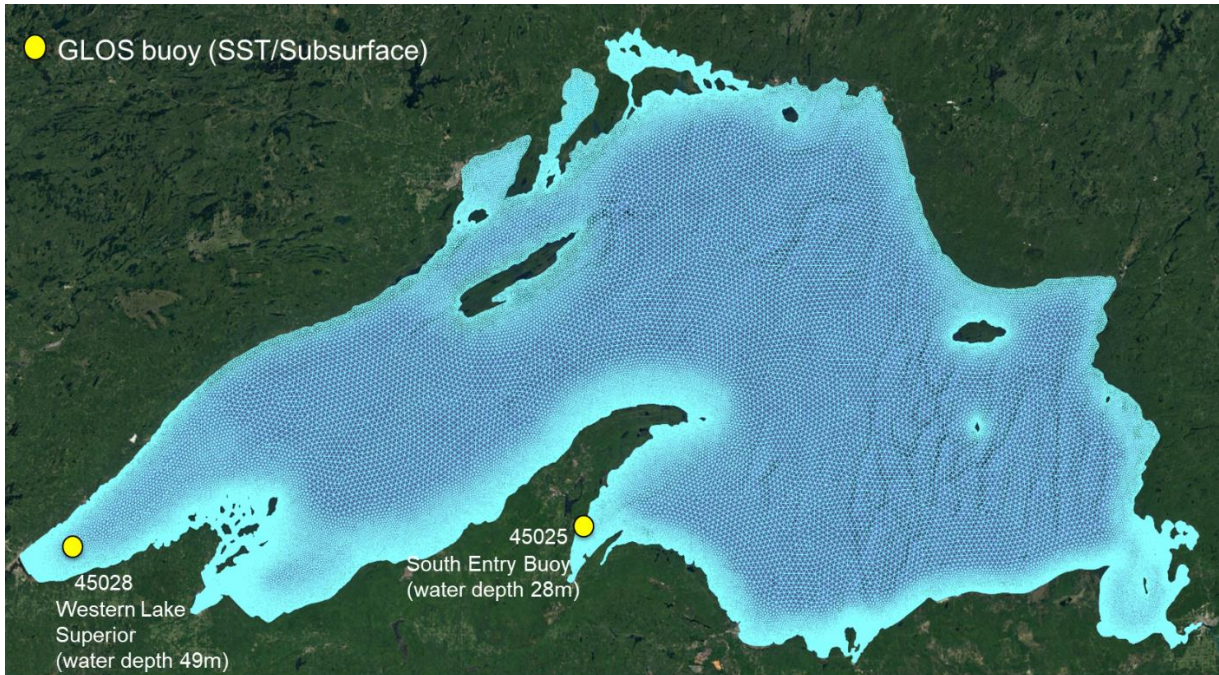


Figure 11. Locations of buoys used to evaluate LSOFS sub-surface water temperature hindcasts. The water depths at the buoys are also depicted.

Table 5. Information about buoys whose subsurface water temperature observations were used to evaluate the LSOFS water temperature hindcasts.

Buoy Name	Agency	Prov. or State	NWS Buoy Platform ID	Water Depth (m)	Coordinates	
					Latitude (deg N)	Longitude (deg W)
South Entry	GLOS	MI	45025	28	46.969	88.398
Western Lake Superior	GLOS	MN	45028	49	46.814	91.829

#### 5.4. Evaluation of Water Currents Hindcasts

The evaluation of hourly hindcasts of water currents was based on comparisons of time series of the hindcasts to observations at the GLOS North Keweenaw Waterway buoy off the west coast of Keweenaw Peninsula in Lake Superior (Fig. 10). The buoy, commonly referred to as the North Entry Buoy, is operated by the Great Lakes Research Center at the Michigan Technological University ([http://uglos.mtu.edu/station\\_page.php?station=45023](http://uglos.mtu.edu/station_page.php?station=45023)). The comparisons were done using SM, RMSE, SD, NOF, POF, MDPO, and MDNO. The point evaluations were conducted by comparing observations to hindcasts of water currents at the nearest grid point to GLOS station and at the approximate depth. Geographic information for the buoy is given in Table 6.



Figure 12. Location of the buoy used to evaluate LSOFS hindcasts of water currents. The numbers of depths at which data are available for 2017 and 2018 are also given.

Table 6. Information about GLOS buoy whose water currents observations were used to evaluate the LSOFS water currents hindcasts.

Name of Currents Meter	Agency	Prov. or State	NWS Buoy Platform ID	NOS Platform ID	Coordinates	
					Latitude (deg N)	Longitude (deg W)
North Entry	GLOS	MI	45023	NA	44.800	87.760

## **6. HINDCAST SKILL ASSESSMENT RESULTS**

The results of the skill assessment of the 2017 and 2018 hindcasts will be presented in this section. In addition, the skill assessment of the operational nowcasts of water levels and surface water temperatures from the present LSOFS during 2017 will also be discussed. The water level assessment will be given first followed by a discussion of the water temperature evaluation results.

### **6.1. Assessment of Water Level Hindcasts**

The standard suite of skill assessment statistics evaluated the ability of the hindcasts to predict hourly and also extreme high and low water levels at NOS/CO-OPS NWLON gages and CHS Water Level Gauging Network during 2017 and 2018. The hindcasts were compared to the de-biased water level observations discussed in Section 5. The results of the assessment of the hourly hindcasts are described in Section 6.1.1 and the assessment results of extreme high and low water events are given in Sections 6.1.2 and 6.1.3.

#### **6.1.1. Hourly Water Levels**

The hourly water level time series plots at different water level gauges of 2017 and 2018 are shown from Figures 11-14. The MAE and RMSE of hindcast are highlighted on all 2017 hindcast time series plots. The 2017 time series plots contain both hindcasts and operational nowcasts (if station output is available) of hourly water levels and MAE and RMSE for both LSOFS-FVCOM and LSOFS-POMGL versus observations. The 2018 plots contain only the LSOFS-FVCOM vs. observations due to the unavailability of LSOFS-POMGL nowcast output at multiple dates. Full statistic tables are available from Table 7 to Table 10. The results are discussed for the U.S. lake shore and then along the Canadian lakeshore.

##### **6.1.1.1. United States Lakeshore**

Along the U.S. shore of Lake Superior, there are five NOS/CO-OPS NWLON gauges that measure the water levels of Lake Superior. Geographic locations of these five stations are labeled from 1 to 5 on the regional map and on the individual water level time series plots in Figure 11.

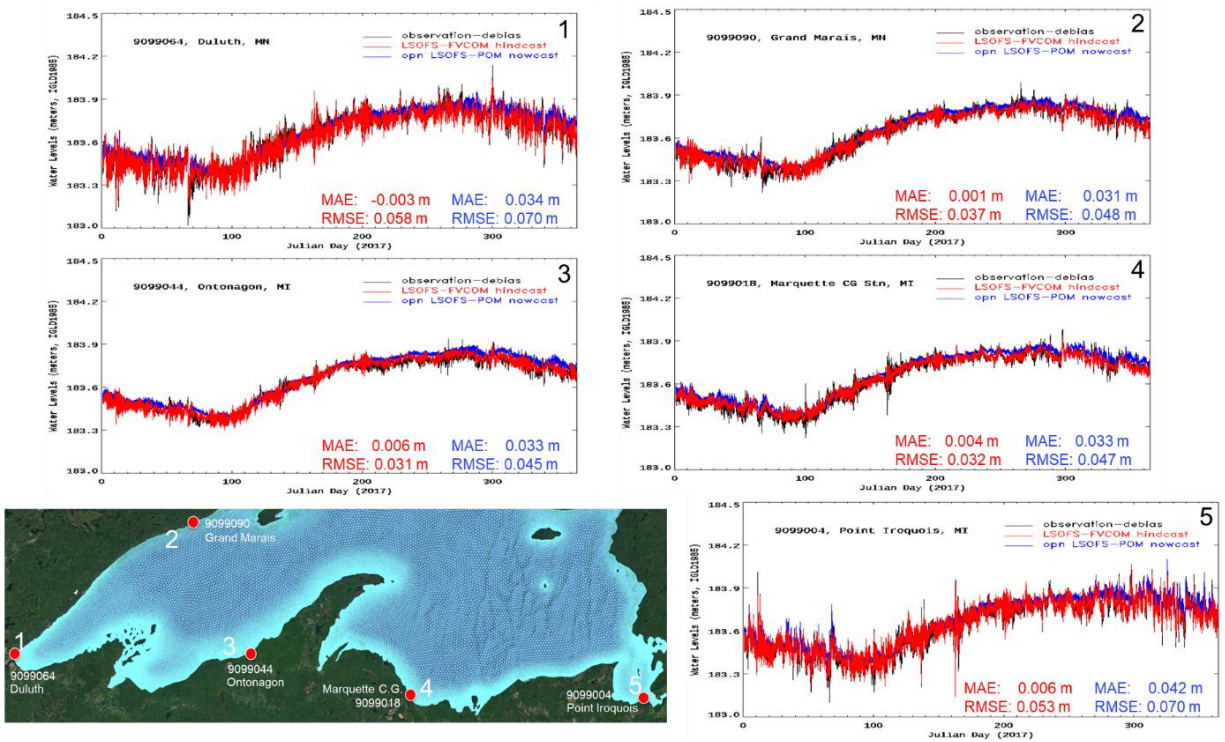


Figure 13. Time series plots of hourly LSOFS-POMGL nowcasts (blue) and LSOFS-FVCOM hindcast of water level (red) vs. bias-corrected observations (black) at NOS/CO-OPS NWLON gauges (1. Duluth, MN, 2. Grand Marais, MN, 3. Ontonagon, MI, 4. Marquette C.G. Station, MI, and 5. Point Iroquois, MI), Lake Superior during 2017. MAE and RMSE (m) at each station are shown individually on each panel.

The skill statistics assessing the ability of the hindcasts to predict the hourly water levels at CO-OPS gauges are given in Table 7 along with skill statistics for operational LSOFS nowcasts. A similar table for 2018 is given in Table 8, but without comparable statistics for the nowcasts from the present operational LSOFS. The MAE for 2017 ranged from -0.3 cm to 0.06 cm and the RMSE from 3.1 cm to 5.8 cm. The MAEs and RMSEs for the hindcasts were smaller than those for the operational nowcasts. The MAEs were all negative indicating a slight underprediction.

The MAE for 2018 ranged from 2.7 cm at Duluth and Grand Marais to -1.5 cm at Ontonagon. The average MAE was 2.2 cm. The RSMES were approximately the same as those for 2017 ranging from 3.2 cm to 6.2 cm. The hindcasts for both 2017 and 2018 passed all NOS acceptance criteria.

Table 7. Summary of skill assessment statistics evaluating the ability of the LSOFS-FVCOM hindcasts and LSOFS-POMGL nowcasts to predict hourly water levels at NOS NWLON gauges in Lake Superior during 2017. Gray shading, if present, indicates that it did not meet the NOS acceptance criteria.

Statistic, Acceptable Error [ ], and Units ( )	9099064 Duluth		9099090 Grand Marais		9099044 Ontonagon	
	<b>FVCOM</b>	<b>POMGL</b>	<b>FVCOM</b>	<b>POMGL</b>	<b>FVCOM</b>	<b>POMGL</b>
N	8761	8759	8704	8702	8761	8759
Mean Alg. Error (m)	-0.003	0.034	0.001	0.031	0.006	0.033
RMSE (m)	0.058	0.070	0.037	0.048	0.031	0.045
SD (m)	0.058	0.061	0.037	0.037	0.030	0.030
NOF [2×15 cm] (%)	0.0	0.0	0.0	0.0	0.0	0.0
CF [15 cm] (%)	98.7	96.1	99.9	99.8	100.0	100.0
POF [2×15 cm] (%)	0.0	0.0	0.0	0.0	0.0	0.0
MDNO [2×15 cm] (hr)	0.0	0.0	0.0	0.0	0.0	0.0
MDPO [2×15 cm] (hr)	0.0	0.0	0.0	0.0	0.0	0.0

Statistic, Acceptable Error [ ], and Units ( )	9099018 Marquette C.G.		9099004 Point Iroquois	
	<b>FVCOM</b>	<b>POMGL</b>	<b>FVCOM</b>	<b>POMGL</b>
N	8761	8759	8761	8759
Mean Alg. Error (m)	0.004	0.033	0.006	0.042
RMSE (m)	0.032	0.047	0.053	0.070
SD (m)	0.031	0.033	0.053	0.056
NOF [2×15 cm] (%)	0.0	0.0	0.0	0.0
CF [15 cm] (%)	99.9	99.9	99.0	97.2
POF [2×15 cm] (%)	0.0	0.0	0.0	0.0
MDNO [2×15 cm] (hr)	0.0	0.0	0.0	0.0
MDPO [2×15 cm] (hr)	0.0	0.0	0.0	0.0

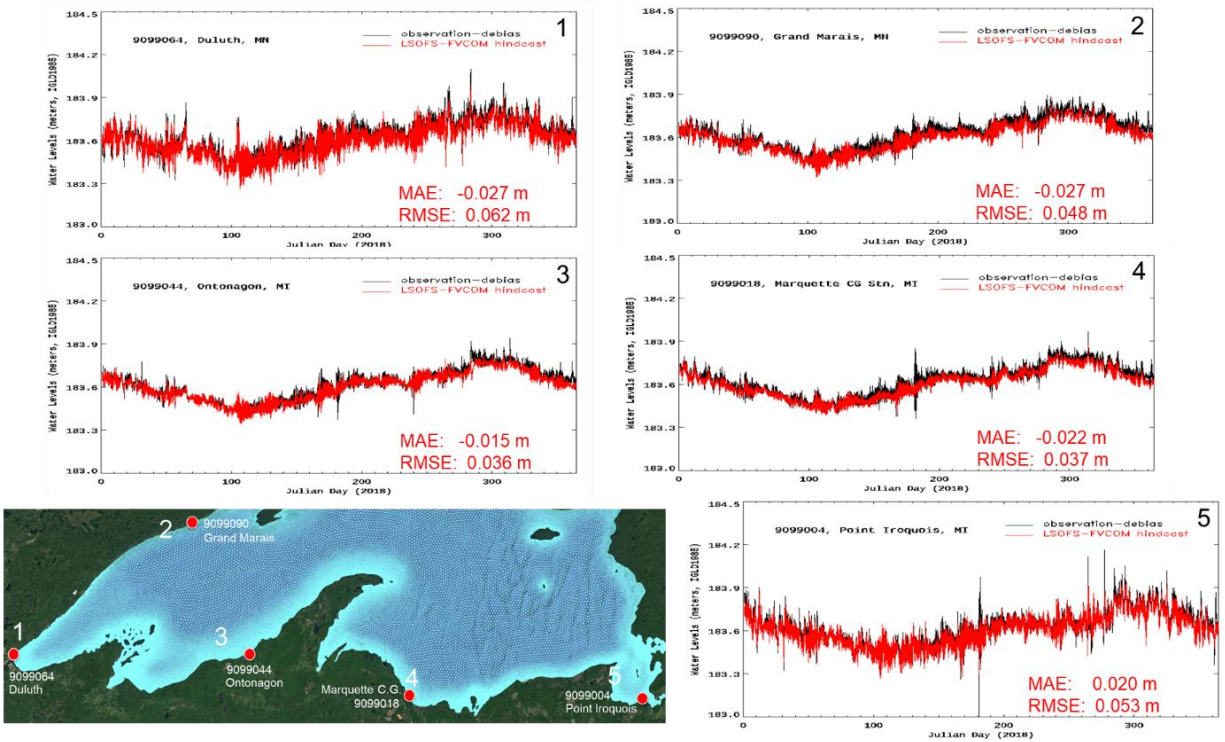


Figure 14. Time series plots of hourly LSOFS-FVCOM hindcasts of water level (red) vs. bias-corrected observations (black) at NOS/CO-OPS NWLON gauges (1. Duluth, MN, 2. Grand Marais, MN, 3. Ontonagon, MI, 4. Marquette C.G. Station, MI, and 5. Point Iroquois, MI), Lake Superior during 2018. MAE and RMSE (m) at each station are shown individually on each panel.

Table 8. Summary of skill assessment statistics evaluating the ability of the LSOFS-FVCOM hindcasts to predict hourly water levels at NOS NWLON gauges in Lake Superior during 2018. Gray shading, if present, indicates that it did not meet the NOS acceptance criteria.

Statistic, Acceptable Error [ ], and Units ( )	9099064 Duluth	9099090 Grand Marais	9099044 Ontonagon	9099018 Marquette C.G.	9099004 Point Iroquois
N	8761	8761	8761	8761	8761
Mean Alg. Error (m)	-0.027	-0.027	-0.015	-0.022	-0.020
RMSE (m)	0.062	0.048	0.036	0.032	0.053
SD (m)	0.055	0.039	0.032	0.030	0.049
NOF [2×15 cm] (%)	0.0	0.0	0.0	0.0	0.0
CF [15 cm] (%)	98.3	99.8	99.7	99.8	99.3
POF [2×15 cm] (%)	0.0	0.0	0.0	0.0	0.0
MDNO [2×15 cm] (hr)	0.0	0.0	0.0	0.0	0.0
MDPO [2×15 cm] (hr)	0.0	0.0	0.0	0.0	0.0

### 6.1.1.2. Canadian Lakeshore

On the Canadian shore of Lake Superior, there are three CHS gauges that measure the water levels of Lake Superior. Geographic locations of the gauges at Thunder Bay, Rosspoint, and Michipicoten are labeled from 1 to 3 on the regional map and on the individual water level time series plots in Figures 13 and 14. The skill statistics assessing the ability of the hindcasts to predict the hourly water levels at CHS gauges are given in Table 9 along with skill statistics for operational LSOFS nowcasts. A similar table for 2018 is given in Table 10, but without comparable statistics for the nowcasts from the present operational LSOFS.

The MAE for 2017 ranged from 0.004 m to 0.008 m and the RMSE from 0.027 m to 0.036 m. The MAEs and RMSEs for the hindcasts were smaller than those for the operational nowcasts. The MAEs were all negative indicating a slight underprediction. The RMSEs for the hindcasts were smaller than for the nowcasts from the operational LSOFS. The average RMSE was 0.017 m less for the hindcasts. The 2017 hindcasts at the CHS gauges passed all NOS acceptance criteria.

For 2018, the MAE and RSME ranged from -0.018 m to -0.015 m and 0.031 m to 0.039 m, respectively. The MAEs were all positive demonstrating an overprediction. The hindcasts for 2017 and 2018 passed all NOS acceptance criteria. The 2018 hindcasts at the CHS gauges passed all NOS acceptance criteria.

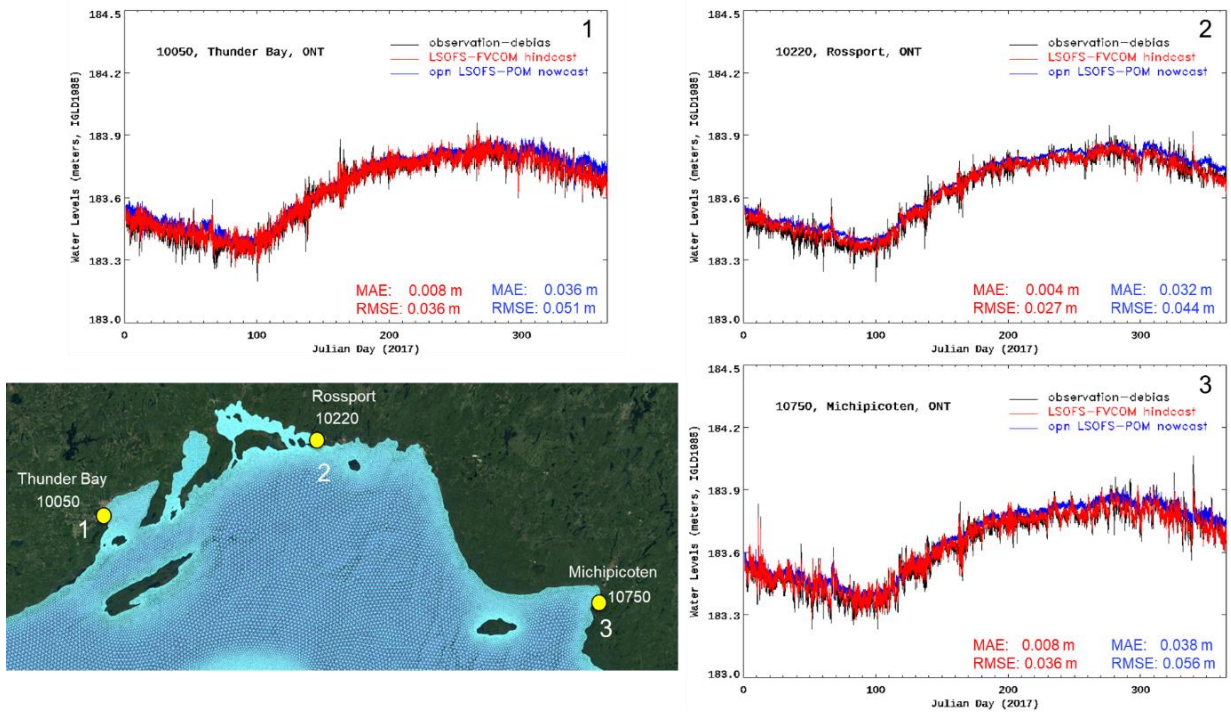


Figure 15. Time series plots of hourly LSOFS-POMGL nowcasts (blue) and LSOFS-FVCOM hindcasts of water level (red) vs. bias-corrected observations (black) at CHS Water Level gauges (1. Thunder Bay, ONT, 2. Rossport, ONT, and 3. Michipicoten, ONT), Lake Superior during 2017. MAE and RMSE (m) at each station are shown individually on each panel.

Table 9. Summary of skill assessment statistics of LSOFS-FVCOM hindcasts and LSOFS-POMGL nowcasts of hourly water levels at CHS gauges in Lake Superior during 2017. Gray shading, if present, indicates that it did not meet the NOS acceptance criteria.

Statistic, Acceptable Error [ ], and Units ( )	C10050 Thunder Bay		C10220 Rosspport		C10750 Michipicoten	
	<b>FVCOM</b>	<b>POMGL</b>	<b>FVCOM</b>	<b>POMGL</b>	<b>FVCOM</b>	<b>POMGL</b>
N	8737	8737	8737	8737	8732	8732
Mean Alg. Error (m)	0.008	0.036	0.004	0.032	0.008	0.038
RMSE (m)	0.036	0.051	0.027	0.044	0.036	0.056
SD (m)	0.036	0.036	0.027	0.029	0.035	0.042
NOF [2×15 cm] (%)	0.0	0.0	0.0	0.0	0.2	0.0
CF [15 cm] (%)	99.9	99.8	100.0	99.9	99.9	99.4
POF [2×15 cm] (%)	0.0	0.0	0.0	0.0	0.0	0.0
MDNO [2×15 cm] (hr)	0.0	0.0	0.0	0.0	0.0	0.0
MDPO [2×15 cm] (hr)	0.0	0.0	0.0	0.0	0.0	0.0

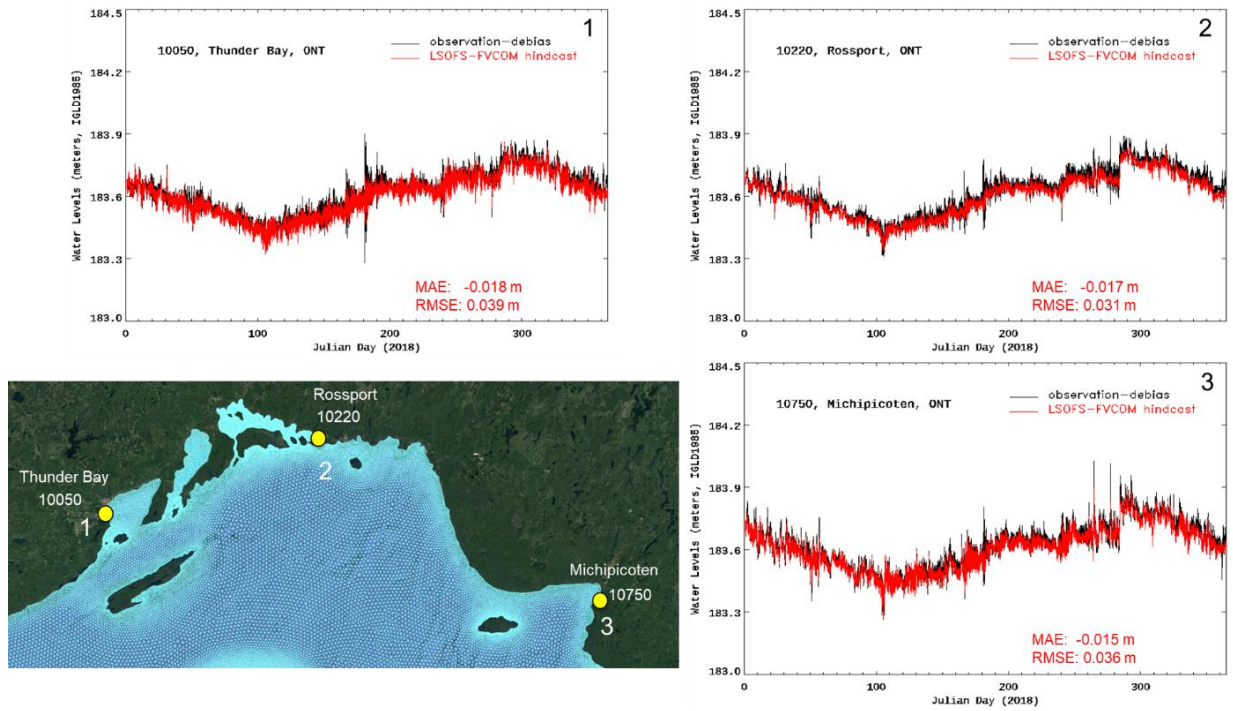


Figure 16. Time series plots of hourly LSOFS-FVCOM hindcasts of water level (red) vs. bias-corrected observations (black) at CHS Water Level gauges (1. Thunder Bay, ONT, 2. Rossport, ONT, and 3. Michipicoten, ONT), Lake Superior during 2018. MAE and RMSE (m) at each station are shown individually on each panel.

Table 10. Summary of skill assessment statistics of LSOFS-FVCOM hindcasts of hourly water levels at CHS gauges in Lake Superior during 2018. Gray shading, if present, indicates that it did not meet the NOS acceptance criteria.

Statistic, Acceptable Error [ ], and Units ( )	C10050 Thunder Bay	C10220 RosSPORT	C10750 Michipocoten
N	8737	8737	8737
Mean Alg. Error (m)	-0.018	-0.017	-0.015
RMSE (m)	0.039	0.031	0.036
SD (m)	0.035	0.026	0.033
NOF [2×15 cm] (%)	0.0	0.0	0.0
CF [15 cm] (%)	99.7	99.9	99.9
POF [2×15 cm] (%)	0.0	0.0	0.0
MDNO [2×15 cm] (hr)	0.0	0.0	0.0
MDPO [2×15 cm] (hr)	0.0	0.0	0.0

### 6.1.2. Extreme High-Water Level Events

The skill statistics assessing the ability of LSOFS-FVCOM hindcasts to predict the amplitude and timing of extreme high-water level events at gauges along the U.S. lakeshore during 2017 and 2018 are given in Tables 11 to 12, respectively. Similar tables for Canada shore are given in Tables 13 to 14. Depending on gauge location and hindcast year, the number of high-water level events at a gauge ranged from two to six. The results are discussed for the U.S. lake shore and then along the Canadian shore.

#### 6.1.2.1. United States Lakeshore

During 2017, the hindcasts underpredicted extreme high-water events at the three U.S. gauges. MAEs ranged from 6.5 cm at Marquette to 7.6 cm at Point Iroquois. The RMSE ranged from 7.5 cm at Grand Marais to 9.9 cm at Pt. Iroquois. Nowcasts from the operational POMGL-based LSOFS were available at these three gauges although the number of high-water level events were not always the same for both hindcasts and nowcasts at each gauge. At the three gauges, the average MAEs for the hindcasts was 8.1 cm while 7.1 cm for the nowcasts. Thus, the hindcasts and nowcasts both underpredicted high events at comparable amounts at two of the gauges, but the nowcasts had a slightly larger MAE at Point Iroquois. The hindcasts for 2017 passed all

NOS acceptance criteria except for CF amplitude at Point Iroquois and for CF phase (time) at Marquette.

A time series of hindcasts vs. observations and nowcasts for the high-water level event of Oct. 27, 2017 (NWS/WFO Duluth, 2017) is given in Fig. 17. An extra-tropical cyclone of Oct. 27-28 caused lake shore flooding in the Twin Ports of Duluth (MN) and Superior (WI) including Canal Park and Brighton Beach in Duluth due to a combination of storm surge and high waves. An examination of the plot points out three facts. First, the hindcasts are better at matching the overall trend of the water levels before, during, and after the high-water level event than the nowcasts. Second, the hindcasts came closer to predicting the amplitude of the high-water level event than the nowcasts but exhibited larger amplitude fluctuations compared to the observations and the nowcasts. Finally, the hindcasts predicted the water level event to start sooner compared to the nowcasts.

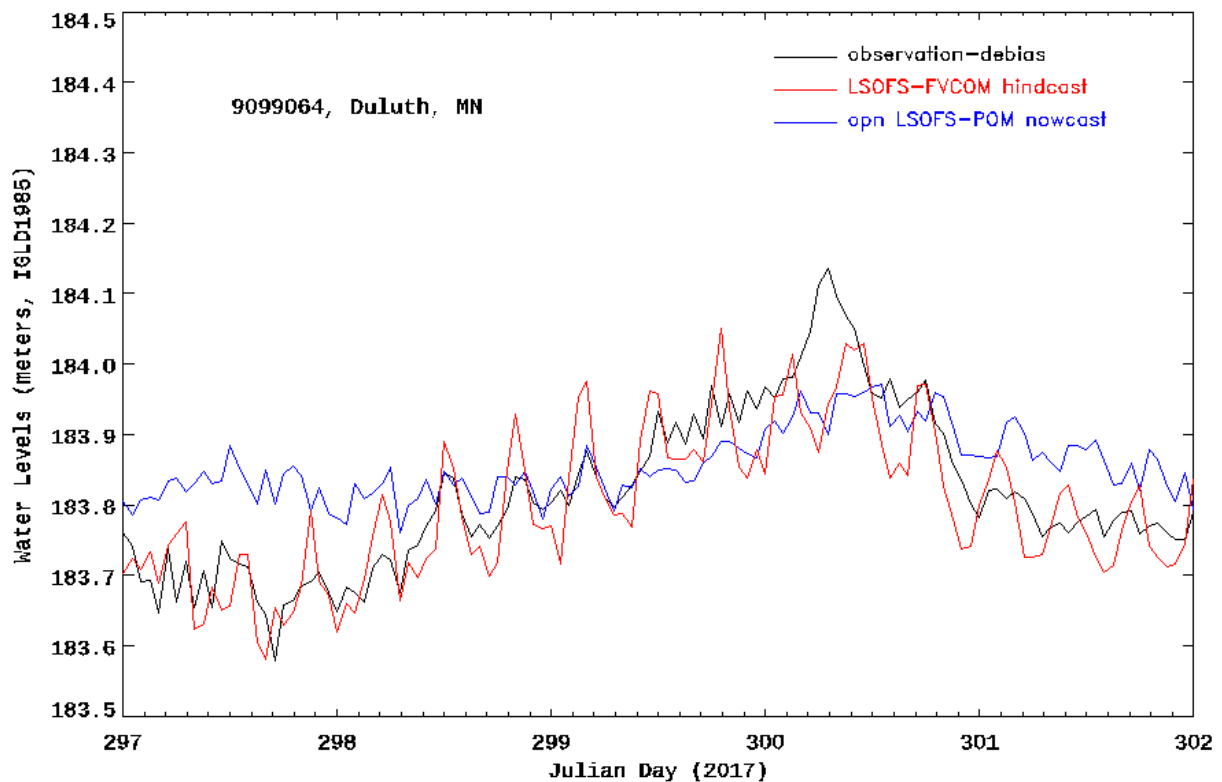


Figure 17. Time series plots of hourly LSOFS-POMGL nowcasts (blue) and LSOFS-FVCOM hindcast of water level (red) vs. bias-corrected observations (black) at NOS/CO-OPS NWLON gauge at Duluth, MN Oct. 24 (297) to Oct. 29, 2017 (302) including the high water level event of Oct. 27 (300), 2017.

During 2018, the hindcasts underpredicted extreme high-water events at the four U.S. gauges. MAEs ranged from -3.3 cm at Duluth to -1.6 cm at Point Iroquois with an average MAE of 10.2 cm. The RMSE ranged from 5 cm at Duluth to 18.6 cm at Point Iroquois with an average RMSE of 11.8 cm. The hindcasts for 2018 passed all NOS acceptance criteria except for CF amplitude at Point Iroquois and phase (time) at Grand Marais and Marquette. Nowcasts from the operational LSOFS in 2018 were not available at four gauges for the evaluation.

A time series of hindcasts vs. observations for the April 13-15, 2018 high water event is given in Fig. 18. The event was caused by a late season blizzard (NWS/WFO DUL, 2018) which caused lake shore flooding in the Twin Ports of Duluth (MN) and Superior (WI) including Canal Park and Brighton Beach due to a combination of storm surge and high. An examination of the plot point that captured the overall trend of the water levels before, during, and after the high-water level but exhibited larger amplitude fluctuations than was evident in the observations, similar to the 2017 high water event. The hindcasts for April 2018 were similar to the October 2017 hindcasts in the fact that both were forced by forecast guidance from HRRR V2.

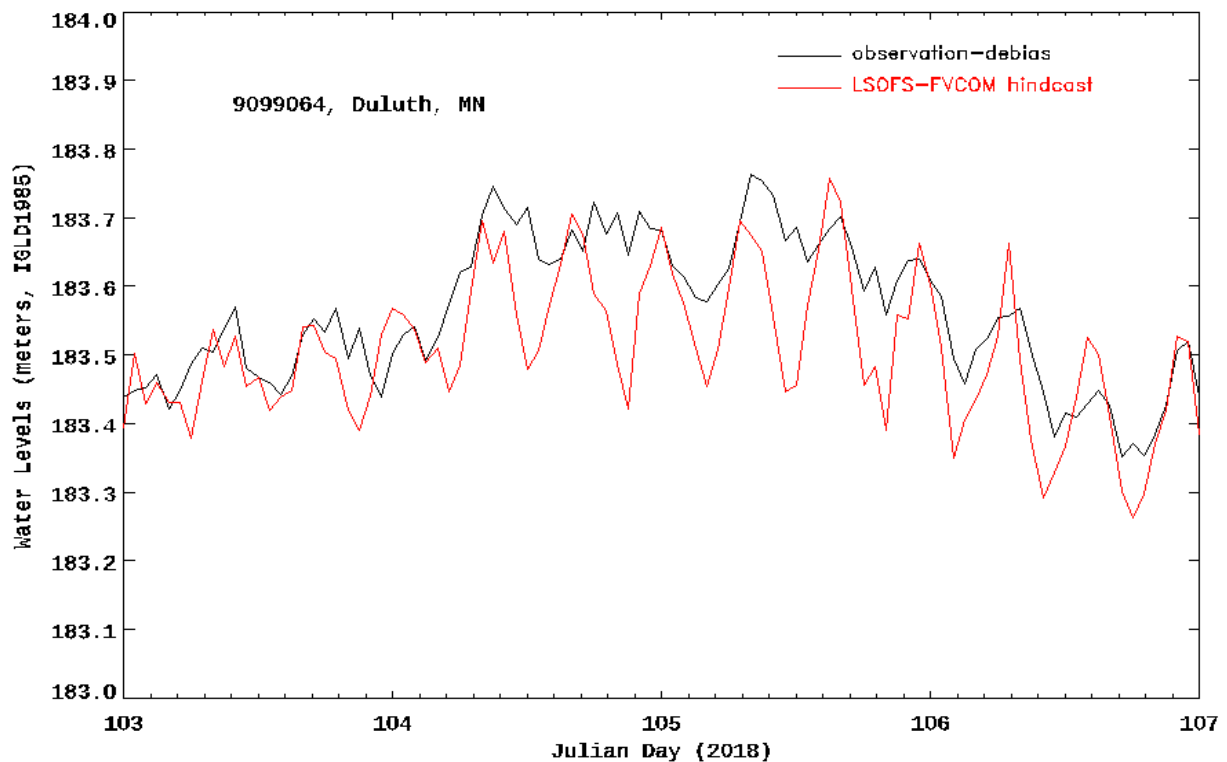


Figure 18. Time series plots of hourly LSOFS-FVCOM hindcast of water level (red) vs. bias-corrected observations (black) at NOS/CO-OPS NWLON gauge at Duluth, MN for the period from April 12 (103) to April 17 (107) 2018 including the high-water level event of April 12 (103) to April 17 (107) 2018 including the high-water level event of April 13-15, 2018.

A time series of LSOFS hindcasts vs. observations for the extra-tropical cyclone of Oct. 9 – Oct. 11, 2018 which caused lake shore flooding in the Twin Ports of Duluth (MN) and Superior (WI) including Canal Park and Brighton Beach in Duluth due to a combination of storm surge and high waves is given in Fig. 19. According to press reports, the Canadian freighter Assiniboine, anchored in Lake Superior just off Duluth, recorded winds up to 102 KPH (64 MPH) and 6 m (20 ft) waves and wind gust of 138 KPH (86 MPH) reported by the Canadian freighter Algowood off the Minnesota North Shore near Castle Danger (Forum News Service, 2018). The hindcasts for October 2018 were forced by forecast guidance from HRRR V4.

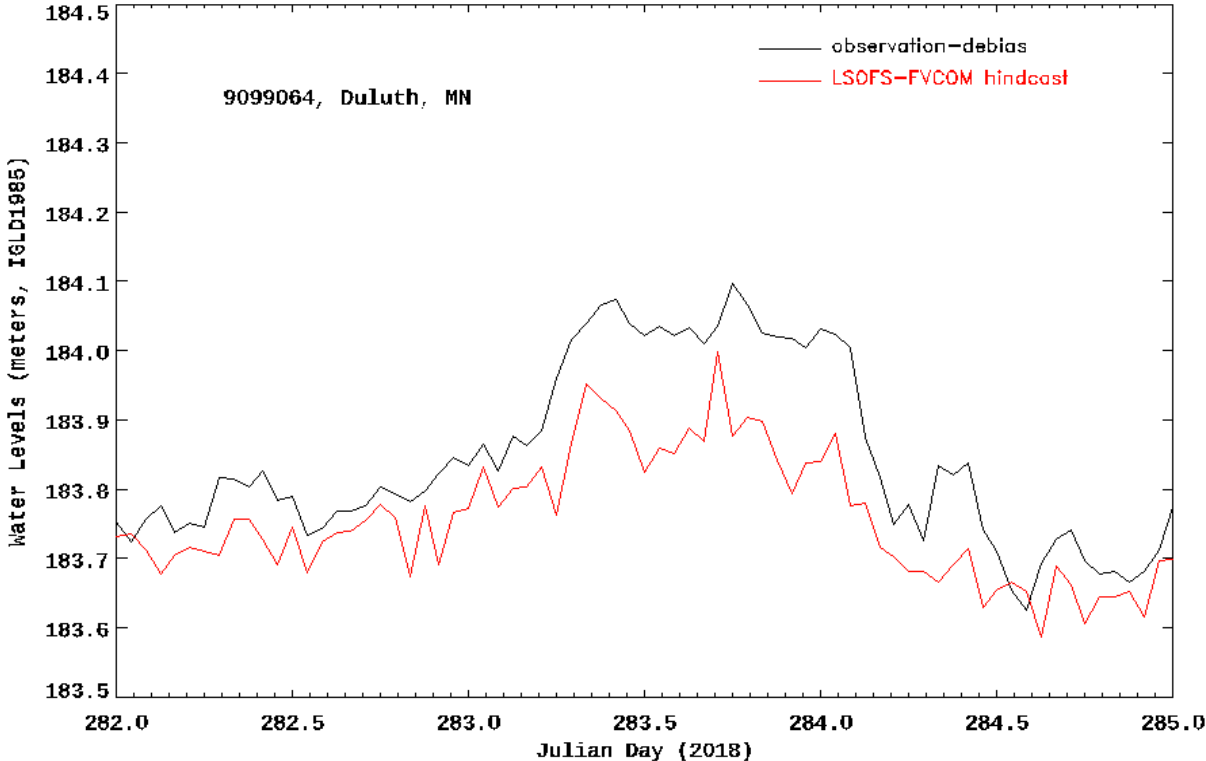


Figure 19. Time series plots of hourly LSOFS-FVCOM hindcast of water level (red) vs. bias-corrected observations (black) at NOS/CO-OPS NWLON gauge at Duluth, MN Oct. from Oct. 9 (282) to Oct. 12 (285), 2018 including the high-water level event of Oct. 10 – 11, 2018.

**6.1.2.2. Canadian Lakeshore**

During 2017, the hindcasts underpredicted extreme high-water events at the two CHS gauges. MAEs were -6.2 cm at Rosspport to -7.7 cm at Michipicoten with an average MAE of -7.1 cm. The RMSEs were 6.3 cm at Rosspport to 7.7 cm at Michipicoten with an average RMSE of 6.9 cm. Nowcasts from the operational POMGL-based LSOFS and the hindcasts were both

available at two of the three gauges although the number of high-water level events were not always the same for both hindcasts and nowcasts at each gauge. At the two gauges, the average MAEs for the hindcasts was -6.9 cm while -7.7 cm for the nowcasts, both the hindcasts and nowcasts both underpredicted high events. The hindcasts passed all the NOS criteria at the two CHS gauges except for POF for timing at Rosspport.

During 2018, the hindcasts underpredicted extreme high-water events at the two Canadian gauges with a MAE of -14.5 cm at Thunder Bay and -7.1 cm at Michipicoten. The RMSE ranged from 9.4 cm at Michipicoten to 15.2 cm at Thunder Bay. The hindcasts passed all the acceptance criteria except for CF at both gauges.

Table 11. Summary of skill assessment statistics evaluating the ability of the LSOFS-FVCOM hindcasts and LSOFS-POMGL nowcasts to predict extreme high water level events at NOS NWLON gauges during 2017. Gray shading, if present, indicates that it did not meet the NOS acceptance criteria.

Statistic, Acceptable Error [ ], and Units ( )	9099064 Duluth			9099090 Grand Marais			
	FVCOM N=0		POMGL N=2	FVCOM N=2		POMGL N=3	
		Amp.	Time	Amp.	Time	Amp.	Time
Mean Alg. Error (m) (hr)		-0.101	0.000	-0.073	-0.500	-0.069	0.667
RMSE (m) (hr)		0.101	1.000	0.075	0.707	0.070	1.155
SD (m) (hr)		0.016	1.414	0.023	0.707	0.012	1.155
NOF [2×15 cm or 90 min] (%)		0.0	0.0	0.0	0.0	0.0	0.0
CF [15 cm or 90 min] (%)		100.0	100.0	100.0	100.0	100.0	66.7
POF [2×15 cm or 90 min] (%)		0.0	0.0	0.0	0.0	0.0	0.0
MDNO [2×15 cm or 90 min] (hr)		0.0	0.0	0.0	0.0	0.0	0.0
MDPO [2×15 cm or 90 min] (hr)		0.0	0.0	0.0	0.0	0.0	0.0

Statistic, Acceptable Error [ ], and Units ( )	9099018 Marquette C.G.				9099004 Point Iroquois			
	FVCOM N=3		POMGL N=3		FVCOM N=4		POMGL N=6	
	Amp.	Time	Amp	Time	Amp.	Time	Amp.	Time
Mean Alg. Error (m) (hr)	-0.065	-1.333	-0.064	0.667	-0.076	-0.750	-0.110	0.833
RMSE (m) (hr)	0.085	1.414	0.066	2.000	0.099	0.866	0.153	1.080
SD (m) (hr)	0.067	0.577	0.022	2.309	0.073	0.500	0.116	0.753
NOF [2×15 cm or 90 min] (%)	0.0	0.0	0.0	0.0	0.0	0.0	0.0	0.0
CF [15 cm or 90 min] (%)	100.0	66.7	100.0	0.0	75.0	100.0	50.0	83.3
POF [2×15 cm or 90 min] (%)	0.0	0.0	0.0	0.0	0.0	0.0	0.0	0.0
MDNO [2×15 cm or 90 min] (hr)	0.0	0.0	0.0	0.0	0.0	0.0	0.0	0.0
MDPO [2×15 cm or 90 min] (hr)	0.0	0.0	0.0	0.0	0.0	0.0	0.0	0.0

Table 12. Summary of skill assessment statistics evaluating the ability of the LSOFS-FVCOM hindcasts to predict extreme high water level events at NOS NWLON stations in Lake Superior during 2018. Gray shading, if present, indicates that it did not meet the NOS acceptance criteria.

Statistic, Acceptable Error [ ], and Units ( )	9099064 Duluth		9099090 Grand Marais		9099018 Marquette C.G.	
	<b>FVCOM</b> N=2		<b>FVCOM</b> N=3		<b>FVCOM</b> N=2	
	Amp.	Time	Amp.	Time	Amp.	Time
Mean Alg. Error (m) (hr)	-0.033	-0.500	-0.133	-1.667	-0.077	-0.500
RMSE (m) (hr)	0.050	0.707	0.134	1.732	0.077	1.581
SD (m) (hr)	0.053	0.707	0.018	0.577	0.006	2.121
NOF [2×15 cm or 90 min] (%)	0.0	0.0	0.0	0.0	0.0	0.0
CF [15 cm or 90 min] (%)	100.0	100.0	100.0	33.3	100.0	50.0
POF [2×15 cm or 90 min] (%)	0.0	0.0	0.0	0.0	0.0	0.0
MDNO [2×15 cm or 90 min] (hr)	0.0	0.0	0.0	0.0	0.0	0.0
MDPO [2×15 cm or 90 min] (hr)	0.0	0.0	0.0	0.0	0.0	0.0

Statistic, Acceptable Error [ ], and Units ( )	9099004 Point Iroquois	
	<b>FVCOM</b> N=3	
	Amp.	Time
Mean Alg. Error (m) (hr)	-0.163	-0.667
RMSE (m) (hr)	0.186	0.816
SD (m) (hr)	0.110	0.577
NOF [2×15 cm or 90 min] (%)	0.0	0.0
CF [15 cm or 90 min] (%)	66.7	100.0
POF [2×15 cm or 90 min] (%)	0.0	0.0
MDNO [2×15 cm or 90 min] (hr)	0.0	0.0
MDPO [2×15 cm or 90 min] (hr)	0.0	0.0

Table 13. Summary of skill assessment statistics evaluating the ability of LSOFS-FVCOM hindcasts to predict extreme high water level events at CHS gauges in Lake Superior during 2017. Gray shading, if present, indicates that it did not meet the NOS acceptance criteria.

Statistic, Acceptable Error [ ], and Units ( )	C10050 Thunder Bay			C10220 RosSPORT		
	<b>FVCOM</b> N=0	<b>POMGL</b> N=2		<b>FVCOM</b> N=2		<b>POMGL</b> N/A
		Amp.	Time	Amp.	Time	
Mean Alg. Error (m) (hr)		-0.064	0.000	-0.062	-2.000	
RMSE (m) (hr)		0.067	0.000	0.063	2.000	
SD (m) (hr)		0.028	0.000	0.012	0.000	
NOF [2×15 cm or 90 min] (%)		0.0	0.0	0.0	0.0	
CF [15 cm or 90 min] (%)		100.0	100.0	100.0	0.0	
POF [2×15 cm or 90 min] (%)		0.0	0.0	0.0	0.0	
MDNO [2×15 cm or 90 min] (hr)		0.0	0.0	0.0	0.0	
MDPO [2×15 cm or 90min] (hr)		0.0	0.0	0.0	0.0	

Statistic, Acceptable Error [ ], and Units ( )	C10750 Michipicoten			
	<b>FVCOM</b> N=3		<b>POMGL</b> N=4	
	Amp.	Time	Amp.	Time
Mean Alg. Error (m) (hr)	-0.077	0.333	-0.096	0.250
RMSE (m) (hr)	0.077	0.577	0.102	0.866
SD (m) (hr)	0.013	0.577	0.038	0.957
NOF [2×15 cm or 90 min] (%)	0.0	0.0	0.0	0.0
CF [15 cm or 90 min] (%)	100.0	100.0	100.0	100.0
POF [2×15 cm or 90 min] (%)	0.0	0.0	0.0	0.0
MDNO [2×15 cm or 90 min] (hr)	0.0	0.0	0.0	0.0
MDPO [2×15 cm or 90min] (hr)	0.0	0.0	0.0	0.0

Table 14. Summary of skill assessment statistics evaluating the ability of LSOFS-FVCOM hindcasts to predict extreme high water level events at CHS stations in Lake Superior during 2018. Gray shading, if present, indicates that it did not meet the NOS acceptance criteria.

Statistic, Acceptable Error [ ], and Units ( )	C10050 Thunder Bay		C10750 Michipicoten	
	<b>FVCOM</b>		<b>FVCOM</b>	
	N=2		N=5	
	Amp.	Time	Amp.	Time
Mean Alg. Error (m) (hr)	-0.145	0.000	-0.071	0.000
RMSE (m) (hr)	0.152	0.000	0.094	0.894
SD (m) (hr)	0.064	0.000	0.068	1.000
NOF [2×15 cm or 90 min] (%)	0.0	0.0	0.0	0.0
CF [15 cm or 90 min] (%)	50.0	100.0	80.0	100.0
POF [2×15 cm or 90 min] (%)	0.0	0.0	0.0	0.0
MDNO [2×15 cm or 90 min] (hr)	0.0	0.0	0.0	0.0
MDPO [2×15 cm or 90 min] (hr)	0.0	0.0	0.0	0.0

### 6.1.3. Extreme Low Water Level Events

The skill statistics assessing the ability of hindcasts to predict the amplitude and timing of extreme low-water level events at gauges along the U.S. and Canadian lakeshore during 2017 and 2018 are given in Tables 15 and 16, respectively. Similar tables for Canada shore are given in Tables 17 and 18. Depending on gauge location and hindcast year, the number of low-water level events at a gauge ranged from two to six. The results are discussed for the U.S. lake shore and then along the Canadian shore.

#### 6.1.3.1. United States Lakeshore

During 2017, the hindcasts overpredicted extreme low-water events at the four U.S. gauges. MAEs ranged from 3 cm at Duluth to 7.5 cm at Ontonagon with an average of 5.0 cm. The RMSE ranged from 4.2 cm Duluth to 9.8 cm at Pt. Iroquois with an average of 6.9 cm. The corresponding average MAE and RMSE for the nowcasts were 16.0 cm and 16.8, respectively. The hindcasts for 2017 passed all NOS acceptance criteria except for CF amplitude at Point Iroquois and for CF phase (time) at Duluth, Ontonagon, and Point Iroquois.

A time series of hindcasts vs. observations and nowcasts for the low-water level events of January 11 and 13, 2017 is depicted in Fig. 20. Both hindcasts and nowcasts captured the Jan. 11<sup>th</sup> event although the hindcasts did better in simulating the amplitude and timing. However, for the Jan. 13<sup>th</sup> event, the hindcasts captured the event well in terms of amplitude but had two events of approximately equal amplitude while the nowcasts had a sole event which was very close to the time of occurrence. As was evident in other events, the hindcasts exhibit higher amplitude fluctuations than seen in the nowcasts or observations. As mentioned in the extreme high water level event section, the hindcasts were forced by guidance from HRRR V2.

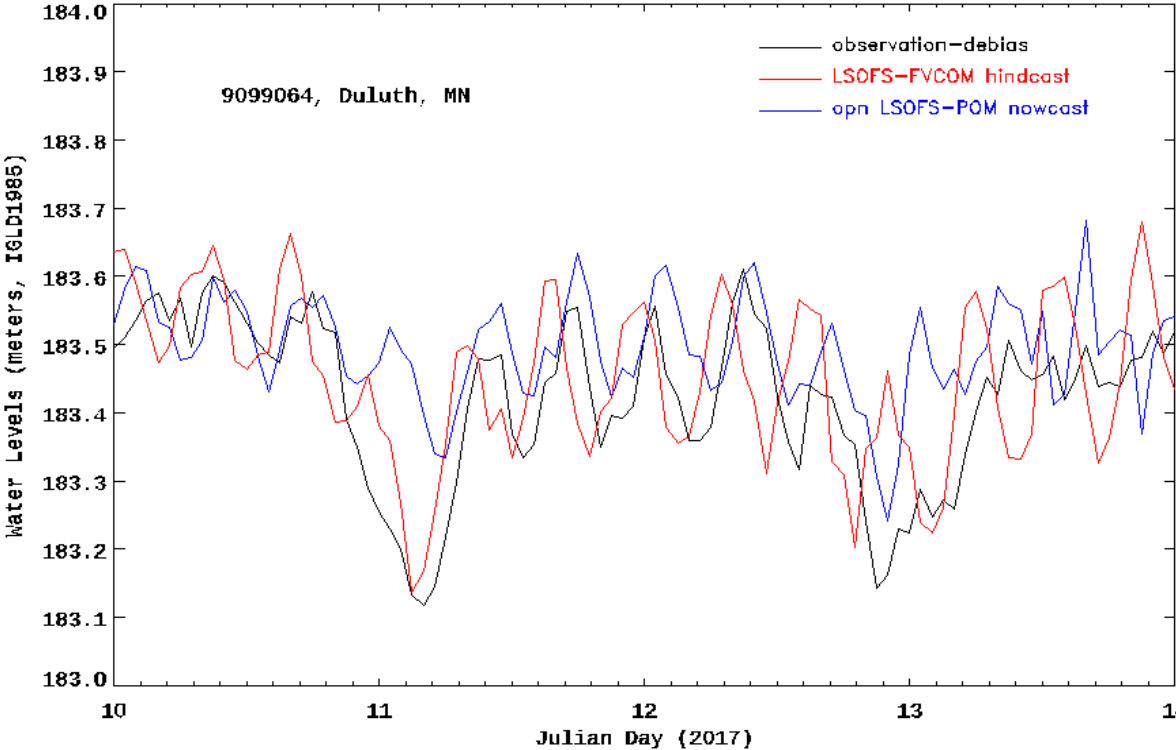


Figure 20. Time series plots of hourly LSOFS-POMGL nowcasts (blue) and LSOFS-FVCOM hindcast of water level (red) vs. bias-corrected observations (black) at NOS/CO-OPS NWLON gauge at Duluth, MN from January 10 to 14, 2017 including low water level events of January 11 and 13, 2017.

During 2018, the hindcasts overpredicted extreme low-water events at the five U.S. gauges. MAEs ranged from 0.4 cm at Duluth to 6.6 cm at Grand Marais with an average of 3.9 cm. The RMSE ranged from 2.0 cm Duluth to 6.9 cm at Pt. Iroquois with an average of 5.0 cm. The hindcasts for 2018 passed all NOS acceptance criteria except for CF for timing at Pt. Iroquois and Ontonagon.

A time series of hindcasts vs. observations for the low-water level events of October 4, 2018 is given in Fig. 21. The hindcasts captured the event both in amplitude and timing. When compared to the Jan. 2017 events, the hindcasts did not exhibit the same high amplitude fluctuations. This may be due to use of surface wind forecast guidance from HRRR V3 to force the hindcast runs starting on July 12, 2018 while predictions from HRRR V2 were used from Jan. 1, 2017 to July 11, 2018.

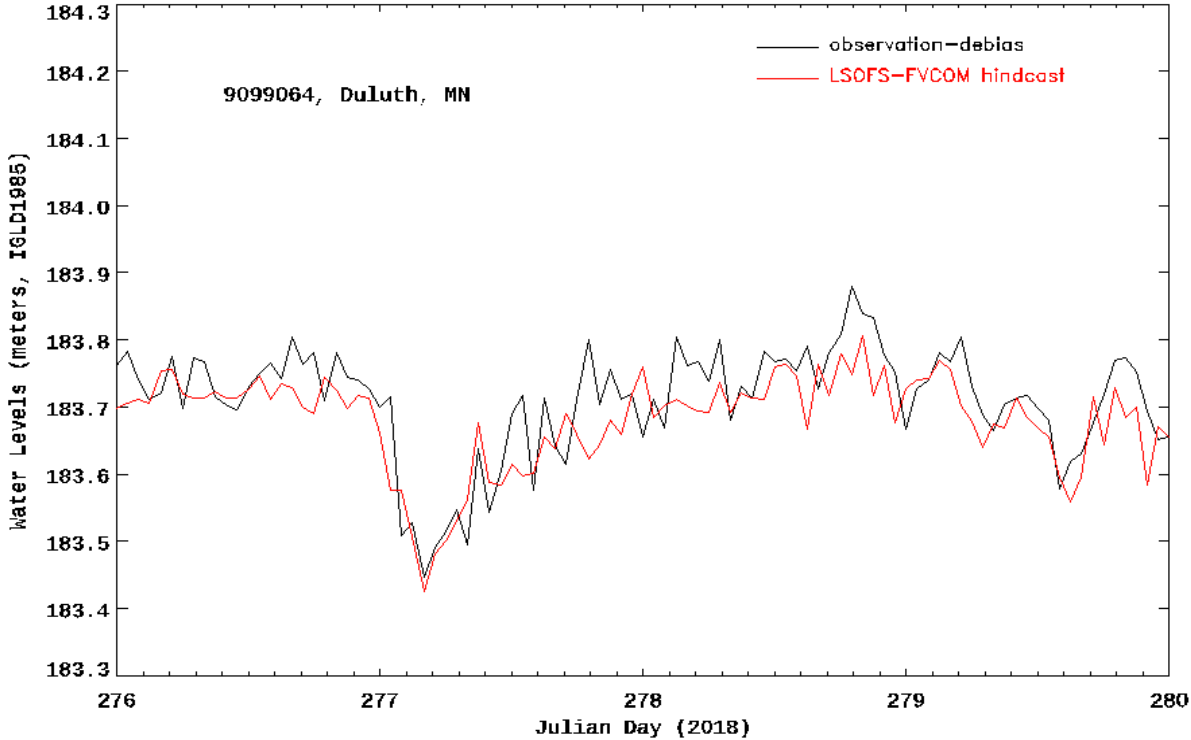


Figure 21. Time series plots of hourly LSOFS-FVCOM hindcast of water level (red) vs. bias-corrected observations (black) at NOS/CO-OPS NWLON gauge at Duluth, MN for the period from Oct. 3 (276) to Oct. 7 (280) 2018 including the low water level event of Oct. 4 (277), 2018.

Table 15. Summary of skill assessment statistics evaluating the ability of the LSOFS-FVCOM hindcasts and LSOFS-POMGL nowcasts to predict extreme low water level events at NOS NWLON gauges in Lake Superior during 2017. Gray shading, if present, indicates that it did not meet the NOS acceptance criteria.

Statistic, Acceptable Error [ ], and Units ( )	9099064 Duluth				9099090 Grand Marais			
	FVCOM N=10		POMGL N=10		FVCOM N=2		POMGL N=2	
	Amp.	Time	Amp.	Time	Amp.	Time	Amp.	Time
Mean Alg. Error (m) (hr)	0.033	-0.400	0.147	0.400	0.054	0.000	0.131	2.000
RMSE (m) (hr)	0.042	1.414	0.152	1.483	0.060	1.000	0.131	2.000
SD (m) (hr)	0.027	1.430	0.039	1.506	0.038	1.414	0.011	0.000
NOF [2×15 cm or 90 min] (%)	0.0	0.0	0.0	0.0	0.0	0.0	0.0	0.0
CF [15 cm or 90 min] (%)	100.0	60.0	50.0	60.0	100.0	100.0	100.0	0.0
POF 2× [15 cm or 90 min] (%)	0.0	0.0	0.0	0.0	0.0	0.0	0.0	0.0
MDNO [2×15 cm or 90 min] (hr)	0.0	0.0	0.0	0.0	0.0	0.0	0.0	0.0
MDPO [2×15 cm or 90 min] (hr)	0.0	0.0	0.0	0.0	0.0	0.0	0.0	0.0

Statistic, Acceptable Error [ ], and Units ( )	9099044 Ontonagon			9099004 Point Iroquois			
	FVCOM N=2		POMGL N/A	FVCOM N=5		POMGL N=7	
	Amp.	Time		Amp.	Time	Amp.	Time
Mean Alg. Error (m) (hr)	0.075	0.000		0.039	0.400	0.201	-0.143
RMSE (m) (hr)	0.075	2.000		0.098	1.265	0.221	1.000
SD (m) (hr)	0.013	2.828		0.100	1.342	0.100	1.069
NOF [2×15 cm or 90 min] (%)	0.0	0.0		0.0	0.0	0.0	0.0
CF [15 cm or 90 min] (%)	100.0	0.0		80.0	80.0	28.6	85.7
POF [2×15 cm or 90 min] (%)	0.0	0.0		0.0	0.0	14.3	0.0
MDNO [2×15 cm or 90 min] (hr)	0.0	0.0		0.0	0.0	0.0	0.0
MDPO [2×15 cm or 90 min] (hr)	0.0	0.0		0.0	0.0	0.0	0.0

Table 16. Summary of skill assessment statistics evaluating the ability of the LSOFS-FVCOM hindcasts to predict extreme low water level events at NOS NWLON stations in Lake Superior during 2018. Gray shading, if present, indicates that it did not meet the NOS acceptance criteria.

Statistic, Acceptable Error [ ], and Units ( )	9099064 Duluth		9099090 Grand Marais		9099018 Marquette C.G.	
	<b>FVCOM</b> N=3		<b>FVCOM</b> N=2		<b>FVCOM</b> N=2	
	Amp.	Time	Amp.	Time	Amp.	Time
Mean Alg. Error (m) (hr)	0.004	0.000	0.066	-0.500	0.048	0.400
RMSE (m) (hr)	0.020	0.816	0.067	0.707	0.057	0.632
SD (m) (hr)	0.024	1.000	0.000	0.707	0.034	0.548
NOF [2×15 cm or 90 min] (%)	0.0	0.0	0.0	0.0	0.0	0.0
CF [15 cm or 90 min] (%)	100.0	100.0	100.0	100.0	100.0	100.0
POF [2×15 cm or 90 min] (%)	0.0	0.0	0.0	0.0	0.0	0.0
MDNO [2×15 cm or 90 min] (hr)	0.0	0.0	0.0	0.0	0.0	0.0
MDPO [2×15 cm or 90 min] (hr)	0.0	0.0	0.0	0.0	0.0	0.0

Statistic, Acceptable Error [ ], and Units ( )	9099004 Point Iroquois		9099044 Ontonagon	
	<b>FVCOM</b> N=10		<b>FVCOM</b> N=2	
	Amp.	Time	Amp.	Time
Mean Alg. Error (m) (hr)	0.044	0.100	0.031	-1.000
RMSE (m) (hr)	0.069	1.049	0.039	1.414
SD (m) (hr)	0.056	1.101	0.033	1.414
NOF [2×15 cm or 90 min] (%)	0.0	0.0	0.0	0.0
CF [15 cm or 90 min] (%)	100.0	80.0	100.0	50.0
POF [2×15 cm or 90 min] (%)	0.0	0.0	0.0	0.0
MDNO [2×15 cm or 90 min] (hr)	0.0	0.0	0.0	0.0
MDPO [2×15 cm or 90 min] (hr)	0.0	0.0	0.0	0.0

### **6.1.3.2. Canadian Lakeshore**

During 2017, the hindcasts overpredicted the extreme low-water events at the three CHS gauges. MAEs ranged from 6.7 cm at Thunder Bay to 9.5 cm at Rosspport. The RMSEs ranged from 7.3 cm at Michipicoten to 9.7 cm at Rosspport. Nowcasts from the operational LSOFS were available at three of the gauges, although the number of events were not the same. At the three gauges, the average MAE for the hindcasts was 7.7 cm while 13.9 cm for the nowcasts. The average RMSE was 8.4 cm for the hindcasts and 14.1 cm for the nowcasts. The hindcasts passed the NOS acceptance criteria at all three gauges but did not for CF for amplitude at Thunder Bay and CF for timing at Thunder Bay and Rosspport.

During 2018, the hindcasts overpredicted the low water events at the three CHS gauges. MAEs ranged from 4.2 cm at Thunder Bay to 7.2 cm at Rosspport with an average MAE of 5.7cm. RMSEs ranged from 5.2 cm at Thunder Bay to 7.7 cm at Rosspport with an average 6.8 cm. The hindcasts passed the acceptance criteria at all three gauges except for CF for timing at Thunder Bay and Rosspport.

Table 17. Summary of skill assessment statistics evaluating the ability of LSOFS-FVCOM hindcasts and LSOFS-POMGL nowcasts to predict extreme low water level events at CHS gauges in Lake Superior during 2017. Gray shading, if present, indicates that it did not meet the NOS acceptance criteria.

Statistic, Acceptable Error [ ], and Units ( )	C10050 Thunder Bay				C10220 Rosspport			
	FVCOM		POMGL		FVCOM		POMGL	
	N=7		N=6		N=3		N=4	
	Amp.	Time	Amp.	Time	Amp.	Time	Amp.	Time
Mean Alg. Error (m) (hr)	0.067	0.143	0.131	1.000	0.095	-0.333	0.152	0.750
RMSE (m) (hr)	0.081	1.254	0.133	1.528	0.097	1.732	0.155	1.323
SD (m) (hr)	0.049	1.345	0.021	1.265	0.027	2.082	0.032	1.258
NOF [2×15 cm or 90 min] (%)	0.0	0.0	0.0	0.0	0.0	0.0	0.0	0.0
CF [15 cm or 90 min] (%)	85.7	71.4	66.7	50.0	100.0	33.3	50.0	75.0
POF [2×15 cm or 90 min] (%)	0.0	0.0	0.0	0.0	0.0	0.0	0.0	0.0
MDNO [2×15 cm or 90 min] (hr)	0.0	0.0	0.0	0.0	0.0	0.0	0.0	0.0
MDPO [2×15 cm or 90min] (hr)	0.0	0.0	0.0	0.0	0.0	0.0	0.0	0.0

Statistic, Acceptable Error [ ], and Units ( )	C10750 Michipicoten			
	FVCOM		POMGL	
	N=5		N=4	
	Amp.	Time	Amp.	Time
Mean Alg. Error (m) (hr)	0.069	-0.200	0.134	0.500
RMSE (m) (hr)	0.073	0.447	0.135	1.000
SD (m) (hr)	0.027	0.447	0.010	1.000
NOF [2×15 cm or 90 min] (%)	0.0	0.0	0.0	0.0
CF [15 cm or 90 min] (%)	100.0	100.0	100.0	75.0
POF [2×15 cm or 90 min] (%)	0.0	0.0	0.0	0.0
MDNO [2×15 cm or 90 min] (hr)	0.0	0.0	0.0	0.0
MDPO [2×15 cm or 90min] (hr)	0.0	0.0	0.0	0.0

Table 18. Summary of skill assessment statistics evaluating the ability of LSOFS-FVCOM hindcasts to predict extreme low water level events at CHS gauges in Lake Superior during 2018. Gray shading, if present, indicates that it did not meet the NOS acceptance criteria.

Statistic, Acceptable Error [ ], and Units ( )	C10050 Thunder Bay		C10220 RosSPORT		C10750 Michipicoten	
	<b>FVCOM</b>		<b>FVCOM</b>		<b>FVCOM</b>	
	N=6		N=3		N=6	
	Amp.	Time	Amp.	Time	Amp.	Time
Mean Alg. Error (m) (hr)	0.042	-0.500	0.072	-0.667	0.057	0.000
RMSE (m) (hr)	0.052	0.913	0.077	1.155	0.076	0.577
SD (m) (hr)	0.034	0.837	0.031	1.155	0.056	0.632
NOF [2×15 cm or 90 min] (%)	0.0	0.0	0.0	0.0	0.0	0.0
CF [15 cm or 90 min] (%)	100.0	83.3	100.0	66.7	100.0	100.0
POF [2×15 cm or 90 min] (%)	0.0	0.0	0.0	0.0	0.0	0.0
MDNO [2×15 cm or 90 min] (hr)	0.0	0.0	0.0	0.0	0.0	0.0
MDPO [2×15 cm or 90 min] (hr)	0.0	0.0	0.0	0.0	0.0	0.0

## 6.2. Assessment of Surface Water Temperature Hindcasts

The results of the skill assessment of hourly hindcasts of surface water temperatures for 2017 and 2018 are given in this section for nearshore and offshore/open lake buoys. The assessment results were separated into these two areas because of the unique water temperature fluctuations found in the observations and hindcasts in these two areas. Buoys in the nearshore have water depths that ranged from 25 to 49 m at 45023 and 45173, respectively while the depths at the buoys in the open lake ranged from 170 to 247 m at 45136 and 45001, respectively. In addition, skill results of POMGL-based LSOFS nowcasts for 2017 are provided as well.

### 6.2.1. Open Lake

The time series plots (Fig. 22) indicate that the hindcasts overestimated the rate and amplitude of the spring warmup at all offshore buoys in 2017. The nowcasts from the operational LSOFS exhibited the same overestimation. The hindcasts and the nowcasts matched the observations very well from approximately Day 220 onwards at the three buoys. The MAEs for the hindcasts ranged from 1.8 to 3.2 °C. The RMSEs ranged from 3.3 to 4.1 °C. The MAEs and RMSEs were similar to those for the nowcasts at the three buoys. The 2017 hindcasts failed to pass the

acceptance criteria for CF, POF, MDNO, and MDPO (Table 19). The 2017 nowcasts also failed to criteria for these statistics.

For 2018, the hindcasts again overestimated the rate and amplitude of the spring warmup (Fig. 23). The MAEs for the hindcasts ranged from 2.2 to 3.2 °C across the four buoys where the hindcasts were evaluated at. The RMSEs ranged from 2.4 to 3.8 °C. The 2018 hindcasts failed to pass the NOS acceptance criteria for POF and MDPO at three of the buoys (Table 20) and failed to pass the CF criteria at all four buoys.

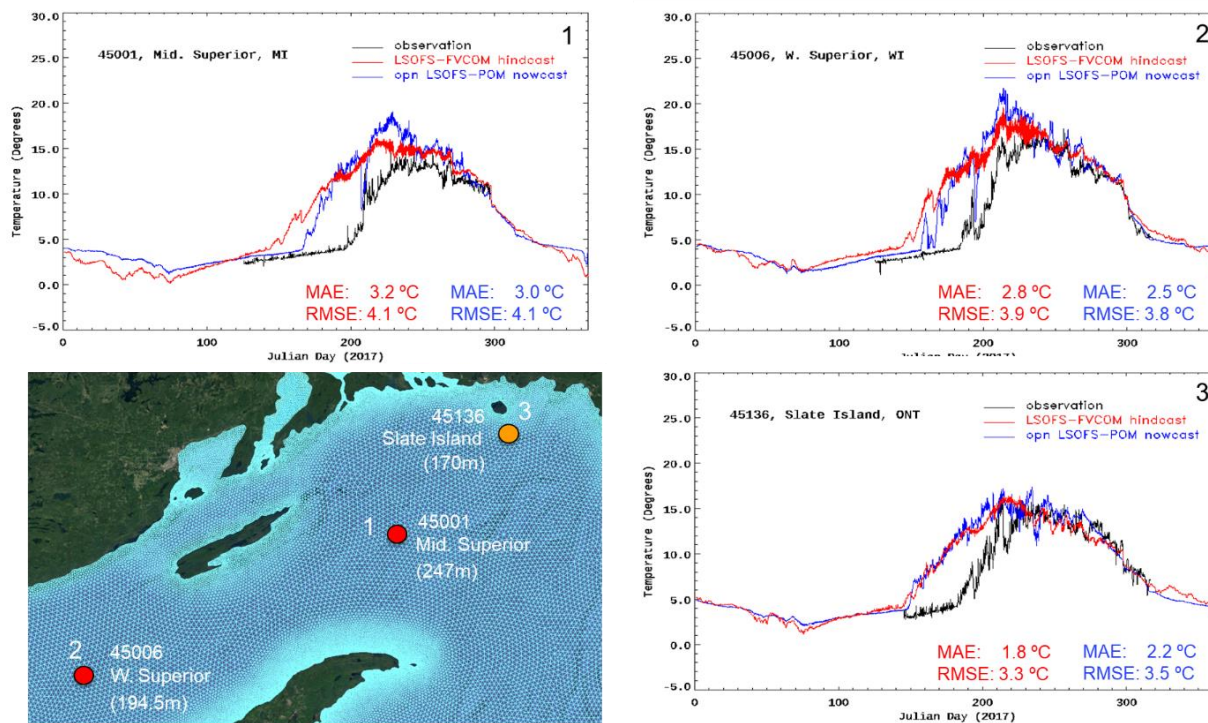


Figure 22. Time series plots of hourly LSOFS-POMGL nowcasts (blue) and LSOFS-FVCOM hindcasts of surface water temperature (red) vs. observations (black) at NDBC and buoys (1. 45001, Mid. Superior, MI, 2. 45006, W. Superior, MI, and 3. 45136, and Slate Island, ON during 2017. MAE and RMSE (°C) at each station are shown individually on each panel.

Table 19. Summary of skill assessment statistics of the hourly LSOFS-FVCOM hindcasts and LSOFS-POMGL nowcasts of surface water temperature at NDBC and ECCC fixed buoys in Lake Superior during 2017. Gray shading, if present, indicates that it did not meet the NOS acceptance criteria.

Time Period, Statistic, Acceptable Error [ ], and Units ( )		45001 Mid. Superior		45006 W. Superior		45136 Slate Island	
Time Period	Begin	06/06/2017		07/08/2017		07/05/2017	
	End	10/23/2017		09/24/2017		11/12/2017	
Model		FVCOM	POMGL	FVCOM	POMGL	FVCOM	POMGL
N		4069	4069	4570	4570	4097	4097
Mean Alg. Error (°C)		3.238	3.015	2.769	2.507	1.816	2.158
RMSE (°C)		4.089	4.101	3.851	3.759	3.299	3.519
SD (°C)		2.498	2.781	2.677	2.801	2.754	2.779
NOF [2×3°C] (%)		0.0	0.0	0.0	0.0	0.0	0.0
CF [3°C] (%)		58.2	62.1	66.9	66.5	65.5	62.7
POF [2×3°C] (%)		20.4	18.6	18.9	16.7	11.3	12.2
MDNO [2×3°C] (hr)		0.0	0.0	0.0	0.0	0.0	0.0
MDPO [2×3°C] (hr)		527.0	493.0	376.0	238.0	119.0	159.0

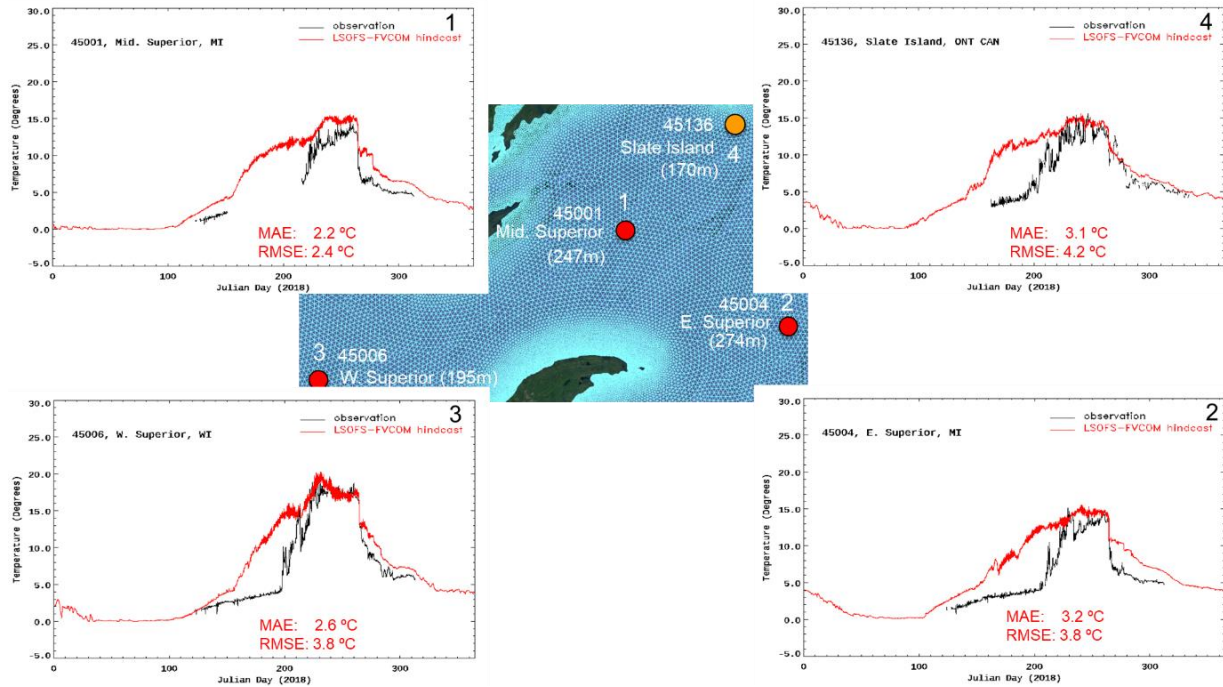


Figure 23. Time series plots of hourly LSOFS-FVCOM hindcasts of surface water temperature (red) vs. observations (black) at NDBC and ECCC buoy (1. 45001, Mid. Superior, MI, 2. 45004, E. Superior, MI, 3. 45006, W. Superior, WI, and 4. 45136, Slate Island, ON, during 2018. MAE and RMSE (°C) at each station are shown individually on each panel.

Table 20. Summary of skill assessment statistics of the hourly LSOFS-FVCOM hindcasts of surface water temperatures at open lake NDBC and ECCC fixed buoys in Lake Superior during 2018. Gray shading, if present, indicates that it did not meet the NOS acceptance criteria.

Time Period, Statistic, Acceptable Error [ ], and Units ( )		45001 Mid. Superior	45004 E. Superior	45006 W. Superior	45136 Slate Island
Time Period	Begin	08/03/2018	07/28/2018	08/17/2018	06/11/2018
	End	11/08/2018	11/08/2018	11/09/2018	07/26/2018
Model		<b>FVCOM</b>	<b>FVCOM</b>	<b>FVCOM</b>	<b>FVCOM</b>
N		2916	4430	4446	3317
Mean Alg. Error (°C)		2.222	3.222	2.628	3.094
RMSE (°C)		2.443	3.837	3.787	4.197
SD ( )		1.016	2.084	2.727	2.835
NOF [2×3°C] (%)		0.0	0.0	0.0	0.0
CF [3°C] (%)		77.2	54.8	69.9	59.7
POF [2×3°C] (%)		0.3	12.4	16.5	26.8
MDNO [2×3°C] (hr)		0.0	0.0	0.0	0.0
MDPO [2×3°C] (hr)		4.0	448.0	624.0	596.0

### 6.2.2. Nearshore Buoys

The hindcasts matched observations more closely at nearshore buoys compared to the open lake buoys (Fig. 24), including the prediction of the spring warmup. When comparing performance among the six the buoys, the hindcasts did not match observations as well at Buoy 45027, located 10 miles off McQuade Harbor, and at Buoy 45025 located at the South Entry of the Keweenaw Waterway. The depth of the water temperature sensors at these two buoys is 3 m. At 45027, the hindcasts exhibited high-frequency fluctuations that were not seen in the observations. At 45025, the hindcasts were cooler than the observations. The MAEs and RMSEs at the four buoys ranged from -2.1 to 0.7 °C and 1.5 to 3.5 °C, respectively. The 2017 hindcasts at three of the nearshore buoys came close to meeting all NOS acceptance criteria, but the hindcasts at 45027 failed to meet the criteria for three statistics (Table 21).

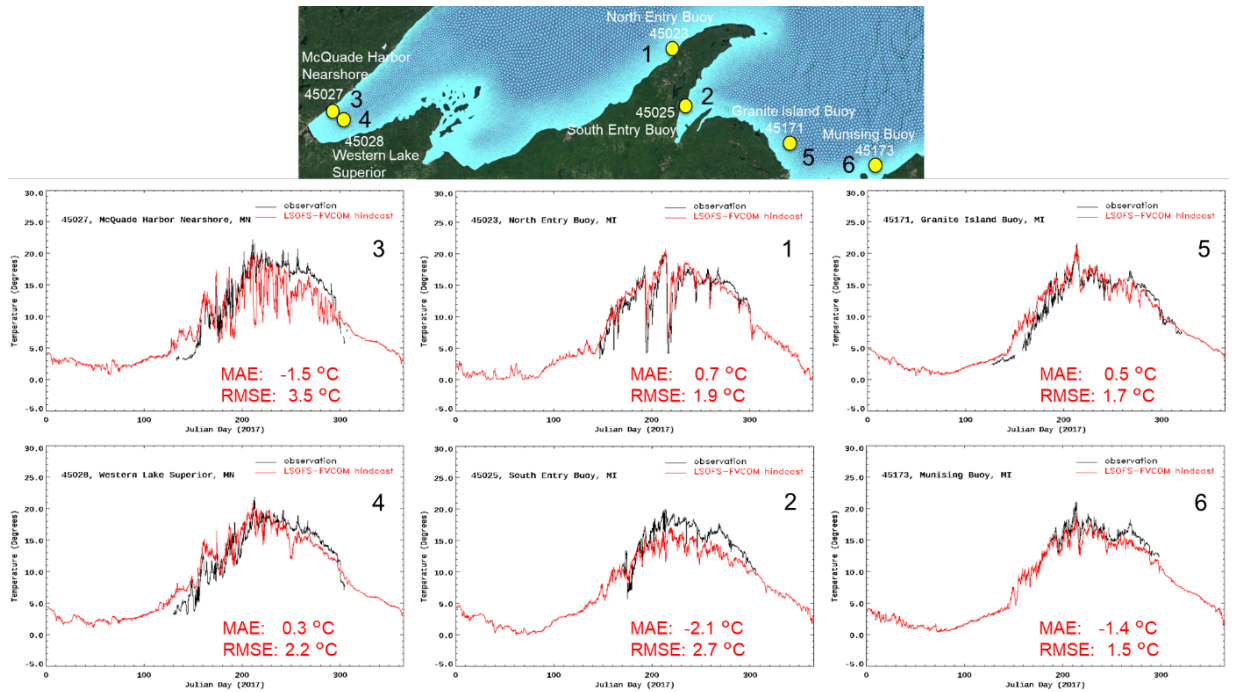


Figure 24. Time series plots of hourly LSOFS-FVCOM hindcasts of surface water temperature (red) vs. observations (black) at GLOS nearshore buoys (1. 45023, North Entry Buoy, MI, 2. 45025 South Entry Buoy, MI, 3. 45027, McQuade Harbor Nearshore, MN, 4. 45028, Western Lake Superior, MN, 5. 45171, Granite Island Buoy, MI, and 6. 45173, Munising Buoy, MI) during 2017. MAE and RMSE (°C) at each station are shown individually on each panel.

Table 21. Summary of skill assessment statistics of the hourly LSOFS-FVCOM hindcasts of surface water temperatures at GLOS stations and the fixed buoys in Lake Superior during 2017. Gray shading, if present, indicates that it did not meet the NOS acceptance criteria.

Time Period, Statistic, Acceptable Error [ ], and Units ( )		45023 North Entry Buoy	45025 South Entry Buoy	45027 McQuade Harbor Nearshore	45028 Western Lake Superior
Time Period	Begin	09/01/2017	06/19/2017	09/05/2017	06/11/2017
	End	10/27/2017	11/01/2017	10/08/2017	10/31/2017
Model		<b>FVCOM</b>	<b>FVCOM</b>	<b>FVCOM</b>	<b>FVCOM</b>
N		3615	3264	3458	4172
Mean Alg. Error (°C)		0.702	-2.119	-1.511	0.329
RMSE (°C)		1.865	2.652	3.548	2.184
SD (°C)		1.728	1.594	3.211	2.159
NOF [2×3°C] (%)		0.0	0.4	8.1	0.1
CF [3°C] (%)		92.0	72.0	59.4	83.2
POF [2×3°C] (%)		1.3	0.0	0.0	0.0
MDNO [2×3°C] (hr)		0.0	12.0	78.0	1.0
MDPO [2×3°C] (hr)		20.0	0.0	0.0	0.0

Time Period, Statistic, Acceptable Error [ ], and Units ( )		45171 Granite Island Buoy	45173 Munising Buoy
Time Period	Begin	09/21/2017	09/21/2017
	End	11/07/2017	10/25/2017
Model		<b>FVCOM</b>	<b>FVCOM</b>
N		4128	2527
Mean Alg. Error (°C)		0.479	-1.362
RMSE (°C)		1.679	1.516
SD (°C)		1.610	0.667
NOF [2×3°C] (%)		0.0	0.0
CF [3°C] (%)		90.0	98.4
POF [2×3°C] (%)		0.0	0.0
MDNO [2×3°C] (hr)		0.0	0.0
MDPO [2×3°C] (hr)		0.0	0.0

The 2018 hindcasts at the nearshore buoys, like the ones for 2017, matched observations more closely than at the open lake buoys (Fig. 25) and the spring warmup. Again, the hindcasts at 45027, exhibited high-frequency fluctuations that were not seen in the observations. The MAEs and RMSEs at the four buoys ranged from -0.5 to 1.2 °C and 1.7 to 3.1 °C, respectively. The hindcasts passed all NOS acceptance criteria at 45173, failed two criteria at 45023, and failed three criteria at 45027 and 45028 (Table 22).

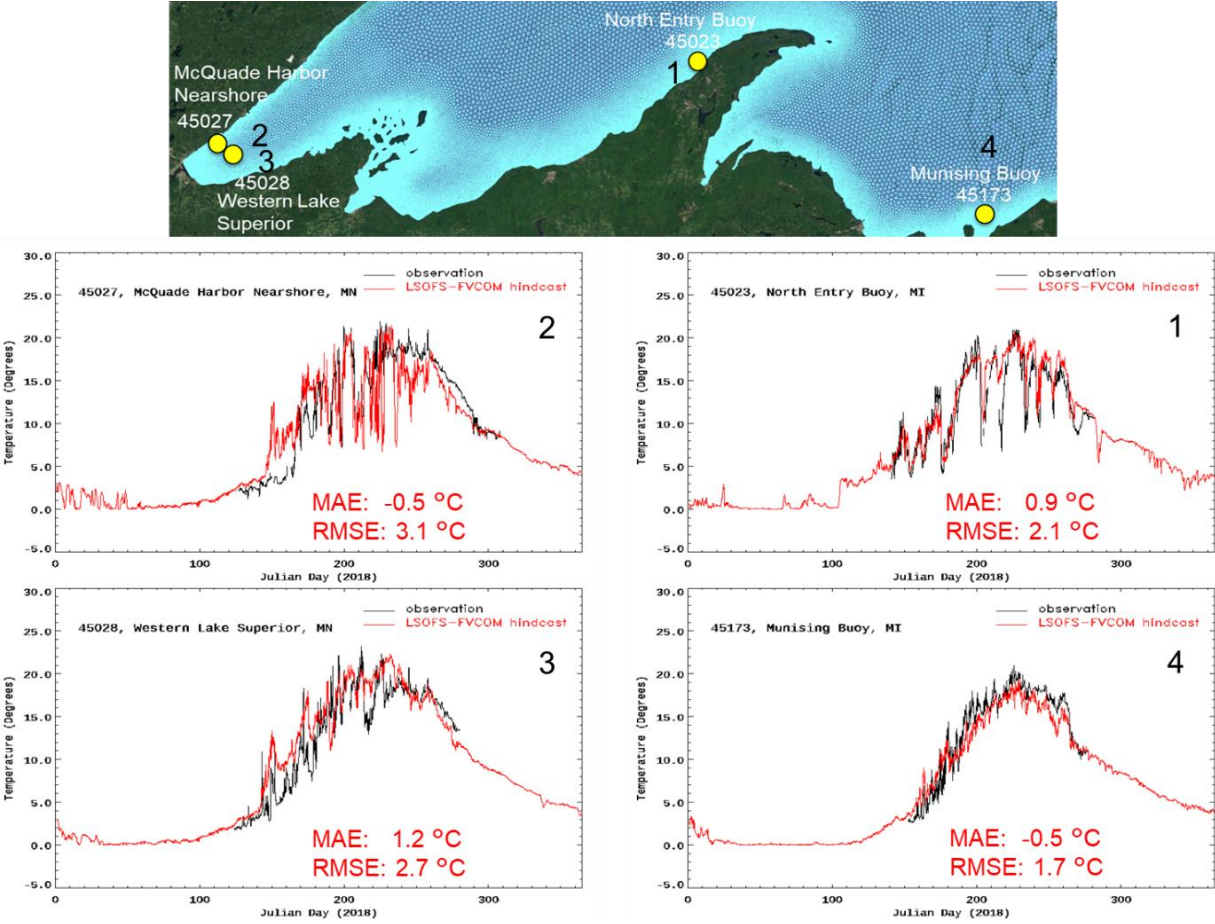


Figure 25. Time series plots of hourly LSOFS-FVCOM hindcasts of surface water temperature (red) vs. observations (black) at GLOS nearshore buoys (1. 45023, North Entry Buoy, MI, 2. 45027, McQuade Harbor Nearshore, MN, 3. 45028, Western Lake Superior, MN, and 4. 45173, Munising Buoy, MI) during 2018. MAE and RMSE (°C) at each station are shown individually on each panel.

Table 22. Summary of skill assessment statistics of the hourly LSOFS-FVCOM hindcasts of surface water temperatures at GLOFS stations and the fixed buoys in Lake Superior during 2018. Gray shading, if present, indicates that it did not meet the NOS acceptance criteria.

Time Period, Statistic, Acceptable Error [ ], and Units ( )		45023 North Entry Buoy	45027 McQuade Harbor Nearshore	45028 Western Lake Superior	45173 Munising Buoy
Time Period	Begin	05/21/2018	09/30/2018	05/04/2018	06/18/2018
	End	07/22/2018	11/04/2018	07/19/2018	06/28/2018
Model		<b>FVCOM</b>	<b>FVCOM</b>	<b>FVCOM</b>	<b>FVCOM</b>
N		3136	3800	3591	2189
Mean Alg. Error (°C)		0.875	-0.505	1.194	-0.470
RMSE (°C)		2.142	3.090	2.699	1.731
SD (°C)		1.955	3.049	2.420	1.666
NOF [2×3°C] (%)		0.0	4.7	0.3	0.0
CF [3°C] (%)		86.5	72.4	71.8	93.7
POF [2×3°C] (%)		2.1	0.7	2.4	0.1
MDNO [2×3°C] (hr)		0.0	45.0	4.0	0.0
MDPO [2×3°C] (hr)		24.0	5.0	38.0	0.0

### 6.3. Assessment of Sub-Surface Water Temperature Hindcasts

Observations of sub-surface water temperature measured by two buoys' thermistor chains (Buoys 45025 and 45028) were used to evaluate the hindcasts of the vertical thermal structure in the western part of Lake Superior. The duration of the observations varied at the two locations in 2017, but were generally from mid-June to Nov. 1<sup>st</sup>. However, for 2018 only observations from the thermistor chain at Buoy 45028 were available. Figures 26 to 28 depicts the hindcasts vs. observations at eight to nine depths ranging from 3 m to 35 m along with MAE and RMSE values. The summary table of the MAEs and RMSEs at the different depths for the 2017 and 2018 hindcasts can be found in Table 23.

At Buoy 45025 located near the south entry to the Keweenaw Waterway in waters of approximately 35 depth, the hindcasts underestimated the water temperatures at the 3 – 12 m depths starting at approximately Day 200 (July 19<sup>th</sup>). The MAEs for these depths ranged from -1.60 to -2.26 °C with the RMSEs of 2.30 °C to 2.88 °C. At the mid and lower depths (16 – 32 m) where observations depicted rapid, high amplitude temperatures, the hindcasts captured the very well timing of these changes of water temperatures until approximately Day 260 (Sept. 17<sup>th</sup>), but not as well for the

amplitudes. However, from Day 260 to approximately Day 300 (Oct. 27<sup>th</sup>), the hindcasts did not simulate well the timing or amplitude of the rapid changes. For the 16 – 32 m depths, MAE values were negative at 16 m and 19 m depths, then positive from 22 m to the final depth at 32 m. RMSE values were around 2.3 °C.

At the buoy 45028 in the western arm of Superior, which is in deeper water (49 m), the average RMSE for the hindcasts was 2.83 °C for 2017. At 3 m and 5 m depths, the hindcasts closely matched observations until approximately Day 230 (Aug. 18<sup>th</sup>) and then were cooler than observations. The MAEs were 0.5 °C or less. For depths 10 to 30 m, the hindcasts were much cooler than observations from about Day 200 (July 19<sup>th</sup>). MAEs ranged from -0.6 °C at 30 m to -2.3 °C at 15 m with RMSEs ranging from 2.7 °C to 3.6 °C. One of the most noticeable differences between hindcasts and observations, was the failure of hindcasts to capture the three peaks centered around Days 200, 230 and 270 (Sept. 27<sup>th</sup>). During the last peak, the observed temperatures rose from 5 °C to 15 °C in a few days which was not seen in the hindcasts.

During 2018, at 45028 the hindcasts overestimated water temperatures at the 3 and 6 m depths until about Day 240 (Aug. 28<sup>th</sup>) and then closely matched observations. MAEs averaged 1.5 °C with an RMSE of 2.8 °C. At depths of 10 to 20 m, the hindcasts ran warmer than observations until about Day 230 (Aug. 18<sup>th</sup>) and then cooler afterwards with MAEs of -0.1 °C to -0.4 °C and RMSEs of 2.3 °C to 2.9 °C. At the lower depths of 25 to 35 m, hindcasts overestimated until about Day 260 (Sep. 17) and then were cooler than observations during an extended spike in the hindcasts which occurred from approximately Day 260 to 280 (Sept. 27<sup>th</sup>). MAEs ranged from -0.2 °C to 0.6 °C with an average RMSE of 2.0 °C. At Duluth International Airport, daily air temperatures ran 10 – 19 °F above normal from Sept. 11<sup>th</sup> through the 17<sup>th</sup> with maximum temperatures around 26.7 °C (80 °F) along with peak wind gusts of 54.7 to 70.8 km/hr (34 to 44 MPH) during Sept. 20-23<sup>rd</sup>.

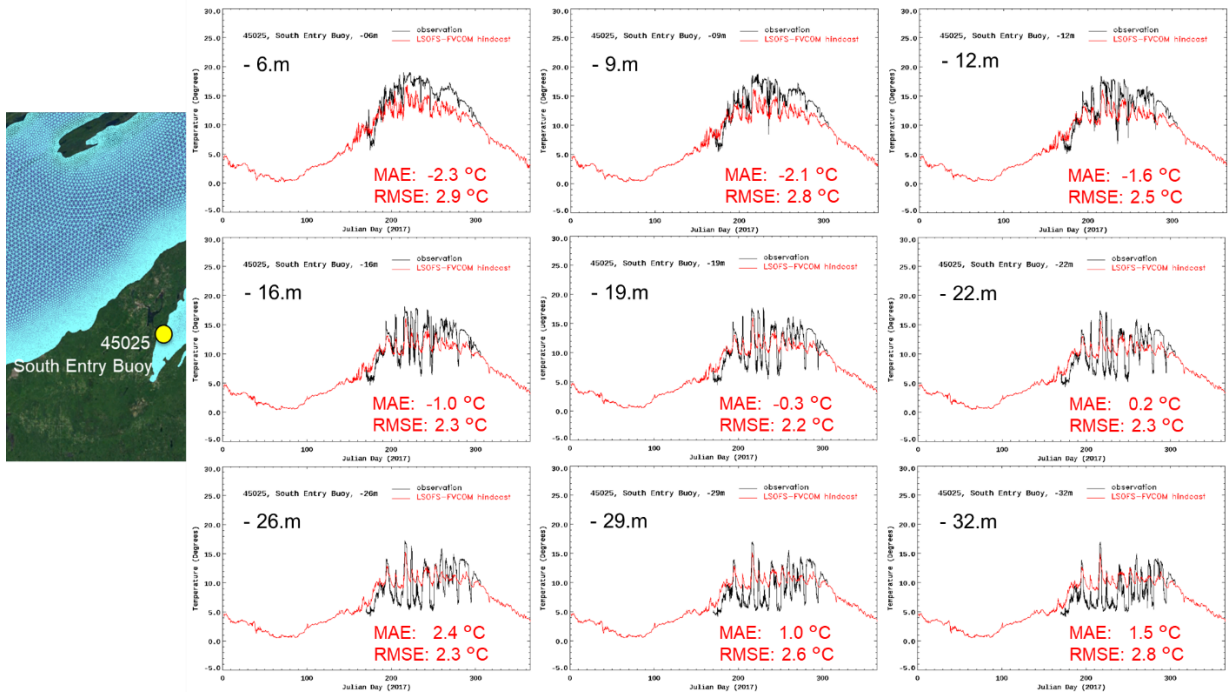


Figure 26. Time series plots of 2017 hourly LSOFS-FVCOM hindcasts of sub-surface water temperature (red) at nine depths vs. observations (black) at the GLOS buoy 45025, South Entry Buoy.

Table 23. Summary of skill assessment statistics of the hourly LSOFS-FVCOM hindcasts of sub-surface water temperatures at GLOS buoys 45025 for 2017 and 45028 for 2017 and 2018.

45025 South Entry Buoy			45028 Western Lake Superior		
Depth (m)	Statistics		Depth (m)	Statistics	
	MAE (°C)	RMSE (°C)		MAE (°C)	RMSE (°C)
	06/19/2017 – 11/01/2017			06/11/2017 – 10/31/2017	
6	-2.260	2.882	3	0.498	2.248
9	-2.087	2.791	5	0.177	2.178
12	-1.601	2.512	10	-1.286	2.764
16	-0.988	2.301	15	-2.261	3.610
19	-0.317	2.228	20	-2.048	3.457
22	0.173	2.290	25	-1.482	3.247
26	0.557	2.394	30	-0.571	2.701
29	1.049	2.566	35	0.099	2.419
32	1.488	2.756			
				05/ 04/2018 – 07/19/2018	
			3	1.607	2.838
			5	1.360	2.757
			10	-0.249	2.878
			15	-0.097	2.773
			20	-0.448	2.348
			25	-0.152	1.987
			30	0.155	1.962
			35	0.634	2.084

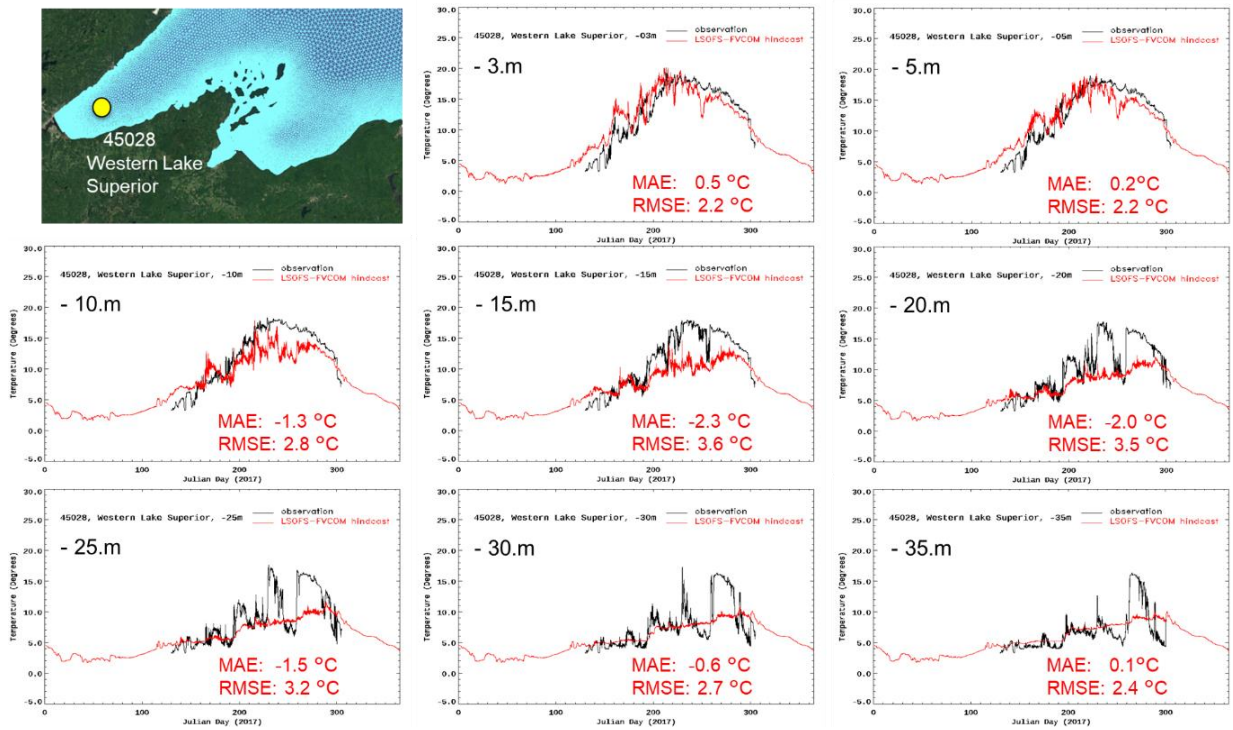


Figure 27. Time series plots of 2017 hourly LSOFS-FVCOM hindcasts of sub-surface water temperature (red) at eight depths vs. observations (black) at GLOS buoy 45028, Western Lake Superior.

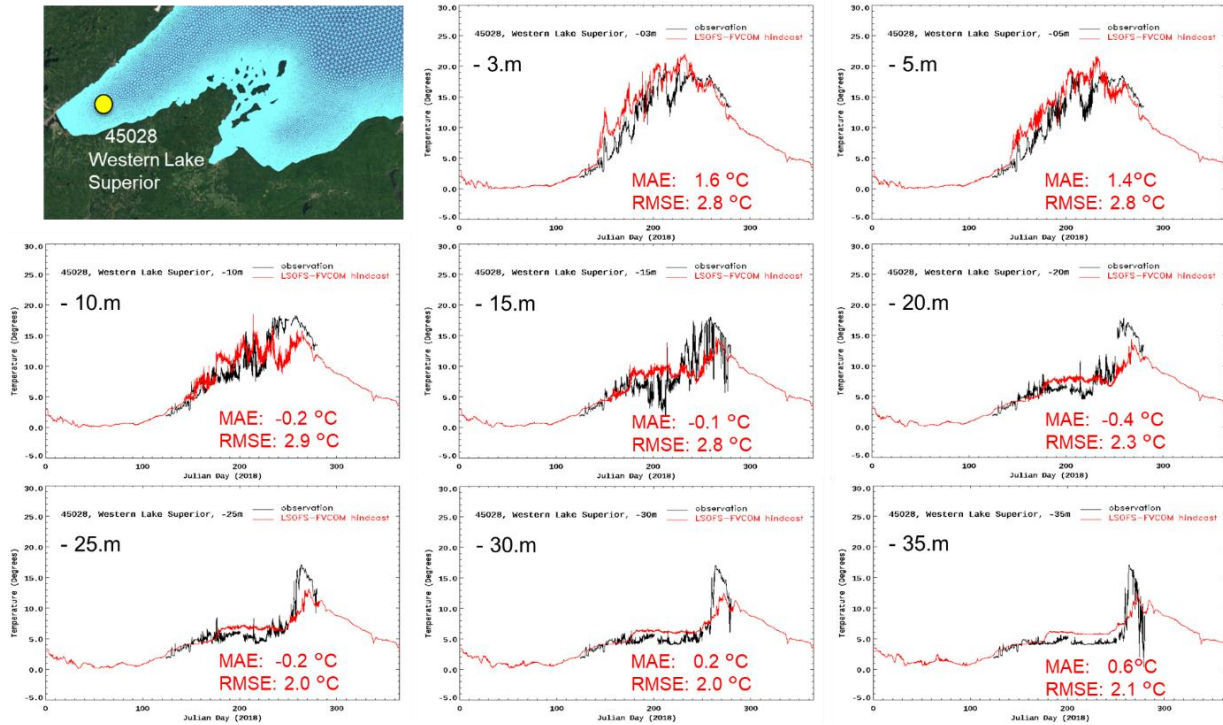


Figure 28. Time series plots of 2018 hourly LSOFS-FVCOM hindcasts of sub-surface water temperature (red) at eight depths vs. observations (black) at GLOS buoy 45028, Western Lake Superior.

#### 6.4. Assessment of Surface Water Currents Hindcasts

Observations of water currents measured at 2 and 5 m depths at the GLOS North Entry Buoy were used to evaluate the hindcasts of surface water currents during 2017 and 2018. The buoy is located at the North Entry of the Keweenaw Waterway. The depth of the water at the buoy is reported to be 25 m. Hindcasts of the direction and speed of the surface water currents vs. observations along with MAE and RMSE at 2 and 5 m depths are depicted in Figures 29 and 30, respectively.

The MAE and RMSE values on the plots are for those hindcasts where both the hindcasts and observations had speeds greater than 0.26 m/s. The NOS model skill assessment software only uses currents greater than 0.26 m/s to calculate skill metrics for water current direction hindcasts. Unlike the coastal ocean, the lake current generally low, ranges from about 5-20 cm/s (<http://www.geo.mtu.edu/KeweenawGeoheritage/Lake/Currents.html>), therefore the CFs and other statistics will not be discussed here.

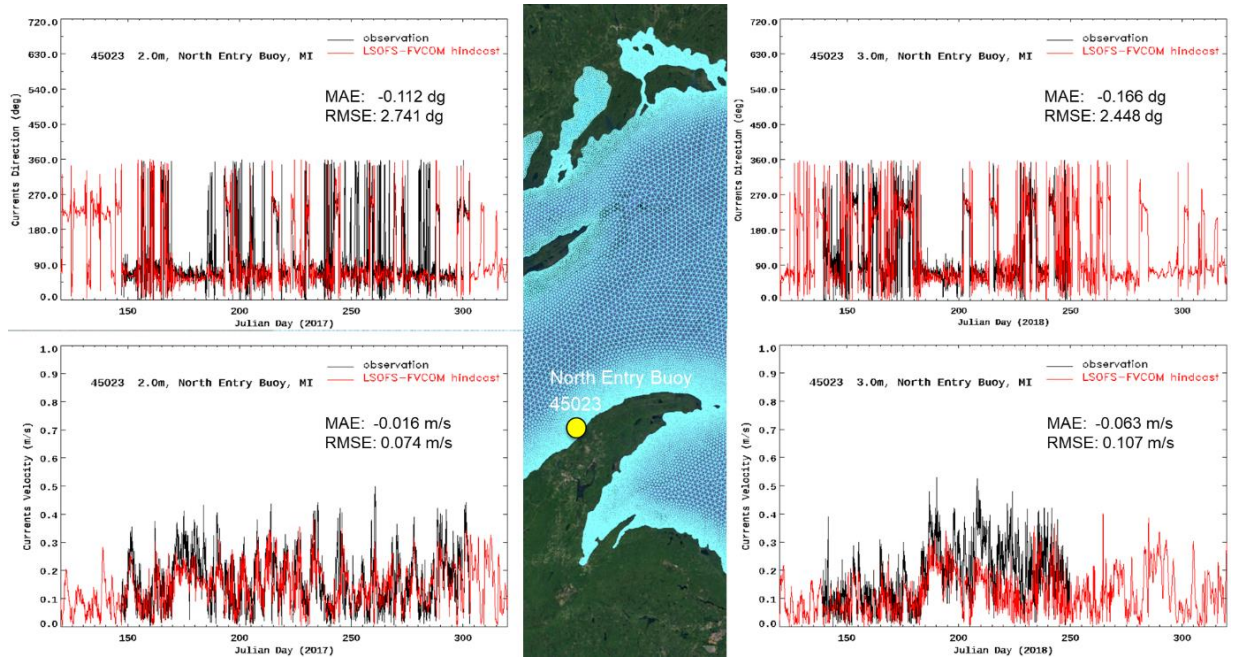


Figure 29. Time series plots of 2017 (left) and 2018 (right) hourly LSOFS-FVCOM hindcasts of water currents at top obs-layer (-2.0 m in 2017, and -3.0 m in 2018) (red) vs. observations (black) at the GLOS North Entry Buoy 45023. The upper plots are current directions in degrees and the lower plots are current speeds in m/s. The MAE and RMSE values on the plots are for those hindcasts where both the hindcasts and observations had speeds greater than 0.26 m/s.

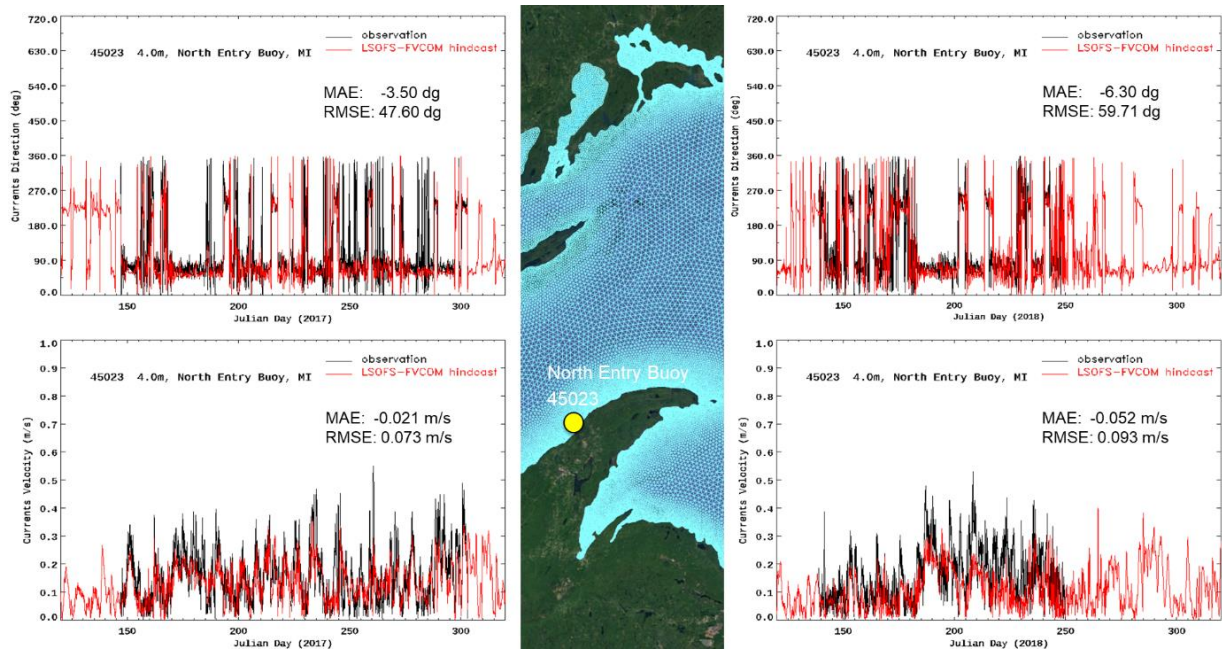


Figure 30. Time series plots of 2017 (left) and 2018 (right) hourly LSOFS-FVCOM hindcasts of water currents at -4.0 m (red) vs. observations (black) at the GLOS North Entry Buoy 45023. The upper plots are current directions in degrees and the lower plots are current speeds in m/s. The MAE and RMSE values on the plots are for those hindcasts where both the hindcasts and observations had speeds greater than 0.26 m/s.



## 7. SUMMARY AND DISCUSSION

NOAA/GLERL ran hindcasts of the FVCOM-based LSOFS using FVCOM V4.3.1 with COARE V2.6. FVCOM was run with the Los Alamos CICE model turned on. Meteorological forcing was based on forecast guidance from NOAA's High-Resolution Rapid Refresh (HRRR) V2 (Jan. 1, 2017 to July 14, 2018) and V3 (July 15 to Dec. 31, 2018). CSDL/CMMB personnel had the responsibility to assess the hindcast skills in collaboration with the GLERL developers.

The hindcasts of water level, water temperature, and currents from the FVCOM-based LSOFS for 2017 and 2018 were compared to in-situ observations in Lake Superior. When possible, the hindcasts were also compared to nowcasts from the present POMGL-based LSOFS. The water level hindcasts were compared to observational data recorded at NOS NWLON and CHS gauges. Due to a linear drift with time in the observations, the water levels were de-biased before comparison to the hindcasts. Water temperature hindcasts were evaluated against observations from NDBC, GLOS, and ECCC fixed buoys, both in the open lake and nearshore. Hindcasts of sub-surface water temperatures were compared to data at two buoys in the western portion of the lake. Hindcasts of surface currents at 2 m and 5 m depths were compared to observations at only one location.

### *Water Levels*

Hindcasts of water levels for 2017 and 2018 demonstrated good skill for simulating hourly water levels during both years. The RMSE ranged from approximately 3 cm to 6 cm at locations at U.S. gauges and 2.7 cm to 4 cm at the Canadian gauges. The NOS acceptance criteria was met at all U.S. and Canadian gauges. In comparison to 2017 nowcasts, the average RMSE for hindcasts at U.S. gages was 4.2 cm while the average for the nowcasts was 5.6 cm. At Canadian gauges, the average RMSE for hindcasts and nowcasts were 3.3 cm and 5.0 cm, respectively. Thus overall, the hindcasts did better at predicting water levels than the nowcasts. However, it is not known whether this is due to FVCOM, the meteorological forcing (i.e. interpolation of in-situ surface weather observations used by present PMGL-LSOFS vs. HRRR predictions for FVCOM-LSOFS). The hindcasts did well at predicting the amplitudes of extreme high and low water level events with the acceptance criteria being met at the majority of gauges. However, the CF criteria for timing was not met at several of the U.S. and Canadian gauges.

### *Surface Water Temperatures*

Hindcasts at open lake buoys for 2017 and 2018 did well in predicting the surface water temperatures from late August into late Autumn. However, the hindcasts overestimated the rate and amplitude of the spring warmup during both years. The same problem also exists in the nowcasts. The MAE for the hindcasts ranged from 1.8 °C to 3.2 °C in 2017 and 2.2 °C to 3.2 °C in 2018. The average RMSE was 3.75 °C for 2017 and 3.57 °C for 2018. For 2017, these values are similar for the nowcasts (nowcasts were not available during 2018). The water temperature

hindcasts at open lake locations did not meet the NOS acceptance criteria for CF, POF, and MDPO at the majority of the buoys during both years.

The hindcasts at nearshore buoys more closely matched observations compared to the hindcasts at the open lake buoys, including the prediction of the rate of the spring warmup during both 2017 and 2018. The MAEs for the hindcasts ranged from -1.5 to 0.7 °C in 2017 and -0.5 °C to 1.2 °C in 2018. The average RMSE was 2.56 °C for 2017 and 2.42 °C for 2018. The hindcasts did the worse at Buoy 45027, 10 miles off McQuade Harbor near Duluth where the hindcast exhibited high frequency fluctuations that were not seen in the observations. At this buoy, the RMSE was 3.5 °C. Similar high frequency fluctuations were seen in the water level hindcasts at the nearby NOS Duluth gauge, especially during extreme water level events and when HRRR V2 predictions were used to force the hindcasts (Jan. 1, 2017 to July 14, 2018). The water temperature hindcasts at nearshore locations came close to meeting all NOS acceptance criteria at the majority of sites but not at 45027.

### *Subsurface Water Temperatures*

The evaluation of the hindcasts of sub-surface water temperatures were limited to just two buoy locations: just offshore of Duluth and at the south entry of Keweenaw Waterway where the lake depth is less than 50 m. The evaluation took place from about June 1<sup>st</sup> to November 1<sup>st</sup> of 2017 and 2018. The average RMSE for both locations across all depths during 2017 was 2.67 °C. During 2018, there were only observations from one buoy. The average RMSE at this buoy across all depths for 2018 was 2.54 °C. The hindcasts had the most difficulty in capturing the sudden high amplitude temperature changes at depths from 15 m to 35 m during 2017 at the buoy off Duluth.

### *Water Currents*

Hindcasts at two depths (2 m and 4 m) were compared to observations at the GLOS North Entry Buoy near Keweenaw Waterway. The MAEs for speed ranged from -1.6 cm/s to -6.3 cm/s and RMSEs ranged from 7.3 cm/s to 10.7 cm/s.

The LSOFS-FVCOM code package was delivered to NOS/CO-OPS for setting up semi-operational nowcast/forecast runs on NOAA's WCOSS in FY2020 Q4. CO-OPS made changes in the specification of the lateral boundary conditions and in the choice of surface meteorological forcing in comparison to the semi-operational runs conducted by GLERL on their computer infrastructure. CO-OPS began semi-operational nowcast/forecast runs in the Autumn of 2020. CO-OPS will continue their runs into 2022. It is anticipated that the upgraded LSOFS will become operational on WCOSS sometime during the summer of 2022 along with the upgraded LOOFS.

## **ACKNOWLEDGEMENTS**

The upgrade of LSOFS to FVCOM, its evaluation, and implementation on NOAA's WCOSS is a collaborative cross-NOAA project between OAR/GLERL, NOS/OCS/CSDL, NOS/CO-OPS, and NWS/NCEP Central Operations.

We express our thanks to the reviewers Wei Wu, Lei Shi, and Mojgan Rostaminia for their helpful comments and suggestions to improve this report.



## REFERENCES

- Anderson, E.J., A. Fujisaki-Manone, J. Kressler, G.A. Lang, P. Y. Chu, J.G.W. Kelley, Y. Chen, and J. Wang, 2018: Ice forecasting in the next-generation Great Lakes Operational Forecast System (GLOFS). *J. Marine Science and Engineering*, 6, 123, doi:10.3390/jmse6040123.
- Bechle, A., C. Wu, D.A.R. Kristovich, E. J. Anderson, D. J. Schwab, and A. B. Rabinovich, 2016: Meteotsunamis in the Laurentian Great Lakes. *Scientific Reports*, 6, 37832, [doi.org/10.1038/srep37832](https://doi.org/10.1038/srep37832).
- Benjamin, S.G., S.S. Weygandt, J.M. Brown, M. Hu, C.R. Alexander, T.G. Smirnova, J.B. Olson, E.P. James, D.C. Dowell, G.A. Grell, H. Lin, S.E. Peckham, T.L. Smith, W.R. Moninger, J.S. Kenyon, and G.S. Manikin, 2016: A North American Hourly Assimilation and Model Forecast Cycle: The Rapid Refresh. *Mon. Wea. Rev.*, 144, 1669–1694. (Available at <https://www.glerl.noaa.gov/pubs/fulltext/2017/20170011.pdf>).
- Boyce, F.M., M.A. Donelan, P.F. Hamblin, C.R. Murthy and T.J. Simons, 1989: Thermal structure and circulation in the Great Lakes, *Atmosphere-Ocean*, 27:4, 607-642, DOI: [10.1080/07055900.1989.9649358](https://doi.org/10.1080/07055900.1989.9649358).
- Brian P. Neff and J.R. Nicholas, 2005: Uncertainty in the Great Lakes Water Balance. Scientific Investigations Report 2004-5100, U.S. Geological Survey, Reston, Virginia: 2005.
- Chen, C., N. Liu, and R. Beardsley, 2003: An unstructured grid, finite-volume, three-dimensional primitive equations ocean model: Application to coastal ocean and estuaries. *J. Atmos. Oceanic Technol.*, 20, 159-186.
- Chen, C., H. Huang, R. Beardsley, H. Liu, Q. Xu, and G. Cowles, 2007: A finite volume numerical approach for coastal ocean circulation studies: Comparisons with difference models. *J. Geophys. Res.*, 112, C03018.
- Chen, C., R. Beardsley, G. Cowles, J. Qi, Z. Lai, G. Gao, D. Stuebe, Q. Xu, P. Xue, J. Ge, S. Hu, R. Tian, H. Huang, L. Wu, and H. Lin, 2013: An Unstructured Grid, Finite-Volume Community Ocean Model FVCOM User Manual, fourth ed., SMAST/UMASSD, Technical Report-13-0701, UMASS-Dartmouth, Dartmouth, MA, 404 pp.

Chu, P., J. G. W. Kelley, A. J. Zhang, and K. W. Bedford, 2007: Skill Assessment of NOS Lake Erie Operational Forecast System (LEOFS). NOAA Technical Memorandum NOS CS 12, Silver Spring, MD, 73 pp (Available at <https://repository.library.noaa.gov/view/noaa/2464>).

Report Prepared by the Vertical Control – Water Levels Subcommittee on behalf of the Coordinating Committee on Great Lakes Basic Hydraulic and Hydrologic Data, 2017: Updating the International Great Lakes Datum (IGLD) (Available at [http://www.greatlakescc.org/wp36/wp-content/uploads/2017/09/IGLD\\_Update\\_20170929\\_220dpi.pdf](http://www.greatlakescc.org/wp36/wp-content/uploads/2017/09/IGLD_Update_20170929_220dpi.pdf))

Fairall, C.W., E.F. Bradley, J.E. Hare, and A.A. Grachev, and J.B. Edson, 2003: Bulk parameterization of air-sea fluxes: updates and verification for the COARE algorithm, *J. Climate*, 16, 571-591.

Foken, T., 2006: 50 Years of the Monin–Obukhov Similarity Theory, *Boundary-Layer Meteorology*, 119, 431–447, doi.org/10.1007/s10546-006-9048-6.

Forum News Service, 2018: Powerful storm hits Duluth; big waves flood Lake Superior shoreline (Available at <https://www.twincities.com/2018/10/10/powerful-storm-hits-duluth-big-waves-flood-lake-superior-shoreline/>).

Fujisaki-Manome, A., G.E. Mann, E.J. Anderson, P.Y. Chu, LE. Fitzpatrick, S.G. Benjamin, E.P. James, T.G. Smirnova, C.R. Alexander, and D.M. Wright, 2020: Improvements to lake-effect snow forecasts using a one-way air-lake model, *Journal of Hydrometeorology*, 21, 2813-2828, (Available at <https://journals.ametsoc.org/view/journals/hydr/21/12/jhm-d-20-0079.1.xml>).

Gill, S. K. 2014: Gap Analysis of the Great Lakes Component of the National Water Level Observation Network (NWLON), NOAA Technical Report NOS 0074, NOAA/National Ocean Service, CO-OPS, Silver Spring, MD (Available at <https://repository.library.noaa.gov/view/noaa/2737>).

Gronewold, A.D., E.J. Anderson and J. Smith, 2019. Evaluating operational hydrodynamic models for real-time simulation of evaporation from large lakes. *Geophysical Research Letters*, 46 (6), 3263-3269. <https://doi.org/10.1029/2019GL082289>.

Heck, J., and M. Craymer, 2021. Updating the International Great Lakes Datum: Enabling the Integration of Water and Land Management in the Great Lakes Region. (Available at

[https://www.fig.net/resources/proceedings/fig\\_proceedings/fig2021/papers/ts05.1/TS05.1\\_heck\\_craymer\\_11046.pdf](https://www.fig.net/resources/proceedings/fig_proceedings/fig2021/papers/ts05.1/TS05.1_heck_craymer_11046.pdf))

Hess, K.W., T. F. Gross, R. A. Schmalz, J.G.W. Kelley, F. Aikman III, E. Wei, and M.S. Vincent, 2003: NOS Standards for Evaluating Operational Nowcast and Forecast Hydrodynamic Model System. NOAA Technical Report NOS CS 17, 48 pp (Available from <https://repository.library.noaa.gov/view/noaa/2460>).

Hunke, E.C., W.H. Lipscomb, A.K. Turner, N. Jeffery, and S. Elliott, 2010: CICE: The Los Alamos Sea Ice Model documentation and software user's manual. Tech. Rep. LA-CC-06-012, 116 pp.

Kantha, L.H. and C.A. Clayson, 2004: On the effect of surface gravity waves on mixing in the oceanic mixed layer. *Ocean Modelling*, 6, 101-124.

Kelley, J.G.W, Y. Chen, E.J. Anderson, G.A. Lang, and J. Xu, 2018: Upgrade of NOS Lake Erie operational forecast system (LEOFS) to FVCOM: Model development and hindcast skill assessment. NOAA Technical Memorandum NOS CS 40, 78 pp (Available at <https://repository.library.noaa.gov/view/noaa/17253>).

Kelley, J.G.W., Y. Chen, E.J. Anderson, G.A. Lang, and M. Peng, 2020: Upgrade of the NOS Lake Michigan and Lake Huron Operational Forecast System to FVCOM: Model Development and Hindcast Skill Assessment. NOAA Technical Memorandum NOS CS 42, 98 pp (Available at <https://repository.library.noaa.gov/view/noaa/23891>).

Mainville, A, and M.R. Craymer, 2005: Present-day tilting of the Great Lakes region based on water level gauges. *GSA Bulletin* (2005) 117 (7-8), 1070-1080 (Available at <https://pubs.geoscienceworld.org/gsa/gsabulletin/article-abstract/117/7-8/1070/2185/Present-day-tilting-of-the-Great-Lakes-region?redirectedFrom=fulltext>).

Mortimer, C. H., E. J. Fee, D. B. Rao and D. J. SchwabFree, 1976: Surface Oscillations and Tides of Lakes Michigan and Superior. *Philosophical Transactions of the Royal Society of London. Series A, Mathematical and Physical Sciences*, Vol. 281, No. 1299 (Jan. 29, 1976), pp. 1-61 (61 pages) (available at <https://doi.org/10.1098/rsta.1976.0020>)

NWS, 2017: Furious Winds and Snow- The October 27th-28th Storm. NWS WFO Duluth, MN (Available at <https://www.weather.gov/dlh/lateoctoberstorm>).

NWS, 2018: Mid-April Storm Review. NWS WFO Duluth, MN (Available at [https://www.weather.gov/dlh/April13th\\_15th2018Stormclc](https://www.weather.gov/dlh/April13th_15th2018Stormclc)).

Peng, M., A. Zhang, E.J. Anderson, G.A. Lang, J.G.W. Kelley, and Y. Chen, 2019: Implementation of the Lakes Michigan and Huron Operational Forecast System (LMHOFS) and the Nowcast/Forecast Skill Assessment, NOAA Technical Report NOS CO-OPS 091, 28 pp. (Available at <https://repository.library.noaa.gov/view/noaa/24001>).

Schmalz, R.A, Jr, 2014: Hydrodynamic model development for the San Francisco Bay Operational Forecast System (SFBOFS), NOAA Technical Report NOS CS 34, Silver Spring, MD, 294 pp (Available at <https://repository.library.noaa.gov/view/noaa/2693>).

Wei, E., Z. Yang, Y. Chen, J.G.W. Kelley, and A. Zhang, 2014: The Northern Gulf of Mexico Operational Forecast System (NGOFS): Model Development and Skill Assessment. NOAA Technical Report NOS CS 33, Silver Spring, MD, 190 pp.

Wei, E., Z. Yang, Y. Chen, J.G.W. Kelley, and A. Zhang, 2015: The Nested Northwest and Northeast Gulf of Mexico Operational Forecast Systems (NWGOFS and NEGOFs): Model Development and Hindcast Skill Assessment. NOAA Technical Report NOS CS 35, Silver Spring, MD, 33 pp.

Zhang, A., K.W. Hess, E. Wei, and E. Myers, 2006: Implementation of Model Skill Assessment Software for Water Levels and Currents. NOAA Technical Report NOS CS 24, 61 pp. (Available at [https://repository.library.noaa.gov/view/noaa/2204/noaa\\_2204\\_DS1.pdf](https://repository.library.noaa.gov/view/noaa/2204/noaa_2204_DS1.pdf)).

Zhang, A., K.W. Hess, and F. Aikman, 2010: User-based skill assessment techniques for operational hydrodynamic forecast systems, *J. Oper. Oceanogr.*, 3(2), 11-24.

## APPENDIX

### Setup Comparisons between LSOFS-POM Nowcast and LSOFS-FVCOM Hindcast

	LSOFS-POM	LSOFS-FVCOM
	Nowcast	Hindcast
Core 3-D Ocean Circulation Model	POMGL	FVCOM V3.2
Surface Heat Flux Algorithm	GLERL's SOLAR Algorithm	Coupled Ocean Atmosphere Response Experiment Bulk Air-Sea Flux Algorithm (COARE V2.6)
Ice Model	N/A	Los Alamos Sea Ice Model (CICE) - Turned ON
Run Schedule	Hourly	6-hourly
Surface Forcing	GLOFS' hourly analyses of sfc marine obs (*Backup: 12km NAM model fcast guidance)	NWS High Resolution Rapid Refresh (HRRR) 1-hr surface forecast guidance (Backup: 2.5km NDFD gridded fcsts)
Lateral Boundary Conditions and Estimate of Lake Level	Avg. of observed water levels at NOS gages in lakes for past 5 days	Inflow/outflow estimates for connecting channels & 2 tributaries WL open boundary condition for one inflow inlet Estimate of residual to take into account P and E and other tributaries Water temperature prescribed for two river inputs